Folkhälsan Research Center
Department of Medical Genetics, Faculty of Medicine,
University of Helsinki

Doctoral Programme in Biomedicine
Faculty of Biological and Environmental Sciences
University of Helsinki
Dissertationes Universitatis Helsingiensis 452/2025

Insights into synaptic physiology from omics analyses in the early disease onset of CSTB-deficient mice modeling EPM1

Katarin Gorski

ACADEMIC DISSERTATION

To be presented, with the permission of the Faculty of Biological and Environmental Sciences of the University of Helsinki, for public examination in lecture hall 2, Biomedicum Helsinki,
on the 5th of December 2025, at 13 o'clock.

Helsinki 2025

Publisher: Helsingin yliopisto
Series: Dissertationes Universitatis Helsingiensis 452/2025

ISBN 978-952-84-1636-4 (print)
ISBN 978-952-84-1635-7 (online)
ISSN 2954-2898 (print)
ISSN 2954-2952 (online)
PunaMusta, Joensuu 2025

Supervised by

Professor and Research Director Anna-Elina Lehesjoki, MD, PhD
Folkhälsan Research Center, Helsinki, Finland, and Medicum, Faculty of Medicine, University of Helsinki, Helsinki, Finland

Associate Professor and Research Director Brendan J. Battersby, PhD
Institute of Biotechnology, University of Helsinki, Helsinki, Finland

Associate Professor Outi Kopra, PhD (deceased)
Folkhälsan Research Center, Helsinki, Finland, and Medicum, Faculty of Medicine, University of Helsinki, Helsinki, Finland

Thesis advisory committee

Associate Professor Aija Kyttälä, PhD
Arctic Biobank, University of Oulu, Oulu, Finland

Associate Professor and Research Director Claudio Rivera, PhD
Neuroscience Center, HiLIFE, University of Helsinki, Helsinki, Finland

Reviewed by

Professor and Research Director Annakaisa Haapasalo, PhD
A.I. Virtanen Institute for Molecular Sciences, University of Eastern Finland, Kuopio, Finland

Associate Professor Nataša Kopitar-Jerala, PhD
Jožef Stefan Institute, Ljubljana, Slovenia, and Jožef Stefan International Postgraduate School, Ljubljana, Slovenia

Opponent

Professor and Research Director Sara Mole, PhD
Great Ormond Street Institute of Child Health, University College London, London, UK

Custos

Professor and Research Director Katariina Öörni, PhD
Molecular and Integrative Biosciences Research Programme, Faculty of Biological and Environmental Sciences, University of Helsinki, Helsinki, Finland

Abstract

Loss of the cysteine protease inhibitor cystatin B (CSTB) causes severe neurological disorders. Partial loss causes childhood-onset progressive myoclonus epilepsy, EPM1, while complete loss causes a rapidly progressing developmental microcephaly with onset soon after birth. In both EPM1 patients and the CSTB-deficient (*Cstb*$^{-/-}$) mouse model, CSTB loss is associated with neuronal hyperexcitability, progressive brain degeneration, and disturbed neuronal signaling. CSTB is implicated in several biological processes, including regulation of epigenetic modifications, protection against oxidative stress and apoptosis, and maintenance of synaptic physiology. However, its full spectrum of molecular and physiological functions remains incompletely understood. Studies in *Cstb*$^{-/-}$ mouse brains have revealed early alterations in key cellular processes, including dysfunction of GABAergic signaling, mitochondrial impairment, and altered inflammatory responses. These processes are crucial for maintaining physiological functions and intercellular interactions, suggesting that CSTB loss drives multi-level dysfunction and widespread neuropathology.

The overall aim of this dissertation was to gain a comprehensive understanding of synaptic alterations preceding and accompanying disease onset in CSTB deficiency, with particular focus on the GABAergic signaling pathway. To accomplish this, synaptosome samples isolated from the cerebella of *Cstb*$^{-/-}$ mice were analyzed using mass spectrometry.

Proteomic analysis of synaptosomes from presymptomatic *Cstb*$^{-/-}$ mice (Study I) revealed significant alterations in mitochondrial function, cytoskeletal dynamics, and translational processes. Moreover, the GABA-transporter protein GAT-1 was significantly reduced at the protein level, and its activity was further assessed by electrophysiological recordings in cerebellar granule neurons from presymptomatic and early symptomatic *Cstb*$^{-/-}$ mice. Despite the protein-level change, no corresponding functional deficit in GAT-1 activity was observed. At clinical symptom onset at one month of age, synaptosomes from early symptomatic *Cstb*$^{-/-}$ mice exhibited pronounced proteome-level alterations in mitochondrial processes, further examined by respirometry (Study II). Although no functional differences were observed at symptom onset, significant dysfunction was detected two weeks later. Interestingly, this occurred without changes in ultrastructural or molecular-level markers of mitochondrial damage, suggesting potential metabolic reprogramming. In addition, early symptomatic *Cstb*$^{-/-}$ synaptosomes displayed significant proteome-level disruptions in the synaptic vesicle cycle and local protein translation. Unpublished transcriptomic data revealed widespread upregulation of neuronal cytokine and apoptotic signaling pathways, consistent with the timing of neuronal apoptotic events and clinical symptom onset in *Cstb*$^{-/-}$ mice.

Together, these comprehensive proteomic, transcriptomic, and functional analyses of synaptosomes from presymptomatic and early symptomatic *Cstb*$^{-/-}$ mice confirm previously reported alterations and uncover novel insights into the molecular and cellular mechanisms driving neuronal dysfunction and degeneration in CSTB deficiency.

Sammanfattning

Förlust av cysteinproteashämmaren cystatin B (CSTB) orsakar allvarliga neurologiska sjukdomar. Partiell förlust leder till progressiv myoklonusepilepsi (EPM1) med debut i barndomen, medan total förlust orsakar en snabbt framskridande utvecklingsbetingad mikrocefali med debut strax efter födseln. Hos både EPM1-patienter och i den CSTB-bristfälliga (*Cstb*$^{-/-}$) musmodellen har CSTB-brist associerats med neuronal hyperexcitabilitet, framskridande hjärndegeneration och störd neuronal signalering. CSTB är involverad i flera biologiska processer, inklusive reglering av epigenetiska modifieringar, skydd mot oxidativ stress och apoptos samt upprätthållande av synaptisk fysiologi. Det fullständiga spektrumet av dess molekylära och fysiologiska funktioner är dock inte fullständigt kartlagt. Forskning i hjärnor från *Cstb*$^{-/-}$ möss har avslöjat tidiga förändringar i kritiska processer, såsom dysfunktionell GABAerg signalering, nedsatt mitokondriell funktion och förändrade inflammatoriska responser. Dessa är avgörande för att upprätthålla fysiologiska funktioner och intercellulära interaktioner, vilket tyder på att CSTB-brist orsakar utbredd neuropatologi och dysfunktion på flera nivåer.

Helhetssyftet med denna avhandling var att få en djupgående förståelse av de synaptiska förändringar som sker före och efter sjukdomsdebuten vid CSTB-brist, med särskild fokus på den GABAerga signalrutten. För att uppnå detta analyserades synaptosomprover isolerade från lillhjärnan hos *Cstb*$^{-/-}$ möss med hjälp av masspektrometri.

Proteomisk analys av synaptosomer från presymptomatiska *Cstb*$^{-/-}$ möss (Studie I) avslöjade signifikanta förändringar i mitokondriella funktioner, cytoskelettdynamik och translationsprocesser. Dessutom var proteinnivån av GABA-transportören GAT-1 betydligt lägre, varmed dess aktivitet undersöktes genom elektrofysiologiska mätningar i cerebellära granulaceller från presymptomatiska och tidigt symptomatiska *Cstb*$^{-/-}$ möss. Trots förändringarna på proteinnivå observerades ingen motsvarande funktionell nedsättning av GAT-1-aktivitet. Vid sjukdomsdebut vid en månads ålder uppvisade synaptosomer från *Cstb*$^{-/-}$ möss betydande proteomiska förändringar relaterade till mitokondriella processer, vilka undersöktes med respirometri (Studie II). Även om inga funktionella skillnader observerades vid symptomdebut, upptäcktes signifikant mitokondriell dysfunktion två veckor senare. Detta skedde utan ultrastrukturella förändringar eller molekylära markörer för mitokondriell skada, vilket tyder på en möjlig metabolisk omprogrammering. Dessutom uppvisade synaptosomer från de tidigt symptomatiska *Cstb*$^{-/-}$ mössen tydliga proteomiska ändringar i synaptiska vesikelcykeln och lokala proteinsyntesen. Opublicerad transkriptomdata visade utbredd uppreglering av neuronala cytokin- och apoptossignaleringsrutter, i linje med tidpunkten för neuronal apoptos och klinisk symptomdebut hos *Cstb*$^{-/-}$ möss.

Sammanfattningsvis bekräftar dessa omfattande proteomiska, transkriptomiska och funktionella analyser av synaptosomer från *Cstb*$^{-/-}$ möss tidigare rapporterade förändringar, samtidigt som de avslöjar nya insikter till de molekylära och cellulära mekanismerna som driver neuronal dysfunktion och degeneration vid CSTB-brist.

Tiivistelmä

Kysteiiniproteaasiestäjä kystatiini B:n (CSTB) puutos aiheuttaa vakavia neurologisia sairauksia. Osittainen puutos aiheuttaa lapsuudessa alkavan etenevän myoklonusepilepsian (EPM1), kun taas täydellinen puutos aiheuttaa nopeasti etenevän kehityksellisen mikrokefalian, joka alkaa pian syntymän jälkeen. Sekä EPM1-potilailla että CSTB-puutteisella (*Cstb*$^{-/-}$) hiirimallilla CSTB:n menetys on yhdistetty hermosolujen yliherkkyyteen, etenevään aivorappeumaan ja hermosolujen signalointihäiriöihin. CSTB osallistuu useisiin biologisiin prosesseihin, kuten epigeneettisten modifikaatioiden säätelyyn, oksidatiiviseltä stressiltä ja apoptoosilta suojautumiseen sekä synaptisen fysiologian ylläpitoon. Sen molekulaaristen ja fysiologisten toimintojen koko kirjo on kuitenkin puutteellisesti tunnettu. *Cstb*$^{-/-}$ -hiirten aivoissa on havaittu varhaisia muutoksia keskeisissä fysiologisissa toiminnoissa, kuten häiriintyneessä GABAergisessä signaloinnissa, heikentyneessä mitokondrioiden toiminnassa sekä muuttuneissa tulehdusvasteissa. Tämä viittaa siihen, että CSTB:n puutoksen aiheuttama laaja-alainen neuropatologia aiheutuu moniulotteisesta toimintahäiriöstä.

Tässä väitöskirjassa tutkittiin CSTB-puutokseen liittyviä synaptisia muutoksia ennen taudin puhkeamista ja sen aikana, keskittyen erityisesti GABAergiseen signalointireittiin. Tämän saavuttamiseksi *Cstb*$^{-/-}$ -hiirten pikkuaivoista eristettyjä synaptosominäytteitä analysoitiin massaspektrometrian avulla.

Presymptomaattisten *Cstb*$^{-/-}$ -hiirten synaptosomien proteomiikka-analyysi (Osatutkimus I) paljasti merkittäviä muutoksia mitokondrioiden toiminnassa, soluntukirangan dynamiikassa ja proteiinitranslaatiossa. Lisäksi GABA-kuljettajaproteiini GAT-1:n määrä oli merkittävästi alentunut, ja sen aktiivisuutta arvioitiin elektrofysiologisin mittauksin *Cstb*$^{-/-}$ -hiirten pikkuaivojen jyvässoluissa. Proteiinitason muutoksesta huolimatta, vastaavaa toiminnallista heikkenemistä ei havaittu GAT-1:n aktiivisuudessa. Kliinisten oireiden alkaessa, varhaisoireisten *Cstb*$^{-/-}$ -hiirten synaptosomeissa havaittiin merkittäviä proteomitason muutoksia mitokondriaalisissa toiminnoissa, joita tutkittiin respirometrian avulla (Osatutkimus II). Vaikka oireiden alkaessa ei havaittu toiminnallisia eroja, kaksi viikkoa myöhemmin ilmeni merkittävä mitokondriaalinen toimintahäiriö. Rakenteellisia muutoksia tai molekulaarisia vaurioon liitettyjä markkereita ei havaittu, mikä viittaa metaboliseen uudelleenohjelmointiin. Lisäksi havaittiin merkittäviä muutoksia synaptisessa vesikkelikierrossa ja paikallisessa proteiinisynteesissä. Julkaisematon transkriptomiikkadata osoitti neuronien sytokiini- ja apoptoosireittien aktivoitumista ajallisesti linjassa neuronaalisen apoptoosin ja kliinisten oireiden puhkeamisen kanssa.

Yhdessä nämä laaja-alaiset proteomiikkaan, transkriptomiikkaan ja toiminnallisiin mittauksiin perustuvat analyysit paljastavat uusia näkökulmia molekyyli- ja solutason mekanismeista, jotka johtavat hermosolujen toimintahäiriöön ja rappeumaan CSTB-puutoksessa.

Table of contents

List of original publications

This thesis is based on the following publications:

I **Gorski, K.**, Spoljaric, A., Nyman, T.A., Kaila, K., Battersby, B.J. and Lehesjoki, A.-E. (2020) Quantitative Changes in the Mitochondrial Proteome of Cerebellar Synaptosomes From Preclinical Cystatin B-Deficient Mice. Frontiers in Molecular Neuroscience, 13, 570640.

II **Gorski, K.**, Jackson, C.B., Nyman, T.A., Rezov, V., Battersby, B.J. and Lehesjoki, A.-E. (2023) Progressive mitochondrial dysfunction in cerebellar synaptosomes of cystatin B-deficient mice. Frontiers in Molecular Neuroscience, 16, 1175851.

In addition, unpublished results are presented.

The publications are referred to in the text by their roman numerals.

List of abbreviations

Abbreviations that appear more than once are presented here.

ADP	adenosine diphosphate
ATP	adenosine triphosphate
bp	base pair
CCL	Chemokine (C-C motif) ligand
CSTB	cystatin B/stefin B
Cstb$^{-/-}$	cystatin B deficient mouse model
CXCL	Chemokine (C-X-C motif) ligand
CXCR	Chemokine (C-X-C motif) receptor
CX3CL	Chemokine (C-X3-C motif) ligand
CX3CR	Chemokine (C-X3-C motif) receptor
DAP	differentially abundant protein
DEG	differentially expressed gene
eEF	eukaryotic translation elongation factor
EEG	electroencephalography
eIF	eukaryotic translation initiation factor
EPM1/ULD	myoclonic epilepsy of Unverricht and Lundborg
FAD/FADH	flavin adenine dinucleotide (oxidized/reduced)
FC	fold change
FDR	false discovery rate
GABA	gamma-aminobutyric acid
GAT-1	GABA transporter-1
GO	Gene Ontology
IL	interleukin
iPSC	induced pluripotent stem cell
kDa	kilodalton
LPS	lipopolysaccharide
MRI	magnetic resonance imaging
mRNA	messenger ribonucleic acid
mtDNA	mitochondrial deoxyribonucleic acid
NAD^+/NADH	nicotinamide adenine dinucleotide (oxidized/reduced)

NF	nuclear factor
NLRP	nucleotide-binding domain, leucine-rich–containing family, pyrin domain–containing
OCR	oxygen consumption rate
omics	high-throughput analysis of biological molecules at different levels
OPA1	Dynamin-like GTPase OPA1, mitochondrial
OXPHOS	oxidative phosphorylation
P	postnatal day
PCA	principal component analysis
PCR	polymerase chain reaction
PSD	postsynaptic density
Rab	Ras-associated binding
RNP	ribonucleoprotein
ROS	reactive oxygen species
RT	reverse transcriptase
SOD1	superoxide dismutase 1
SUIT	substrate-uncoupler-inhibitor-titration
TCA	tricarboxylic acid
TEM	transmission electron microscopy
TMS-EEG	transcranial magnetic stimulation and electroencephalography
TNF	tumor necrosis factor alpha
UMI	unique molecular identifier

1 Introduction

The concept of the *Finnish disease heritage*, a group of diseases more common in Finland than elsewhere, emerged from a medical mystery in the 1950s. At the Children's Hospital of the University of Helsinki, doctors observed a concerning pattern: newborns with a confusing treatment-resistant form of nephrosis that invariably resulted in death. Unlike typical cases, this condition was clearly hereditary, prompting a nationwide investigation led by Harri Nevanlinna and Ilmari Kantero. Their study, completed in 1966, identified the disease, now known as congenital nephrosis (CNF), as autosomal recessive, with consanguinity common among affected families. In addition, the findings revealed an unexpected overrepresentation of rare genetic diseases in the Finnish population.

Today, the Finnish disease heritage includes nearly 40 rare genetic disorders significantly more common in Finland than elsewhere. These conditions are often severe, leading to disability or premature death. Most follow an autosomal recessive inheritance pattern, though two autosomal dominant and two X-linked diseases have also been identified. From the 1960s to 1980s, more of these disorders were clinically recognized, and with the rapid development of genomic technologies in the 1990s and 2000s, the causative genes for nearly all were identified. Advances in genetic testing and whole-exome sequencing have improved diagnostics and care, while genetic counseling and prenatal testing remain crucial for families at risk. Still today, around 60 children are born each year in Finland with one of these diseases, for which many have no curative treatment.

Many of the Finnish diseases affect the brain, causing epilepsy and progressive neurological decline, the most common being Unverricht-Lundborg disease, EPM1. Although the causative gene was identified over two decades ago, it has not led to effective therapies. The underlying molecular and cellular mechanisms remain poorly understood, and current care is limited to symptom management. This gap between gene discovery and therapeutic progress is not unique to EPM1 as it reflects a broader challenge in rare disease research. Yet beneath their rarity lie universal biological mechanisms that, once understood, may offer insights far beyond single diseases. By investigating the synaptic and molecular dysfunctions in EPM1, this thesis aims to help bridge that gap by deepening our understanding of a disease that belongs to the Finnish disease heritage, but also by contributing to the broader effort of turning scientific knowledge into care.

2 REVIEW OF THE LITERATURE

2.1 THE BRAIN

2.1.1 Anatomical and functional organization

The human brain is a complex system from which our thoughts, memories, motor skills, and mind originate. It is located inside a supportive and protective bony structure, the cranium, which consists of 22 bones connected by cranial sutures (Anderson et al., 2023). The brain is surrounded by three covering and protecting layers of meninges and cushioning cerebrospinal fluid, and it can be divided into three basic units, the forebrain, midbrain, and hindbrain (**Figure 1A**) (Maldonado and Alsayouri, 2023). These originate from the tip of a three-millimeter-long neural tube that begins to form three to four weeks after conception, and develops into the human brain (Ackerman, 1992). The forebrain is the largest unit of the brain and consists of the cerebrum, thalamus and hypothalamus (Maldonado and Alsayouri, 2023). The outermost layer, the cerebral cortex, is greyish-brown in color and is hence called grey matter (**Figure 1B**). Approximately 40% of the brain consists of grey matter that is composed of neuronal cell bodies, and 60% of white matter, the deeper brain tissue, primarily made up of dendrites and axons, the projections of neuronal cell bodies. The cerebrum is divided into two halves, the left and right hemispheres, which are connected by white matter called the Corpus callosum (**Figure 1C**). These hemispheres are further divided into four pairs of lobes: the frontal, temporal, parietal and occipital lobes (**Figure 1D**), which in turn are divided into areas that process highly specific functions such as voluntary movement, sensory information, and perception of physical sensations from the body (**Figure 1E**). Although most neurons reside in the grey matter, there are collections of neurons located deep in the white matter, such as the thalamus and hypothalamus (**Figure 1A**). These control and regulate the broader functions of the brain, such as transmission of sensory information from the body to the cerebral cortex, and the regulation of hormonal functions. The other basic units of the brain, the midbrain and the hindbrain, function as a relay system for vision and hearing and control the vital functions of the body, such as respiration and heart rate (Ackerman, 1992).

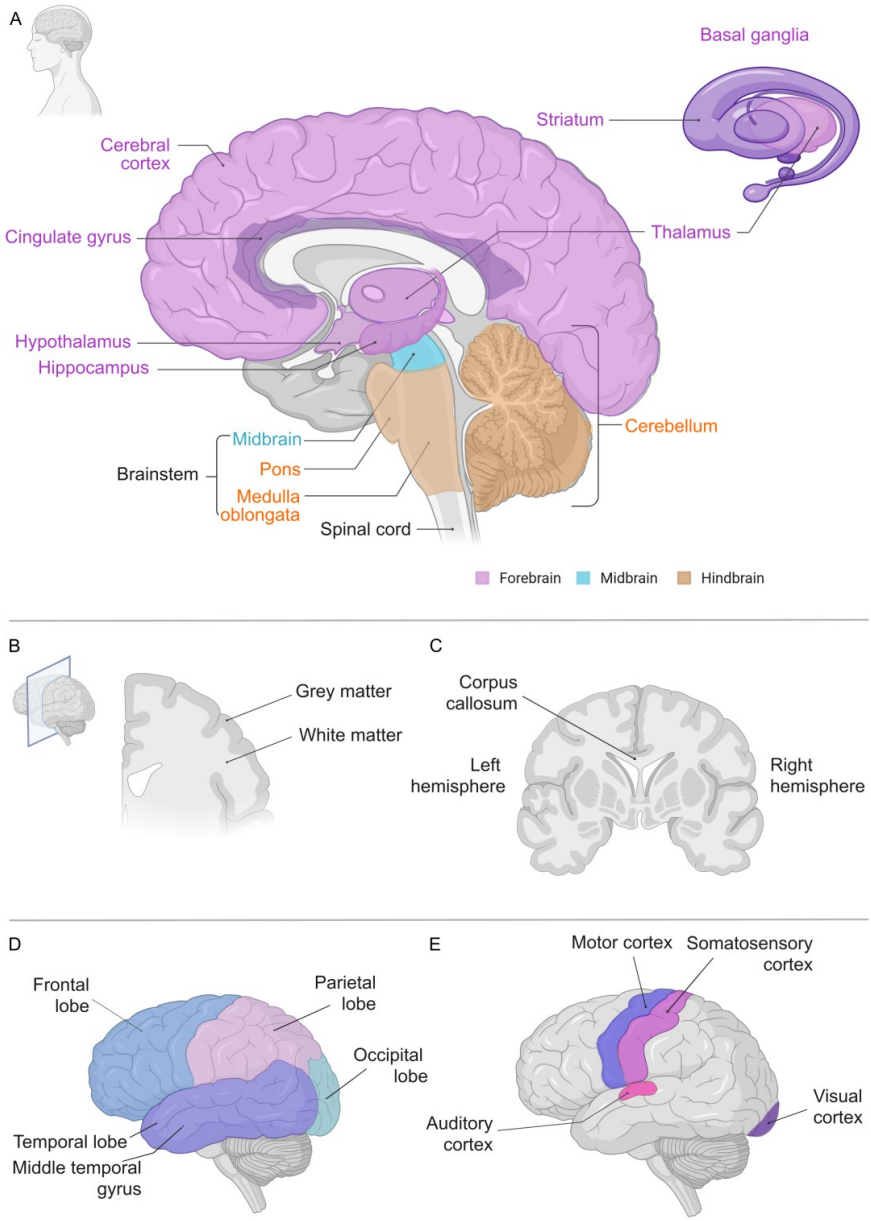

Figure 1 **Anatomical and functional organization of the human brain.** (A) The basic units of the brain gives rise to its different structures. Purple = forebrain; turquoise = midbrain; orange = hindbrain. A magnified view of the thalamus, striatum, and basal ganglia are presented on the right-hand side for clarity. (B) Coronal cross section of brain indicating grey and white matters. (C) Coronal cross section indicating left and right hemispheres, connected by the Corpus callosum. (D) Cerebral hemispheres divided into the frontal (blue), parietal (lilac), temporal (violet), and occipital (green) lobes. (E) Cortical areas of the brain, indicating the motor cortex (blue), somatosensory cortex (plum), auditory cortex (pink), and visual cortex (purple). Figure partly created using BioRender.com.

The midbrain comprises the upper part of the brainstem, while the lower part, consisting of the pons and medulla oblongata, originates from the hindbrain (**Figure 1A**). The hindbrain also gives rise to the cerebellum, the second-largest structure in the brain (Silverthorn, 2009; Maldonado and Alsayouri, 2023). For more information on the cerebellum, see 2.1.2.

2.1.1.1 Major cell types

The average human brain contains approximately 100 billion neurons, organized in sheet-like layers and distributed across dozens of anatomically distinct regions (Amunts and Zilles, 2015). Neuronal morphology consists of three main parts: cell soma, axon and dendrites (**Figure 2A**) (Ludwig et al., 2023). The soma houses the nucleus of the cell and is where transcription of genes takes place. An axon is an extension of the cell body, and an electrically propagating signal at its terminal triggers the release of chemical neurotransmitters, which are received by the dendrites of neighboring cells. Dendrites are branches of the cell body and receive information from nearby axon terminals. There are numerous neuronal subtypes, each with characteristic morphology and distinct molecular signatures (Siletti et al., 2023): for example, 24 types of excitatory and 45 types of inhibitory neurons in the middle temporal gyrus of the human cortex (Hodge et al., 2019), enhancing and suppressing neural signaling, respectively. The balance of excitatory and inhibitory neurons is critical for the proper functioning of the nervous system: lack of proper inhibition causes excess excitation and irrelevant sensory information, which can lead to epileptic seizures and cellular damage (Scharfman, 2007). Thus, excitatory and inhibitory neurons are found in all regions of the brain.

The physical basis of the higher-order functions of the brain lies in the networks formed by the two major types of cells, neurons and glia (**Figure 2B**) (Maldonado and Alsayouri, 2023). Neurons mediate the principal information processing, while glial cells facilitate signal transmission by providing support through nutrition, homeostasis maintenance, and myelin formation (Ludwig and Das, 2025). The ratio of neurons to glial cells varies across brain regions, being high in the cerebellum (25:1) and low in subcortical nuclei such as the thalamus (1:17) and the ventral pallidum of the basal ganglia (1:12) (Herculano-Houzel, 2009). Based on their developmental origin, glial cells are classified into microglia and macroglia, the latter of which are further divided into astrocytes and oligodendrocytes (Skoff, 1980).

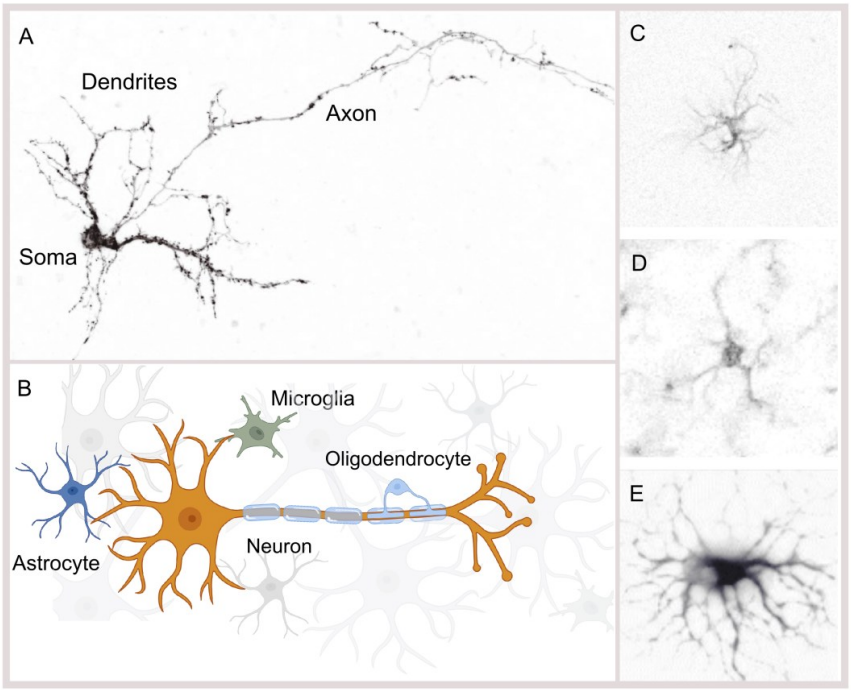

Figure 2 Major cell types in the central nervous system. (A) Microscopy image of a mouse cerebellar granule neuron after 16 days in culture, showing key structural components. The soma, dendrites, and axon are labeled to illustrate the main morphological features; (B) Schematic illustration of a central neuron (orange) and its relation to astrocytes (dark blue), microglia (green), and oligodendrocytes (light blue); (C) Glial fibrillary acidic protein (GFAP)-immunolabeled astrocyte in mouse brain; (D) Ionized calcium binding adaptor molecule 1 (IBA1)-immunolabeled microglial cell in mouse brain; (E) Acetylated alpha-tubulin-immunolabeled oligodendrocyte precursor cell from rat brain in culture. Image A acquired by the author; image B partly created using BioRender.com; images C-D by Saara Tegelberg, Folkhälsan Research Center; image E adapted from Grigoletto et al., 2017 with permission.

Astrocytes (**Figure 2C**), the star-shaped cells of the central nervous system, maintain and modulate the neuronal extracellular homeostasis by forming close contact with neurons, blood capillaries, and cerebrospinal fluid (Araque et al., 1999; Lee et al., 2022). They form a complex functional unit known as the tripartite synapse, interacting with pre- and postsynaptic neuronal elements to provide metabolic support for neurotransmission (see 2.2.3.1 and **Figure 7** for more details). Astrocytes also regulate synaptic formation, transmission, and plasticity (Araque et al., 1999). Upon central nervous system injury, they undergo morphological, functional, and molecular remodeling, becoming heterogeneous cells that contribute to both pathology and repair.

Microglia, the resident macrophages of the central nervous system (**Figure 2D**), also play a vital role in the function of neuronal networks (Li and Barres, 2018). During development, they remodel neural circuits and adopt distinct

morphological, molecular, and secretory profiles required for normal brain maturation (see 2.1.3 for more details). In response to injury or disease, reactive microglia proliferate and migrate to the damaged sites where they phagocytose cellular debris and release cytokines, chemokines, and/or trophic factors (Vilhardt, 2005). Finally, oligodendrocytes, the predominant cell type in the white matter (**Figure 2E**), support neurons by forming and maintaining myelin (Jahn et al., 2009; Simons and Nave, 2015). Myelin, a lipid-rich membrane, is wrapped in sheets around neuronal axons (**Figure 2B**) where it speeds up conduction by electrically insulating and reducing the axonal transverse capacitance (Gerevich et al., 2023). Action potentials, the fundamental units of neuronal communication, propagate by saltatory conduction across the nodes of Ranvier, the periodically located small segments between myelin sheets, enabling rapid and efficient signal propagation along the axon.

2.1.2 The cerebellum

The cerebellum, meaning "little brain", is located beneath the occipital lobes posterior to the brainstem, where it processes sensory input from the spinal cord along with motor commands from the cerebral cortex (Roostaei et al., 2014). Anatomically and physiologically, it is organized into distinct functional compartments comprising regularly arranged neuronal groups, each sharing a conserved microcircuit structure. The anatomy of the cerebellum is highly conserved across mammals (Larsell, 1970; Voogd and Glickstein, 1998), consisting of a narrow midline region, the cerebellar vermis, that connects the two lateral hemispheres (**Figure 3A**). The cerebellum is further divided into three lobes: the anterior, posterior, and flocculonodular lobes (Roostaei et al., 2014), which are in turn subdivided into ten transverse lobules, designated by the roman numerals I-X (Larsell, 1952). The surface of these is further organized into thin, parallel transverse folds called folia (Roostaei et al., 2014).

The cerebellar cortex comprises highly convoluted grey matter that surrounds a branching trunk of white matter known as the arbor vitae ("tree of life") (**Figure 3B**). Embedded within the white matter are three pairs of deep cerebellar nuclei (Roostaei et al., 2014), which serve as the primary output structures of the cerebellum. The cortex itself is organized into a highly conserved three-layered structure that remains consistent across cortical regions, regardless of functions or connectivity patterns (Roostaei et al., 2014). These layers are known as the molecular layer, the Purkinje cell layer, and the granular layer. The deepest layer, the granular layer, is densely populated by a large number of granule cells along with inhibitory Golgi interneurons and serves as the primary input layer for the cerebellar cortex (**Figure 3C**). In the middle lies a narrow layer called the Purkinje layer, containing mainly cell bodies of Purkinje cells and Bergmann glial cells,

serving as the output layer for the cerebellar cortex. The most superficial layer, the molecular layer, is composed of flattened dendritic trees of Purkinje cells, axons of granule cells that ascend into the molecular layer and make horizontal contacts with the dendritic trees of Purkinje cells, and inhibitory interneurons such as stellate and basket cells. Together, these neural circuits are critical for coordinating and adjusting voluntary movement, maintaining posture and balance, and regulating muscle tone and limb position (Roostaei et al., 2014).

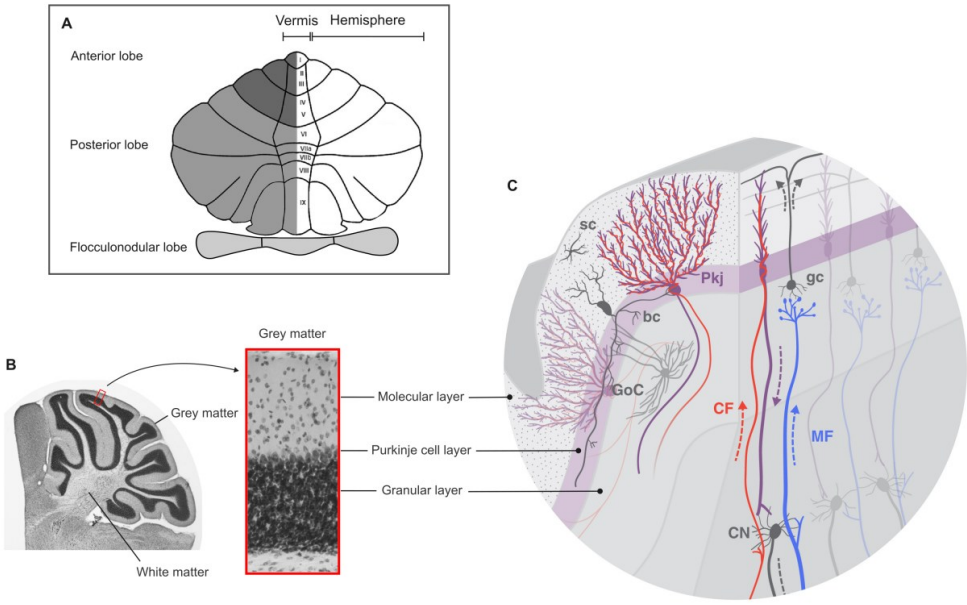

Figure 3 Anatomical organization of the cerebellum and its major cell types. (A) Schematic representation of the cerebellar hemispheres and the midline vermis, showing the anterior, posterior, and flocculonodular lobes divided into ten lobules (I-X). Image adapted from (Fernandez et al., 2020) with permission. (B) Representative histological image of a Nissl-stained mouse cerebellum illustrating the arrangement of white and grey matter and showing the laminar structure of the cerebellar cortex: molecular layer, Purkinje cell layer, and granular layer. Image by Saara Tegelberg/Folkhälsan Research Center. (C) The circuitry of the cerebellar cortex with major cell types and pathways illustrated, including Purkinje cells (Pkj), basket cells (bc), stellate cells (sc), Golgi cells (GoC), and granule cells (gc). Afferent inputs include climbing fibers (CF, red) and mossy fibers (MF, blue), which synapse on Purkinje cells and granule cells, respectively. Purkinje cells send inhibitory outputs to the deep cerebellar nuclei (CN). Figure adapted from Carey, 2024 with permission.

2.1.2.1 Cerebellar neuron development

The majority of neurons in the brain are located in the cerebellum (Herculano-Houzel, 2009), and they are derived from neural progenitor cell populations in

specialized regions called germinal zones: in the cerebellum, excitatory glutamatergic neurons arise from the rhombic lip, and inhibitory gamma-aminobutyric acid (GABA)-ergic neurons from the ventricular zone (Leto et al., 2016). The cerebellum has a protracted developmental course, extending from early embryogenesis into postnatal life (**Figure 4**). In humans, it undergoes its major growth during the third trimester and the first year of life (Kiessling et al., 2014; Leto et al., 2016), and in mice, during the first two postnatal weeks (Leto et al., 2016).

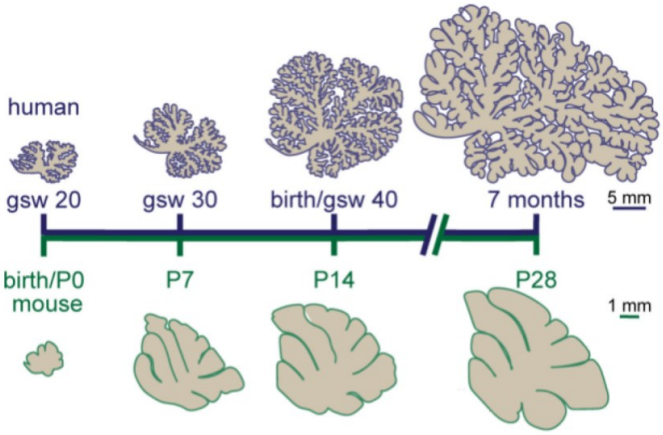

Figure 4 Comparison of cerebellar growth during development in human and mouse. The figure depicts the relative size and morphological progression of the developing cerebellum at key time points in human (gestational weeks (gsw) 20, 30, and 40, and 7 months postnatal) and in mouse (postnatal days (P) 0, 7, 14, and 28). Despite differences in timing, the stages illustrate conserved patterns of cerebellar maturation across species. Image adapted from van der Heijden et al., 2021 with permission.

Neuronal development is initiated by three complex processes: 1) the generation of undifferentiated, lineage-specific neural cells; 2) the migration of these cells to predetermined locations in the brain; and 3) their differentiation into specific cell types appropriate for those locations (Ackerman, 1992). These processes are regulated by the expression of internal transcription factors and by extracellular cues. Unlike some other mammalian brain regions that develop from the core outward, cerebellar development involves overlapping and directional migration of cells that build the cerebellar structure both inside-out and outside-in. GABAergic Purkinje cells and interneurons migrate radially from the ventricular zone outward, whereas glutamatergic granule cell precursors first migrate tangentially from the rhombic lip to form the external granule layer, and then radially to settle in the internal granule layer. The migration of undifferentiated cells is guided by adhesion molecules arranged on radial glial cells and guidance molecules present on the surfaces of axons, leading to the formation of the distinct neuronal layers (**Figures**

3B and **C**). After migration, cerebellar neurons complete their differentiation by acquiring characteristic biochemical properties, forming receptor sites, and developing distinct morphologies, thereby establishing the form and function of cerebellar circuits.

Neuronal migration and differentiation are followed by axonal growth, which is guided by attractive and repulsive cues and regulated by local messenger RNA (mRNA) translation (Ackerman, 1992; Jung et al., 2012). Once axons reach their targets, countless connections between neurons begin to form: between the axon of one neuron and the dendrite of another, the axon and the cell body of another, or between axons, dendrites, or cell bodies themselves. The prosperous formation of synapses in the developing brain is regulated by several messenger molecules, including brain-derived neurotrophic factor (BDNF), whose effects are different in the mature brain, where it modulates synaptic transmission and plasticity (Cohen-Cory et al., 2010; Edelmann et al., 2014; Kowiański et al., 2018). The early quantities of neurons and synapses are overtly large, as some cell populations become permanent while others are programmed to exist only briefly.

The final developmental stage is the selective elimination, or pruning, of many synaptic connections and axons, and the stabilization of those that remain (Changeux and Danchin, 1976; Schafer and Stevens, 2010). This developmental reorganization is common across mammalian species (Juraska and Drzewiecki, 2020) and is crucial for the maturation of synaptic connections. Synaptic fate is influenced by activity: activity promotes maintenance, while less active synapses are eliminated (Nagappan-Chettiar et al., 2023). Eliminated axons are retracted, degraded, or partially absorbed for reuse, and entire cells are allowed to die and are cleared from the system via microglial phagocytosis (Neumann et al., 2009). Elimination is mediated by complex interactions between neurons and glial cells. For example, astrocytes play key roles in both the strengthening and elimination of synapses: they enhance synaptic strength by trafficking postsynaptic receptors to the synapse (Chung et al., 2015) and promote synapse elimination by inducing the expression of complement component C1q, a key signal for synaptic elimination (Stevens et al., 2007). C1q expression activates the complement pathway, which stimulates microglia to phagocytose the synapse. Insufficient or excessive synaptic elimination chronically alters neural circuits, as synapses fail to mature properly, leading to both morphological and functional deficits (Chu et al., 2010; Washbourne, 2015). These abnormalities have been proposed to underlie several neurodevelopmental disorders, including autism, schizophrenia and epilepsy.

2.1.2.2 Developmental plasticity

Neuronal plasticity refers to the adaptive ability of neurons to modify specific circuits in response to different stimuli (Citri and Malenka, 2008). These

modifications on activity and organization are based on previous neuronal activity and are often defined as the molecular form of learning, memory, and development. Plasticity occurs throughout life, but it is particularly important during the developmental period of the brain (Ismail et al., 2017). As neurons mature, the formation of correct circuit connections depend on homeostatic mechanisms that ensure their spontaneous activity, with the best characterized form being synaptic scaling. This refers to activity-induced compensatory changes in synaptic strength with the purpose of firing synapses at stable rates despite changes in network activity (Turrigiano, 2008). Homeostatic plasticity is affected by external factors such as the cytokine tumor necrosis factor alpha (TNF), which is secreted by microglial cells in response to pathological conditions. TNF enhances translocation of neurotransmitter receptors to the postsynapse, increasing the current amplitudes of neurons (Stellwagen and Malenka, 2006).

2.2 THE SYNAPSE

2.2.1 Synaptic organization

Neuronal circuits are formed by populations of neurons interconnected through specialized cell-to-cell connections, called synapses. The concept of a synapse is partly morphological and partly physiological, as it refers to a separation between two membrane-surrounded terminal enlargements that have the property of transmitting nervous impulses from one to the other. Structural and physiological elements of the synapse were described already in the 19th century by the Spanish neuroscientist Santiago Ramón y Cajal (1852–1934), who postulated that nervous information travel across gaps between cells. Cajal's original description of the synaptic structure was confirmed in the 1950s, as electron microscopic observations became available, enabling the identification of several elements characteristic of the pre- and postsynapses, i.e. the transmitting and receiving sides (**Figure 5**) (Palay, 1956).

The presynaptic side has a collection of fine vesicles that cluster into a membrane-anchored electron-dense structure, the active zone, that is facing the interspace between the pre- and postsynaptic side. This synaptic cleft is a region of separation that is approximately 20-30 nanometers (nm) wide between neurons of the central nervous system. The postsynaptic side is characterized by an electron-dense region, the postsynaptic density (PSD), which is associated with the postsynaptic membrane and represents a macromolecular protein complex. The presynaptic side has tightly packed mitochondria and other cytoplasmic elements not usually found on the postsynaptic side.

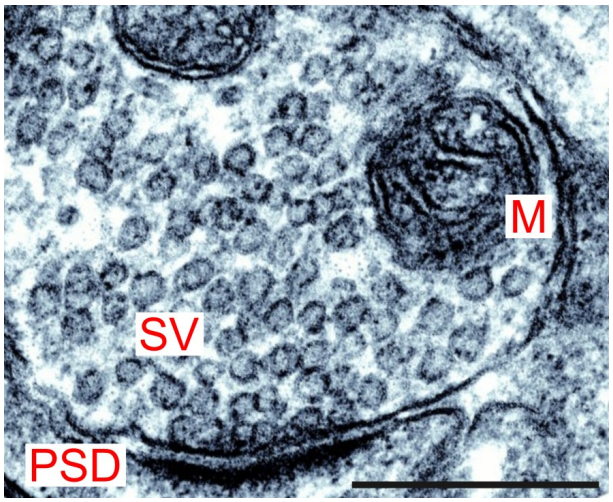

Figure 5 Electron microscopy image of a synapse. The presynaptic terminal with synaptic vesicles (SV), mitochondria (M), and other structural components is separated by a synaptic cleft from an opposing postsynaptic terminal (PSD) with neurotransmitter receptors. Scale bar 400 nm. Adapted from Kennedy, 2000 with permission.

2.2.2 Synaptic transmission

Synaptic transmission refers to an event where electric signals that propagate along the axon within one neuron are chemically transmitted to dendrites of another neuron. This interneuronal communication takes place at chemical synapses, where action potentials cause depolarization of the plasma membrane and initiate a cascade of events: voltage-gated calcium channels in the presynapse open and calcium is released into the synapse (Purves, 2012). The high concentration of calcium ions trigger the fusion and exocytosis of synaptic vesicles with the active zone plasma membrane, resulting in neurotransmitter release into the synaptic cleft (Sudhof, 2004). The neurotransmitter molecules bind and activate receptors on the postsynaptic membrane, whereas the synaptic vesicles are recycled through endocytosis. Activation of postsynaptic receptors leads to either excitation or inhibition of the postsynaptic neuron, depending on the neurotransmitter and receptor type. In excitation, sodium channels on the postsynaptic side open, causing depolarization of the plasma membrane, while in inhibition, chloride channels open, causing membrane hyperpolarization (Purves, 2012). The predominant excitatory and inhibitory neurotransmitters in brain are glutamate and GABA, respectively. The combined effect of several synapses on the postsynaptic neuron determines whether or not the signal propagates. After an effect on the postsynaptic side has been elicited, the neurotransmitter molecule is removed from the receptor, causing the receptor to close. The neurotransmitter is inactivated as a result of

reuptake or degradation by neurons, or uptake and metabolism by glial cells (Sudhof, 2004; Lee et al., 2022).

2.2.3 Synaptic physiology

2.2.3.1 Mitochondrial bioenergetics

Neurons are morphologically polarized and metabolically active cells whose synaptic function, plasticity, and survival depend on high energy levels, tight local calcium regulation and remodeling of the proteome (Rossi and Pekkurnaz, 2019). To meet these local energy and physiological needs, synaptic regions are rich in mitochondria.

Mitochondria are organelles of eukaryotic cells that perform a wide variety of functions, the best described being the aerobic production of cellular energy in the form of adenosine triphosphate (ATP). The metabolic pathways that catabolize nutrients and generate energy and precursors for essential metabolites are interconnected through a series of chemical reactions, in which the product of one reaction serves as the substrate for the next. The central pathways are glycolysis, beta-oxidation, and protein catabolism that are responsible for the breakdown of glucose, fatty acids, and proteins, respectively (**Figure 6**) (Lehninger et al., 2005). The end products of these pathways serve as substrates for the tricarboxylic acid (TCA) cycle in the mitochondria.

Cytoplasmic glycolysis is divided into two distinct phases: the preparatory phase, which consumes ATP and generates intermediates for anabolic biosynthetic reactions, and the energy-conserving phase, which produces ATP, nicotinamide adenine dinucleotide (NADH), and substrates for further catabolism. One of the key end-products of glycolysis is pyruvate, which enters mitochondria through protein complexes formed by mitochondrial pyruvate carriers MPC1 and MPC2 in the inner mitochondrial membrane (McCommis and Finck, 2015). Pyruvate is then metabolized to acetyl coenzyme A (acetyl-CoA), the primary substrate of the TCA cycle. In parallel, mitochondrial beta-oxidation catabolizes fatty acids, derived from dietary lipids, into acetyl-CoA, also feeding the TCA cycle. Both beta-oxidation and the TCA cycle generate high-energy electron carriers, NADH and flavin adenine dinucleotide ($FADH_2$), through stepwise enzymatic reactions (Lehninger et al., 2005). Fatty acids vary structurally in carbon chain length and in the presence and number of double bonds, and depending on their chain length, beta-oxidation yields a variable number of acetyl-CoA, NADH, and $FAHD_2$ units.

The TCA cycle uses acetyl-CoA as its main substrate to produce reduced NADH and $FADH_2$ in a cyclic series of reactions (Lehninger et al., 2005). These electron carriers are then utilized by the oxidative phosphorylation (OXPHOS) system to generate ATP and retain cellular pools of oxidized NAD^+ and FAD (Mitchell, 1961).

However, the metabolic pathways are not isolated or unidirectional. For example, intermediates from the TCA cycle can serve as biosynthetic precursors for amino acids, nucleic acids, and fatty acids, depending on cellular needs. Similarly, products from amino acid degradation can enter the TCA cycle, and the direction and flux of these pathways are influenced by the availability of substrates, enzymes, and cofactors.

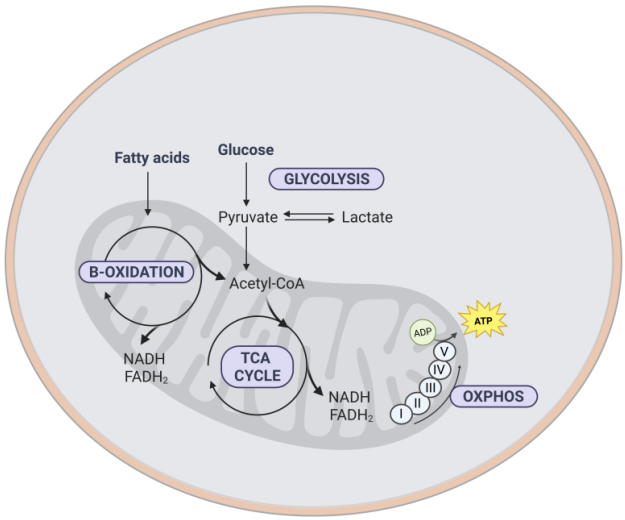

Figure 6 Overview of cellular energy metabolism and mitochondrial ATP production. Glucose is metabolized to pyruvate via glycolysis in the cytosol. Pyruvate is either converted to lactate or transported into mitochondria where it is converted to acetyl-CoA. Fatty acids are metabolized through mitochondrial beta-oxidation, also yielding acetyl-CoA along with NADH and $FADH_2$. Acetyl-CoA enters the tricarboxylic acid (TCA) cycle, producing reducing equivalents (NADH, $FADH_2$) that feed into the electron transport chain (ETC) for oxidative phosphorylation (OXPHOS). The ETC (complexes I-IV) generates a proton gradient that drives ATP synthesis via ATP synthase (complex V), coupling mitochondrial respiration to cellular energy production. Figure partly created using BioRender.com.

Oxidative phosphorylation refers to both the mitochondrial ATP production machinery and the biochemical process through which ATP is generated via the oxidation of NADH and $FADH_2$. This oxidation drives the formation of an electrochemical proton gradient across the inner mitochondrial membrane, which powers ATP synthesis (Mitchell, 1961). Electron transfer and membrane potential generation are carried out by four multiprotein electron carrier complexes (complexes I-IV), embedded in cristae invaginations of the inner mitochondrial membrane, along with soluble electron carriers (Lehninger et al., 2005). Collectively, these are referred to as the electron transport chain or the respiratory chain. As electrons are transferred through complexes I, III, and IV to the final electron acceptor, molecular oxygen, protons are pumped from the mitochondrial

matrix into the intermembrane space, generating both a proton gradient and membrane potential. This stored electrochemical energy is then used by complex V (ATP synthase) to form ATP in a two-component mechanism: protons flow back into the matrix through the membrane-embedded F_0 domain of ATP synthase, inducing its rotation. This rotational motion is transmitted via the γ subunit to the F_1 catalytic domain located in the matrix, causing conformational rearrangements that catalyze the covalent attachment of inorganic phosphate to adenosine diphosphate (ADP), forming ATP (Mitchell, 1961; Jonckheere et al., 2012). In addition to energy production, the activity of the OXPHOS complexes also generates reactive oxygen species (ROS), which are highly reactive radicals that serve as important signaling molecules under both physiological and pathological conditions.

Most cells can balance between glucose and fatty acid catabolism for ATP production, yet neurons primarily use glucose as their energy source due to its readily accessible energy (Dienel, 2012; Mergenthaler et al., 2013). Astrocytes, with their endfeet around blood vessels and perisynaptic processes surrounding synapses, are thought to support neuronal energy metabolism by taking up glucose from the bloodstream, metabolizing it into pyruvate and subsequently to lactate, which is then redistributed to neurons (**Figure 7**) (Pellerin and Magistretti, 1994; Pellerin et al., 2007). In neurons, lactate is metabolized back to pyruvate and oxidized by the TCA cycle. The glucose-lactate shuttle hypothesis suggests that astrocytic glucose uptake is coupled to neuronal activity, although the extent and physiological significance of astrocyte-to-neuron metabolic support remains debated (Dienel, 2017).

In the presynapse, ATP is used for the generation of action potentials, calcium clearance from the cytoplasm, neurotransmitter uptake, and the mobilization of mitochondria and vesicles (Attwell and Laughlin, 2001; Harris et al., 2012). In the postsynapse, ATP is primarily used to mediate synaptic currents. The vast majority of this ATP is produced by mitochondrial OXPHOS (Hall et al., 2012), and its production increases in response to synaptic activity, triggered by increasing levels of ADP and calcium (Rangaraju et al., 2014). To enable rapid adaptation of ATP levels, mitochondria formed in the cell soma are transported along microtubule tracks to axonal sites with high energy demand (Cai et al., 2011). Approximately two-thirds of axonal mitochondria are stationary, while one-third are bidirectionally mobile in response to local bioenergetic needs under various physiological and pathological conditions (Kang et al., 2008; Saxton and Hollenbeck, 2012). In neurons, mitochondria are enriched in areas with a particularly high energy demand, such as active synapses, growth cones and the nodes of Ranvier (Cai et al., 2011). Mitochondrial ATP is also critical for axonal mRNA translation (Spillane et al., 2013). Although direct evidence that synaptic energetics failure causes neuronal dysfunction and degeneration is lacking, several

findings support this possibility. For example, the acute loss of a mitochondrial protein in an *in vitro* model of the neurodegenerative Leigh syndrome leads to decreased ATP levels, which blocks synaptic vesicle endocytosis and impairs synaptic function (Pathak et al., 2015). Similarly, a loss-of-function mutation affecting mitochondrial distribution results in the absence of mitochondria at synapses and an inability to sustain neurotransmission during intense stimulation in the fruit fly, *Drosophila melanogaster* (Verstreken et al., 2005).

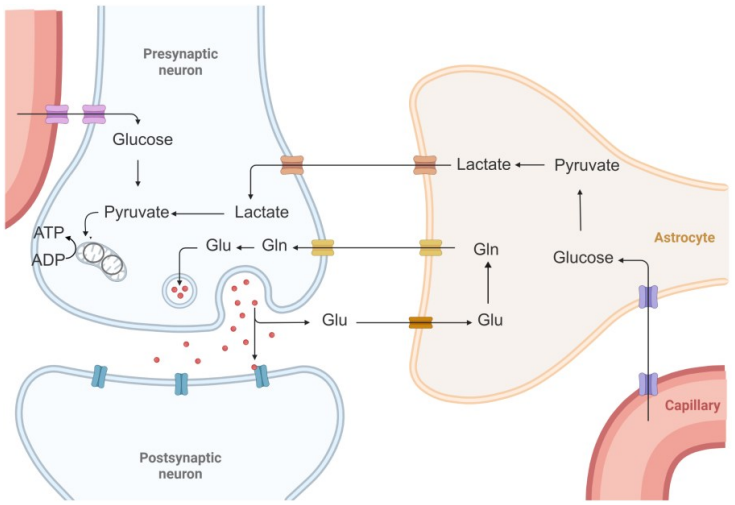

Figure 7 Neuron–astrocyte metabolic coupling at the synapse. The tripartite synapse illustrates the interplay between neurons and astrocytes in regulating synaptic energy metabolism and neurotransmitter recycling. Glucose is taken up from blood capillaries by neurons and astrocytes and metabolized to pyruvate. Pyruvate is converted to lactate in astrocytes, which is shuttled to neurons where it fuels mitochondrial ATP production via conversion back to pyruvate. Glutamate (Glu) released from presynaptic neurons during synaptic transmission is taken up by astrocytes and converted into glutamine (Gln), which is transported back to neurons and reconverted to glutamate for reuse in neurotransmission. This glutamate–glutamine cycle, together with the astrocyte-neuron lactate shuttle, supports both the energetic and functional demands of synaptic activity. Figure partly created using BioRender.com.

In mammalian cells, the anterograde transport of mitochondria, i.e. movement away from the cell soma, is driven by motor protein kinesin-1 adapters that interact with the mitochondrial outer membrane protein Mitochondrial Rho GTPase 1 (MIRO1) (Reis et al., 2009). Neuronal activity regulates movement and distribution, as local calcium concentrations induce mitochondrial arrest and retention at sites where calcium buffering and ATP production are needed (Yi et al., 2004; Maday et al., 2014). Interestingly, mitochondria have also been reported to

transfer between different cell types: for example, neurons have been shown to release damaged mitochondria for astrocytic degradation (Davis et al., 2014), and astrocytes have released functional mitochondria for neuronal uptake (Hayakawa et al., 2016; Liu et al., 2021).

2.2.3.2 Synaptic proteome turnover and remodeling

Neurons are post-mitotic cells, and therefore the turnover and remodeling of the synaptic proteome is a critical factor for their physiology and plasticity. Synaptic proteome turnover involves local protein synthesis, protein degradation, and antero- and retrograde protein transport between the soma and synapse (Garner and Mahler, 1987; Hanus and Schuman, 2013). In addition to these, post-translational modifications remodel the proteome in response to various signals (Tweedie-Cullen et al., 2009). The overall protein turnover rate appears to be positively correlated with plasticity-induced synaptic activity (Schanzenbächer et al., 2016; Dörrbaum et al., 2020; Jähne et al., 2021), and diverse strategies exist to regulate turnover and abundance: to elevate the abundance of a given protein, its synthesis can be elevated or its degradation can be suppressed, and to reduce the abundance of a particular protein, its synthesis can be suppressed or its degradation can be elevated. The regulation is different for different proteins.

Each synapse contains between one thousand and several thousand of different proteins, existing in copy numbers ranging from a few tens to over 20 000 (Sun and Schuman, 2022). The relative stoichiometry between these protein species contributes to synaptic diversity and function. Neuronal proteins generally exhibit longer half-lives than those in other cell types, with turnover rates ranging from less than one day to more than twenty days (Karunadharma et al., 2015; Dörrbaum et al., 2018). Median protein half-lives have been estimated at approximately 5.4 days *in vitro* (Dörrbaum et al., 2018) and around 8 days *in vivo* (Fornasiero et al., 2018). The half-life is widely affected by protein type, function, and subcellular localization, but also by age of subject, and diet regimen: for example, postsynaptic receptor and membrane proteins have significantly shorter half-lives than synaptic vesicle, ribosomal, or mitochondrial proteins (Dörrbaum et al., 2018), and proteins of the electron transport chain exhibit significantly longer half-lives in old than in young mice (Karunadharma et al., 2015). Synaptic activity accelerates turnover (Soykan et al., 2021), and degradation pathways differ between cytosolic and membrane-bound proteins (Zhao et al., 2022). Interacting proteins and proteins of the same multi-protein complexes often exhibit similar half-lives, suggesting coordinated turnover of protein complexes (Price et al., 2010; Cohen et al., 2013; Fornasiero et al., 2018).

Synaptic development, maintenance, and plasticity rely on the long-distance transport of various cargoes that are synthetized in the cell body and delivered to

distal regions (Maday et al., 2014). While the prevailing hypothesis suggests that protein and organelle degradation and recycling primarily occur in the soma (Cai et al., 2011; Maday et al., 2014), a competing view proposes that significant degradation also takes place in axons and synapses (Ashrafi et al., 2014). Biochemical and functional studies indicate that the motor proteins kinesin-1, dynein, and myosin are the primary mediators of anterograde and retrograde transport (Maday et al., 2014). These and several scaffolding adaptor proteins mediate transport through repeated cycles of ATP hydrolysis, cytoskeletal filament binding, and conformational changes that move cargoes along tracks formed by microtubules and actin filaments (Guedes-Dias and Holzbaur, 2019).

Cargo properties influence transport mechanisms: proteins with membrane-spanning or membrane-anchoring domains are packed into vesicles and transported at higher velocity, whereas cytosolic proteins are presumably transported as spontaneously assembled multiprotein complexes at much slower rates (Scott et al., 2011; Roy, 2014). The exact mechanism underlying the slow transport remain unclear, largely due to the challenges of imaging soluble proteins, but current models suggest that these proteins hitchhike short distances on passing vesicles (Tang et al., 2012; Roy, 2014). Despite the inefficiency of the slower transport, the constant delivery of newly synthetized proteins seems to outweigh that of the fast transport and is thus critical for synaptic function and survival. Although the complete regulatory mechanisms of axonal transport, including cargo recognition, binding, and unloading, remain incompletely understood, both direct and indirect regulatory mechanisms have been identified. For example, synaptic activity (Hu et al., 2008) and changes in redox balance (Wilson and González-Billault, 2015) can directly affect cytoskeletal filaments, inducing structural rearrangements and post-translational modifications that influence motor protein binding and stability. Additionally, synaptic activity and elevated calcium levels recruit motile mitochondria to active synapses (Chen and Sheng, 2013).

Protein degradation is initiated in response to misfolded proteins, excessive protein production, and the presence of non-functional proteins (Soykan et al., 2021). Most short-lived and cytosolic proteins undergo targeted degradation via the ubiquitin-proteasome pathway, while endocytosed membrane proteins, proteins with longer half-lives, and aggregated proteins are degraded via lysosomes, either through the endolysosomal degradation pathway or the autophagy-lysosome pathway (Fuertes et al., 2003; Paudel et al., 2023). The contribution of the different pathways in protein degradation is not known, but the ubiquitin-proteasome pathway is estimated to account for more than 70% of protein degradation in mammalian cells (Sha et al., 2018). The majority of mitochondrial protein turnover is mediated by proteases: the cytosolic ubiquitin-proteasome system degrades damaged or mislocalized proteins associated with mitochondria, while mitochondrial proteases eliminate damaged proteins within the organelle itself

(Quirós et al., 2015; Song et al., 2021). When damage is severe or prolonged, entire mitochondria can be removed via selective autophagy, a process known as mitophagy (Kim et al., 2007). Live-cell imaging in mouse primary neurons has shown that autophagosomes at various maturation stages transport both organelles and soluble cargoes, including mitochondria, that are targeted for degradation toward the soma, where they fuse with proteolytically active lysosomes, which are predominantly located in this region (Cai et al., 2011; Maday et al., 2012).

2.2.3.3 mRNA transport and local translation

Synaptic local translation is a conserved mechanism thought to have evolved to provide distal axons and dendrites with new proteins in a rapid timescale, enabling intracellular functions for development, synaptogenesis, plasticity, and survival. Initially, the low number of axonal mRNAs detected was thought to suggest that local translation played only a minor role in the synaptic proteome, but with the advancement of modern technologies and improved detection precision, this original hypothesis has been disproven. To date, approximately 2500 mRNA species have been identified in the dendrites and axons of hippocampal pyramidal neurons (Cajigas et al., 2012), and in a recent study, more than 800 of nearly 8000 mRNA transcripts showed significantly increased translation levels in rat hippocampal dendrites and axons compared to the soma (Glock et al., 2021), indicating that the predominant source of these proteins is local translation. In recent years, the process of local translation has been shown to be disturbed in several neurodegenerative disorders, demonstrating its relevance in neuronal physiology (Pushpalatha and Besse, 2019).

Local translation is carried out regularly both in the absence and in response to exogenous stimulation. It is not fully known which mRNA species are translated constitutively and which are translated on demand, but a recently published study examined local translation across different developmental stages in axons of mouse retinal cell ganglions and showed that over 25% of more than 2500 transcripts were actively translated at all developmental stages examined (Shigeoka et al., 2016). Several of these were synapse and axon-specific proteins. In addition to constitutive protein synthesis, two mechanisms have been identified to induce local translation: chemotropic signaling in development, and neurotrophic signaling in injury and regeneration (Zheng et al., 2001; Cioni et al., 2018). A single cue typically triggers the specific regulation of approximately 100 proteins in the axonal compartment, inducing distinct proteomic signatures (Cagnetta et al., 2018). Both development and injury shape the local proteome by inducing the translation of local transcripts, but they also initiate a slower response involving the nuclear transcription of genes. This nuclear response is induced by the local translation of a regulatory protein, cAMP-responsive element (CRE)-binding protein (CREB) in development (Cox et

al., 2008) and importin-beta in axonal injury (Hanz et al., 2003). The newly synthetized regulatory proteins form complexes with other proteins and are retrogradely transported to the nucleus, where they activate the transcription of a subset of genes, eliciting responses essential for neuronal survival (Cox et al., 2008; Rishal and Fainzilber, 2014).

Nuclear-encoded mRNAs are transcribed in the soma and transported to axons and dendrites, where local translation takes place (Holt et al., 2019). The mRNA remains in a translationally repressed state during transport, preventing unwanted protein expression at inappropriate locations and ensuring that the transcript maintains uncommitted to protein synthesis until translation is activated (Rodriguez et al., 2008). Specific trans-acting translational repressors bind to cis-regulatory elements within their target mRNAs, coordinating both mRNA localization and translational repression (Dictenberg et al., 2008). In neurons, two major forms of mRNA transport have been identified: 1) mRNAs repressed at the initiation step of translation, which are transported without large ribosomal subunits as mRNA transport particles, and 2) mRNAs repressed at the elongation step of translation, transported as stalled polysomes containing components of the translation machinery (Krichevsky and Kosik, 2001; Elvira et al., 2006; Sossin and DesGroseillers, 2006; Pushpalatha and Besse, 2019). These ribonucleoprotein (RNP) complexes are trafficked along cytoskeletal tracks via interactions with motors proteins (Pushpalatha and Besse, 2019). Recent findings have revealed that RNP complexes and ribosomes can also hitchhike bound to the membranes of rapidly moving organelles, such as lysosomes, and use them as a mobile platform for mRNA translation (Salogiannis and Reck-Peterson, 2017). Originally identified in filamentous fungi, this mechanism has since been observed in cultured primary cortical neurons from rat and in zebrafish axons (Liao et al., 2019).

The regulation of local translation is spatially and temporally dynamic and is often triggered by extracellular cues. Regulatory inputs include receptor-ribosome coupling, ribosome-binding proteins (RBP)-mRNA interactions, RNA modifications, ribosomal RNA and protein compositions, mitochondria, and cytoskeletal organization (Li et al., 2021). A recently proposed mechanism for local translation regulation involves the dynamic remodeling of ribosomes through the incorporation of locally synthesized ribosomal proteins (Shigeoka et al., 2016). Here, locally translated ribosomal proteins are incorporated into pre-existing ribosomes, repairing and modifying the ribosomal composition and generating specialized ribosomes for specific mRNA translation (Jung et al., 2014; Shigeoka et al., 2016). Inhibition of this local ribosomal protein translation reduces the local translation activity and disrupts axon branching *in vivo* (Shigeoka et al., 2016), implying that axonal protein translation modifies the local ribosomal function in axons.

A widely recognized model for recruiting mRNAs for translation is called the synaptic sushi belt (Doyle and Kiebler, 2011). In this model, nonspecific RNP species move bidirectionally in axons and dendrites and are selectively recruited to synapses for translation. While the mechanism of how elongating ribosomes on mRNA are reversibly stalled and unstalled is still unclear, analysis of stalled ribosomes has identified an enrichment of the fragile X mental retardation protein (FMRP). FMRP is a negative regulator of translation, loss-of-function of which causes over-abundance of certain proteins and the neurodevelopmental disorder fragile X syndrome (Garber et al., 2008; Anadolu et al., 2023).

2.2.3.4 Neuronal chemokines

Chemokines are small proteins originally identified in immune cells (Yoshimura et al., 1987) that induce a wide variety of cellular responses. Since their discovery in the late 1980s, several detailed studies have determined that chemokines have a neuromodulatory function in the brain, affecting all types of brain cells (Sowa and Tokarski, 2021), and playing a key role in physiological processes such as neurodevelopment and synaptic transmission (Rostène et al., 2007). Chemokines mediate chemotactic interactions primarily through paracrine signaling, where they bind to specific receptors on the surface of target cells and activate intracellular signaling pathways. These pathways are diverse and affect numerous biological processes, including cell migration, transcription, secretion, and apoptosis.

Studies on neuronal chemokines are limited. The first chemokine shown to be expressed in neurons was chemokine (C-X3-C motif) ligand 1 (CX3CL1), which is highly expressed in various regions of the brain (Harrison et al., 1998), and constitutively expressed in human, macaque, rat and mouse neurons *in vitro* and *in vivo* (de Haas et al., 2007). Hereafter, the neuronal expression of chemokine (C-C motif) ligand 2 (CCL2), CCL3, CCL4, C-X-C motif chemokine ligand 10 (CXCL10), CXCL12, and CXCL13 among others, have been described, mainly after insult, in post-mortem patient samples, and in animal and cellular models of neurodegenerative conditions (de Haas et al., 2007; Jiang et al., 2016). Neuronal chemokines appear to be expressed either constitutively, such as CX3CL1, CXCL12, and CCL2 (de Haas et al., 2007), or induced by inflammation and infection, such as CXCL8, CXCL9, CXCL10, CXCL11, and CXCL13 (Jiang et al., 2016; Watson et al., 2020). The subcellular localization of neuronal chemokines has not been extensively addressed, but both somal and synaptic location have been reported (Banisadr et al., 2005; Bhattacharyya et al., 2008; Callewaere et al., 2008; Dansereau et al., 2008; Van Steenwinckel et al., 2011). Vesicle-mediated transport of CCL21 into synapses has been demonstrated *in vitro* (de Jong et al., 2005), which has also been indicated for CCL2 (Van Steenwinckel et al., 2011). Several of the

neuronally expressed chemokines presented in this doctoral dissertation have other, more commonly known aliases, which are presented in **Table 1**.

Neuronal chemokine expression has been studied mainly under pathological conditions. Induced neuronal expression using inflammatory mediators is transient and detectable within a few hours of injury, in contrast to astrocytic chemokine expression, which appears only days later and persists for weeks (Wang et al., 1998; Che et al., 2001). *In vitro* studies have shown that neuronal chemokine expression is induced by different inflammatory mediators than glial chemokines, and that the total amount of chemokines secreted by neurons is lower than that of microglia or astrocytes (Ashutosh et al., 2011). Considering these, it seems that chemokines secreted by neurons and glial cells play different roles in the immunological signaling cascades of the central nervous system (Rostène et al., 2007; Sowa and Tokarski, 2021).

Table 1 Neuronally expressed chemokines and their aliases

Official name	Also known as
CCL2	Monocyte chemoattractant protein-1 (MCP-1)
CCL3	Macrophage inflammatory protein 1-alpha (MIP-1-alpha)
CCL4	Macrophage inflammatory protein 1-beta (MIP-1-beta)
CCL21	6Ckine; Exodus-2; Secondary lymphoid-tissue chemokine (SLC)
CXCL8	Interleukin-8
CXCL9	gamma-interferon-induced monokine; Monokine induced by interferon-gamma (HuMIG; MIG); Small-inducible cytokine B9
CXCL10	Interferon gamma-induced protein 10 (IP-10)
CXCL11	Interferon-inducible T-cell alpha chemoattractant (I-TAC); Interferon-gamma-inducible protein 9 (IP-9)
CXCL12	Stromal cell-derived factor 1 (SDF-1)
CXCL13	B lymphocyte chemoattractant (BLC); B cell-attracting chemokine 1 (BCA-1)
CX3CL1	Fractalkine

Information on chemokine aliases was compiled from Human Gene Nomenclature Committee (HGNC), UniProt, and Zlotnik and Yoshie, 2012.

Astrocytes, microglia and neurons express chemokine receptors under physiological and pathological conditions *in vivo* and *in vitro*, and for inflammatory chemokines, receptor expression is maximal under disease peak (Watson et al., 2020). An *in vitro* interaction, in which chemokines secreted by damaged neurons bind to microglial chemokine receptors and induce their activation and migration,

has been experimentally demonstrated (Harrison et al., 1998). Whether neurons can induce such response *in vivo* is not known. Chemokine-mediated neuron-glia interactions in the progression of neuronal disorders have been studied: the CX3CL1 - C-X-3-C motif chemokine receptor 1 (CX3CR1) axis in many common neurodegenerative disorders (Luo et al., 2019; Subbarayan et al., 2022) and the CXCL13 - C-X-C motif chemokine receptor 5 (CXCR5) axis in amyotrophic lateral sclerosis (ALS) (Jiang et al., 2016). These interactions are of particular interest as activated microglia migrate, proliferate, secrete inflammatory and neurotrophic factors, phagocytose damaged cells and present antigens (Town et al., 2005), which are important factors in the progression of a variety of disorders.

2.2.4 Modeling synapses in experimental research

2.2.4.1 Isolation of synaptosomes

Synaptic fractions can be enriched and isolated from homogenized brain tissue. These so called *synaptosomes* are functional nerve terminals that contain pre- and postsynaptic elements and can be used for structural, biochemical, metabolic, and pharmacological studies. The enrichment of synaptic fractions was first reported in the late 1950s (Hebb and Whittaker, 1958), and the basis of the preparation protocol has remained: fresh brain tissue is gently homogenized in an ion-free, iso-osmotic buffer with a glass-Teflon homogenizer that pinches off nerve terminals. These spontaneously reseal to form synaptosomes. A crude enrichment is achieved by low-speed centrifugation of the homogenate to pellet debris, and high-speed centrifugation of the supernatant to yield a microsomal P2 pellet. This fraction can be further purified using sucrose-density gradient centrifugation or fractionated into further subcellular particles such as synaptic vesicles and the postsynaptic density (**Figure 8**). Several variations to the original fractionation protocol have been published, some of which aim to improve sample purity or isolate specific synaptosomal subpopulations (Docherty et al., 1987; Bradford et al., 1989; Wolf and Kapatos, 1989; Gylys et al., 2000), while others modify the protocol to meet the physiological requirements for follow-up studies (Dunkley et al., 2008). Methods used for these include immunoaffinity and fluorescence-activated cell sorting (FACS) for isolations of synaptosomal subpopulations, and Percoll-density gradient centrifugation for modification of the protocol.

Electron microscopic observations have confirmed that isolated synaptosomes resemble the synaptic structures in tissue (Dodd et al., 1981). Each synaptosome is 0.5-1.0 μm in diameter and contains tens to hundreds of synaptic vesicles and usually one or several mitochondria. The synaptosome is often attached to the postsynaptic density, presumably due to trans-synaptic protein complexes connecting the pre- and postsynapse. Quantitative electron microscope

examination of synaptosome preparations has shown that synaptosomes make up approximately half of the visible structures, myelin about 3%, and free mitochondria 1% (Dodd et al., 1981). A majority of the remaining structures are unidentified and are most likely of glial origin. This has also been demonstrated by proteomic analyses of synaptosomes, where the identified proteins cover a wide range of pre- and postsynaptic proteins, but also known glial proteins indicating glial contamination (Schrimpf et al., 2005). These include astrocytic glutamate transporter 1 (GLT1), microglial ionized calcium binding adapter molecule 1 (IBA1), and myelin proteolipid protein (PLP) representing myelin (Pines et al., 1992; Imai et al., 1996; Greer and Lees, 2002).

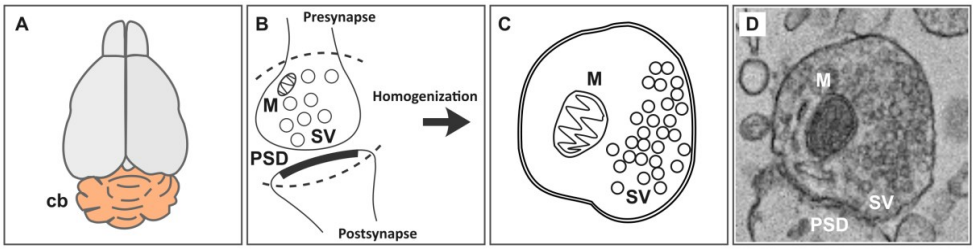

Figure 8 Preparation and content of synaptosomes. (A) Schematic representation of a mouse brain used as starting material for synaptosomes. The cerebellum (cb) is highlighted in orange color. (B) Schematic representation of a synapse with indication of where the pre- and postsynaptic terminals are pinched off following homogenization (dotted lines) forming a synaptosome. Circles within the presynapse indicate synaptic vesicles (SV) and the oval shape with a zigzag inside indicate a mitochondrion (M). The thick rim within the postsynapse indicate the postsynaptic density (PSD). (C) Schematic representation of a mouse cerebellar synaptosome, illustrating the presynaptic features in B. (D) Electron micrograph of a mouse brain synaptosome, illustrating the pre- and postsynaptic features in B. Electron micrograph image by Christopher Jackson, University of Helsinki.

2.2.4.2 Mass-spectrometry based synaptosome proteomics

Mass spectrometry-based synaptosome proteomics offers a powerful tool for profiling the global landscape of synaptic proteins, making it particularly useful for investigating physiological or pathological conditions in experimental models. However, studying synapses poses challenges due to the regional specificities of both brain and neurons: whole-brain tissue preparations consist of diverse cell types, and are thus unspecific for synaptic proteins, whereas synaptosome preparations are enriched for synaptic proteins but contain different neuronal subtypes (Bai and Witzmann, 2007). As a result, synaptosomal proteomics typically reflect an average protein composition, which complicates data interpretation. This is particularly relevant when studying biological mechanisms or specific signaling pathways.

Various proteomics techniques offer different protein enrichment and resolution strategies (Chandramouli and Qian, 2009), but each has specific advantages and limitations. All proteomic techniques have an intrinsic bias towards detecting a certain subset of proteins. For example, standard mass spectrometry-based approaches tend to preferentially detect the most abundant proteins, even though biological samples like synaptosomes contain thousands of proteins expressed at a wide range of copy numbers. Consequently, a single approach is insufficient for comprehensive proteome coverage. Instead, complementary proteomic techniques are often required a achieve a more complete picture (Wu et al., 2006).

Over the past decade, significant advantages in mass spectrometry technologies and bioinformatic tools have expanded the analytical capabilities of proteomics, establishing it as a central approach for generating biological insights in the life sciences (Aebersold and Mann, 2016). Liquid chromatography coupled to tandem mass spectrometry (LC-MS/MS) is a commonly used method for protein identification and quantification (Aebersold and Mann, 2003). In a method called shotgun proteomics, one of the most comprehensive methods, proteins are enzymatically digested into peptides, separated via liquid chromatography, ionized, and analysed in a mass spectrometer. The process involves a survey scan (MS1) to detect ionized peptides, followed by generation of a fragment ion spectra (MS2) to identify peptide sequences based on their mass-to-charge (m/z) ratios (Domon and Aebersold, 2006). These peptide spectra are then matched to reference databases to infer the parent proteins.

Despite technological advances, challenges remain. One major limitation is the poor solubility and digestibility of hydrophobic and membrane-bound proteins, which are key components of synapses (Plum et al., 2015). These proteins are often poorly digested by standard proteases such as trypsin and are difficult to separate using techniques like isoelectric focusing. Improving digestion efficiency may require additional treatments, such as formic acid or heat, to reduce protein hydrophobicity and facilitate enzymatic cleavage (Lee et al., 2011).

The advances in isolation techniques and mass spectrometry sensitivity are reflected in studies of the synaptic proteome. For example, a recent study using microdissection and fluorescence activated synaptosome sorting (FASS) analyzed five brain regions and defined 18 neuronal synapse types based on distinct synaptic protein abundance profiles (Van Oostrum et al., 2023). Interestingly, synapse diversity was explained by neuronal subtype but not the brain region. Earlier proteomic analyses of immunoisolated neurotransmitter-specific synaptic vesicles revealed only little difference in their biochemical composition (Grønborg et al., 2010). Together these data suggest that functional differences between synapses of different neuron types are not determined solely by neurotransmitter specificity but

also on physiological properties such as protein copy number, post-translational modifications, and protein interactions (O'Rourke et al., 2012).

Post-translational modifications have emerged as a critical player of synaptic regulation, influencing nearly all aspects of synaptic function, including neurotransmitter release, synaptic vesicle recycling, ion channel activity, and local protein translation (Rizzoli, 2014; Vallejo et al., 2017; Dalla Costa et al., 2021; Corti and Duarte, 2023). Mass spectrometry-based proteomics has also been successfully applied to characterize changes in the synaptic proteome in a variety of experimental models of neurological conditions. For example, synaptosome proteomics has revealed molecular alterations in spinal cord ganglia after spinal nerve injury and in a rat model of antipsychotic resistance (Bai and Witzmann, 2007; Ji et al., 2009; Singh et al., 2009).

2.3 MYOCLONIC EPILEPSY OF UNVERRICHT AND LUNDBORG

Myoclonic epilepsy of Unverricht and Lundborg (OMIM: 254800) is the single most common type of progressive myoclonus epilepsies, a group of inherited, clinically and etiologically heterogeneous disorders manifesting with myoclonus, epilepsy, and progressive neurological deterioration (Classification of progressive myoclonus epilepsies and related disorders. Marseille Consensus Group, 1990). The disease was initially described by Heinrich Unverricht (1853-1912) and Herman Lundborg (1868-1943) and over the years it became known as Unverricht-Lundborg disease. Today, the established abbreviations are ULD and EPM1, the latter of which is used in this doctoral dissertation.

2.3.1 Clinical presentation

EPM1 is characterized by symptoms affecting movement and motor coordination. Onset is between six and fifteen years of age and the first symptoms are involuntary muscle twitches (myoclonus) and generalized tonic-clonic epileptic seizures (Lehesjoki and Kälviäinen, 2020). Epilepsy can usually be treated with appropriate antiepileptic drugs, but myoclonus is both treatment-resistant and sensitive to stimuli, which makes the lives of the patients' considerable difficult. Myoclonic jerks are induced by voluntary movements or sensory stimuli such as light, touch or sound, and they mainly affect the proximal muscles of the body. During the first 5-10 years, myoclonus becomes more severe, and the patients' clinical condition deteriorates before disease progression stabilizes. A few years after the onset, patients develop additional symptoms including dysarthria, intention tremor, and incoordination.

The severity of EPM1 varies: some patients are able to walk, while others are severely disabled and wheelchair bound. Intellectual performance is usually preserved or slightly declined, but depression, anxiety and emotional lability is common. For this reason, patients need continuous psychological and rehabilitative support throughout their lives. Nowadays, the life expectancy of EPM1 patients has improved and is comparable to that of the general population until approximately 40 years of age, after which it begins to decline (Sipilä et al., 2020).

2.3.2 Neuroimaging and neurophysiology

Brain structure and connectivity in different stages of EPM1 have been studied using imaging techniques such as magnetic resonance imaging (MRI), functional MRI (fMRI) and a combination of MRI-navigated transcranial magnetic stimulation and electroencephalography (TMS-EEG). These studies have shown that the reduction in brain volume is progressive and particularly affects the motor, sensory and somatosensory areas of the cerebral cortex as well as the brainstem, cerebellum, basal ganglia and thalamus (Mascalchi et al., 2002; Koskenkorva et al., 2009, 2012; Manninen et al., 2013). The results also show that cortical thinning correlates with both myoclonus severity and disease progression but is not observed at the time of diagnosis. TMS-EEG has shown that reactivity to physiological stimuli is altered in the primary motor cortex of EPM1 patients, showing increased excitability, reduced inhibition, and impaired coherence (Danner et al., 2009; Julkunen et al., 2013). Older EEG studies have reported abnormalities such as photosensitivity, spike-wave discharges, and polyspike discharges during rapid eye movement (REM) sleep (Koskiniemi et al., 1974b; Franceschetti et al., 1993). These are more pronounced during the initial stages of the disease and reduce in parallel with the epileptic seizures (Ferlazzo et al., 2007), as does the background activity, which varies from normal to mildly slowed at the beginning of the disease and stabilizes over time (Ferlazzo et al., 2007). Taken together, the clinical presentation, neurophysiological assessment, and pharmacological response to drugs in EPM1 patients suggest that the myoclonus and motor disturbances are of cortical or subcortical origin (Kälviäinen et al., 2008).

A limited number of studies on neurotransmitter homeostasis and metabolism in EPM1 have been conducted, focusing mainly on the GABAergic and dopaminergic systems. Impairment of GABAergic signaling has been indicated by immunostainings, where cortical synapses from a deceased EPM1 patient showed reduced immunopositivity for the vesicular GABA transporter (VGAT) protein, a marker of the inhibitory GABAergic system (Buzzi et al., 2012), and by TMS-induced short-term intracortical inhibition (SICI), which was reduced in 21 EPM1 patients compared to controls (Silvennoinen et al., 2023). Also, in the 1980s, before molecular diagnostics for EPM1 was available, fifteen clinically diagnosed EPM1

patients were found to have reduced GABA concentrations in the cerebrospinal fluid (Airaksinen and Leino, 1982). Dopamine metabolism was studied in four EPM1 patients using [11C]-raclopride positron emission tomography (PET), showing higher D2 receptor availability in the striatum of the basal ganglia and thalamus (Korja et al., 2007). Together with the studies assessing brain connectivity, these results suggest that the underlying defects in the brains of EPM1 patients could arise from pathological changes at the neurotransmitter level.

2.3.3 Neuropathology

Neuropathological examinations have identified a variety of changes in the brains of EPM1 patients, including grey and white matter degeneration (Haltia et al., 1969; Koskiniemi et al., 1974a; Eldridge et al., 1983; Cohen et al., 2011). Post-mortem examinations are scarce, and the reported findings are often heterogeneous and based on observations from single patients. In addition, several autopsy reports originate from patients who have used the anti-epileptic drug phenytoin (Haltia et al., 1969; Koskiniemi et al., 1974a), which has been found to aggravate the neurological symptoms and accelerate the cerebellar atrophy in EPM1 patients (Eldridge et al., 1983). However, the main findings are consistent: reduced thickness of the motor cortex and neuron loss in the cerebral cortex, striatum, thalamus and brainstem, as well as loss of cerebellar granule neurons and Purkinje cells, and changes in the motor neurons of the spinal cord. No systematic evidence of accumulated storage material has been observed.

2.3.4 Molecular genetics of EPM1

EPM1 is an autosomal recessively inherited disorder that is caused by biallelic pathogenic variants of the cystatin B (*CSTB*) gene (OMIM: 601145; HGNC:2482). To date, a total of sixteen pathogenic or likely pathogenic disease-associated variants have been described in literature (**Table 2**).

The most commonly observed pathogenic variant is an expansion of a dodecamer repeat sequence (5'-CCCCGCCCCGCG-3') located in the promoter region of the *CSTB* gene (Kälviäinen et al., 2008). This expansion results in significantly reduced expression of the *CSTB* gene and protein (Joensuu et al., 2007). Healthy individuals have 2-3 copies of the dodecamer repeat, whereas more than 30 copies are associated with EPM1 (Lalioti et al., 1997). Evidence suggests that the number of repeats correlates with the age of disease onset, although it shows only modulating effects on symptom severity (Hypponen et al., 2015). Experimental studies using blood leukocytes, derived from EPM1 patients homozygous for the repeat expansion variant, have demonstrated a reduction in *CSTB* mRNA and protein expression to less than 10% of that in control subjects

(Joensuu et al., 2007). The mechanism by which the dodecamer expansion suppresses *CSTB* expression remains unknown, but several hypotheses have been proposed, including unstable promoter activity (Lalioti et al., 1999; Alakurtti et al., 2000), DNA hypermethylation (Lalioti et al., 1997), and altered spacing between regulatory elements and the transcription start site (Lalioti et al., 1999). In lymphoblastoid cells from EPM1 patients, reduced CSTB expression and the consequent decreased inhibitory activity leads to increased activity of its target proteases, cathepsins B, L, and S (Rinne et al., 2002).

Other pathogenic *CSTB* variants include small base substitutions, and insertions or deletions within the coding region, resulting in amino acid alterations, premature termination of protein translation, or altered splicing (**Table 2**). The missense variants are predicted to alter protein folding, leading to loss of protein interaction sites, whereas truncating and spicing variants are predicted to cause significantly reduced or absent (null allele) *CSTB* expression. Nearly all genetically confirmed EPM1 patients are either homozygous for the dodecamer repeat expansion or compound heterozygous, carrying one expansion allele in combination with another pathogenic *CSTB* variant.

Individuals who are compound heterozygous for the repeat expansion and another pathogenic *CSTB* allele typically develop a more severe clinical phenotype of EPM1, with earlier age of onset, more severe myoclonus, and poorer cognitive performance (Koskenkorva et al., 2011; Canafoglia et al., 2012; Assenza et al., 2017). To date, nine individuals, including three sibling pairs, have been reported with truncating variants in both *CSTB* alleles. These patients exhibit a clinically distinct neurodevelopmental disorder with significantly more severe clinical and neuropathological features than in EPM1 (Mancini et al., 2016; O'Brien et al., 2017; Abdel-Hamid et al., 2025). Reported clinical findings include neonatal onset of symptoms, profound developmental delay, microcephaly, dysmorphic facial features, and dyskinesia, with brain MRI revealing progressive cerebral atrophy and disturbances in myelination.

Table 2 Disease-causing *CSTB* variants

Variant	Effect	References
Dodecamer repeat expansion (5'-CCCCGCCCCGCG-3')	Reduced expression	Lafrenière et al., 1997; Lalioti et al., 1997a; Virtaneva et al., 1997
c.10G>C p.(Gly4Arg)	Missense	Lalioti et al., 1997b; Abdel-Hamid et al., 2025
c.66G>A p.(Gln22=)	Altered splicing	Pinto et al., 2012
c.67-1G>C	Altered splicing	Pennacchio et al., 1996; Lafrenière et al., 1997; Lalioti et al., 1997b; Canafoglia et al. 2012; Abdel-Hamid et al., 2025
c.125C>A[1] p.(Ser42*)	Null variant (nonsense)	Erdinç et al., 2010
c.132-134del p.(Lys44_Ser45delinsAsn)	In-frame variant changes length of protein coding region	Assenza et al., 2017
c.136C>T p.(Gln46*)	Null variant (nonsense)	Canafoglia et al., 2012 (erratum: Canafoglia et al., 2013)
c.149G>A p.(Gly50Glu)	Missense	Joensuu et al., 2007
c.168G>A p.(Lys56=)	Predicted to alter splicing	Kagitani-Shimono et al., 2002
c.168+1_18del	Altered splicing	Joensuu et al., 2007
c.168+2_168+21delinsAA	Altered splicing	Canafoglia et al., 2012 (erratum: Canafoglia et al.,2013)
c.169-2A>G	Predicted to alter splicing	Lalioti et al., 1997b
c.202C>T p.(Arg68*)	Null variant (nonsense)	Pennacchio et al., 1996; Lafrenière et al., 1997; Mancini et al., 2017; Abdel-Hamid et al., 2025
c.212A>C p.(Gln71Pro)	Missense	de Haan et al., 2004
c.218dupT p.(His75Serfs*2)	Null variant (frameshift)	O'Brien et al., 2017; Abdel-Hamid et al., 2025
c.218_219delTC p.(Leu73Profs*3)	Null variant (frameshift)	Bespalova et al., 1997b; Lafrenière et al., 1997; Lalioti et al., 1997b

[1] The patient also carried a c.121C>A missense variant in the same allele, but premature stop of *CSTB* cDNA suggested that the c.125C>A variant is disease-causing.
* Premature stop

2.4 CYSTATIN B

2.4.1 Biochemical and cellular functions

CSTB, also known as stefin B, is an evolutionary conserved intracellular inhibitor of thiol proteases, including cysteine cathepsins (Green et al., 1984; Turk and Bode, 1991). CSTB belongs to the cystatin superfamily, which consists of intracellular type 1 cystatins (cystatins A and B), secreted type 2 cystatins (cystatins C, D, E/M, F, S, SA, SN) and intravascular type 3 cystatins.

The *CSTB* transcript is translated into a small protein consisting of 98 amino acids and a molecular mass of approximately 11 kDa (Järvinen and Rinne, 1982). The CSTB protein has a neutral pH optimum and several isoelectric variants. Conformational changes, including S-glutathionylation, dimerization, and oligomerization, are induced by post-translational modifications and prevent the inhibitory activity of CSTB (Green et al., 1984; Wakamatsu et al., 1984; Pol and Björk, 2003; Cabras et al., 2012). Overexpression causes the formation of oligomers and amyloid-like fibrils *in vivo* and *in vitro* (Zerovnik et al., 2002; Cipollini et al., 2008).

CSTB inhibits the proteolytic activity of cysteine cathepsins by tight and reversible binding (Turk and Bode, 1991). Biochemical experiments have shown that binding is strongest against cathepsins H, L and S and weaker against cathepsins B and C (Järvinen and Rinne, 1982; Green et al., 1984; Brömme et al., 1991). CSTB has also been suggested to form complexes and interact with structural proteins such as beta-spectrin and neurofilament light chain, scaffold and adapter proteins such as Receptor Protein Kinase C (RACK1) and myotubularin-related protein, and the antioxidant enzyme Superoxide dismutase 1 (SOD1) (Frappier et al., 1991; Macioce et al., 1999; Giaimo et al., 2002; Ulbrich et al., 2014).

The subcellular localization of CSTB is both cytoplasmic and nuclear, depending on the cellular differentiation status. In dividing and undifferentiated cells, CSTB localization is predominantly nuclear, where it likely participates in the regulation of gene expression by inhibiting nuclear cathepsin L-mediated histone tail proteolysis, and by interacting with histones (Riccio et al., 2001; Alakurtti et al., 2005; Ceru et al., 2010; Daura et al., 2021). In the cytoplasm, CSTB is diffusely distributed, although its association with lysosomes has been demonstrated (Alakurtti et al., 2005). It has been suggested to function as a gatekeeper, inhibiting the activity of leaking lysosomal cathepsins (Turk et al., 2002; Houseweart et al., 2003b). Upon induced inflammation, CSTB localization to mitochondria has been observed by immunofluorescence microscopy (Maher et al., 2014).

CSTB expression is ubiquitous among various tissues and cell types, but it is particularly high in immune cells such as blood leukocytes, placental macrophages, and hepatic lymphocytes (Davies and Barrett, 1984; Luciano-Montalvo et al.,

2008). In cultured primary cells of the mouse central nervous system, *CSTB* mRNA is highly expressed in microglial cells, in contrast to astrocytes and neurons, where its expression is significantly lower (Okuneva et al., 2015). *CSTB* expression is increased upon pro-inflammatory lipopolysaccharide (LPS) stimulation in microglia (Okuneva et al., 2015) and upon hydrogen peroxide-induced oxidative stress in neurons (Lehtinen et al., 2009). Its expression is also increased in several pathological conditions, including many cancer types, human immunodeficiency virus (HIV) infection, and status epilepticus (D'Amato et al., 2000; Rivera et al., 2014; Verbovšek et al., 2014; Takaya et al., 2015), and therefore its function has been implicated in cellular and biological processes such as immune function, apoptosis, and cell cycle progression. Although extensively studied, it is not known how partial loss of CSTB leads to the clinical and neuropathological phenotype of EPM1.

2.4.2 The *Cstb*-deficient mouse model

Shortly after the identification of the gene causing EPM1, a *Cstb* knock-out (*Cstb*$^{-/-}$) mouse model was generated by inserting a neomycin cassette into *Cstb* exon 1 (Pennacchio et al., 1998). This disrupts the reading frame and creates a nonsense codon, which at the translational level is predicted to lead to nonsense-mediated mRNA decay with no protein produced. The overall clinical phenotype of the *Cstb*$^{-/-}$ mouse resembles that of EPM1 patients, but is influenced by the genetic background of the mouse: mice with a pure 129Sv background develop the disease phenotype, in contrast to mice with a mixed C57BL/6 and 129Sv background, which have only a partial disease phenotype (Pennacchio et al., 1998). In this doctoral dissertation, *Cstb*$^{-/-}$ mice refer to mice with a pure 129Sv background.

2.4.2.1 Phenotype

Cstb$^{-/-}$ mice appear to be born healthy and develop normally until the prepubescent stage of adolescence at one month of age (Pennacchio et al., 1998). From here forward, mice start developing myoclonic seizures in their sleep and their coordination gradually deteriorates (**Figure 9**) (Pennacchio et al., 1998; Pollari et al., 2023). Unlike EPM1 patients, *Cstb*$^{-/-}$ mice do not exhibit photosensitivity or tonic-clonic seizures. From approximately six months forward, a severe condition affecting motoric tasks develops, formerly thought to be cerebellar ataxia (Pennacchio et al., 1998). However, recent detailed characterizations of the mouse phenotype have shown that this motor impairment is not ataxia, suggesting that the symptoms in EPM1 patients are due to advanced myoclonus (Pollari et al., 2023). In the original report describing the phenotype of the *Cstb*$^{-/-}$ mouse (Pennacchio et al., 1998), approximately one-third of adolescent mice were reported with increased

tearing of the eyes that developed into inflammatory corneal opacification. This phenotype has not been reported in EPM1 patients and has only been observed sporadically in the Helsinki-colony of *Cstb*$^{-/-}$ mice (unpublished observations). Heterozygous *Cstb*$^{+/-}$ mice do not develop symptoms, although reports of mild ataxia at older ages and myoclonus upon handling have been presented (Kaasik et al., 2007).

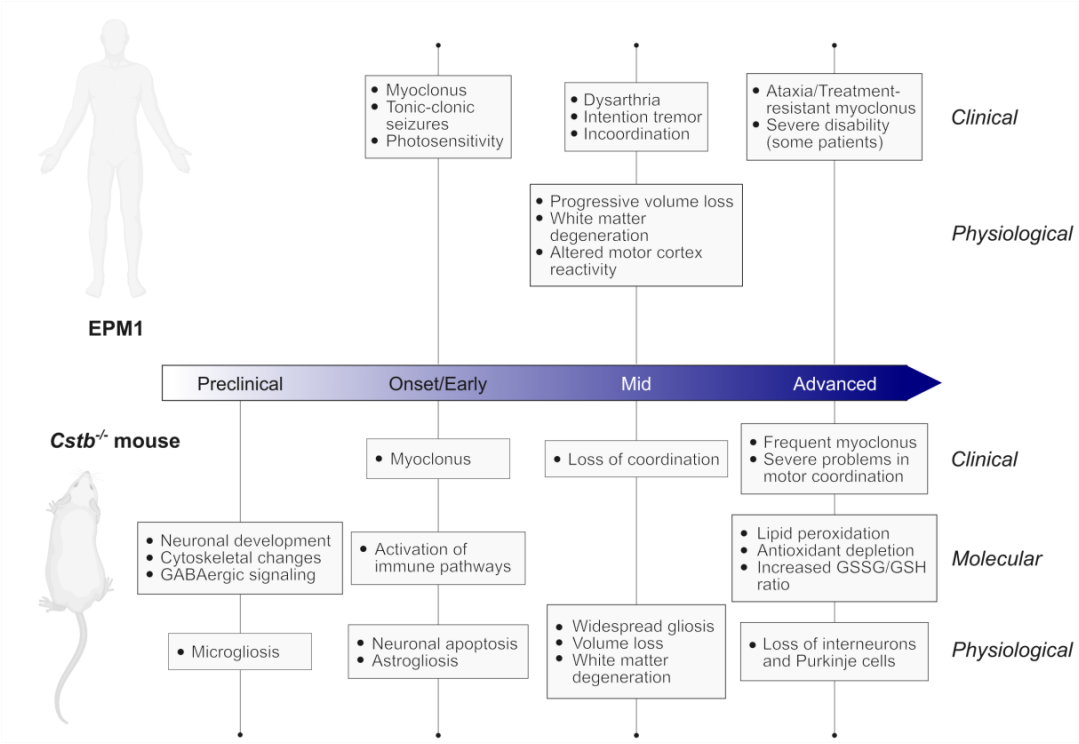

Figure 9 Timeline of clinical, molecular, and physiological findings in EPM1 patients and *Cstb*$^{-/-}$ mice. The figure illustrates the progression of Unverricht-Lundborg disease (EPM1) across distinct stages: preclinical, onset/early, mid-stage, and advanced, highlighting key clinical symptoms and physiological alterations observed in EPM1 patients, as well as presents clinical, molecular, and physiological findings in the *Cstb*$^{-/-}$ mouse model. Findings demonstrate parallels in disease trajectory and support the mouse model's relevance for studying EPM1 pathophysiology. GABA=gamma-aminobutyric acid; GSSG=glutathione disulphide; GSH=glutathione.

2.4.2.1 Pathological findings in the brain and other organs

The first neuropathological signs in the brains of *Cstb*$^{-/-}$ mice are observed already before the appearance of clinical symptoms, as microglial activation is detected in distinct brain areas from two weeks of age onwards (Tegelberg et al., 2012). This is followed by astrocyte activation and neuroinflammation with increased expression of pro-inflammatory markers, and a drastic and progressive apoptotic loss of

cerebellar granule neurons beginning at one month of age, coinciding with the onset of myoclonus (Pennacchio et al., 1998; Tegelberg et al., 2012; Okuneva et al., 2015). Peripheral inflammation, with higher concentrations of pro-inflammatory cytokines and chemokines, is detected in blood serum shortly after (Okuneva et al., 2016).

The majority of the morphological observations in *Cstb*$^{-/-}$ mice brains have been performed by neuropathological or neuroimaging studies in older animals with an advanced disease. In these mice, progressive and widespread gliosis and atrophy have been observed in histopathological analyses from two months onwards, particularly in the cerebellum, hippocampus, entorhinal cortex and somatosensory thalamocortical areas that mediate motor and sensory information (Pennacchio et al., 1998; Shannon et al., 2002; Franceschetti et al., 2007; Tegelberg et al., 2012). Longitudinal *in vivo* MRI volumetry and *ex vivo* diffusion tensor imaging in one to six months-old mice have shown early and progressive signs of white matter atrophy in all major tracts of the brain (Manninen et al., 2014), presumably due to local axonal degeneration (Manninen et al., 2013).

The cerebellum is the most affected brain region in *Cstb*$^{-/-}$ mice, although its pathology is not notably observed in examinations of EPM1-patients (Koskenkorva et al., 2009). Starting at two months of age, there is a widespread and progressive reduction in cerebellar volume, affecting all cerebellar layers (Tegelberg et al., 2012). At the age of six months, the cerebellum of *Cstb*$^{-/-}$ mice is reduced in size by nearly half. Hallmarks of oxidative damage, including lipid peroxidation, depleted antioxidant levels, and an increased ratio of oxidized to reduced glutathione, are also evident in the cerebellum (Lehtinen et al., 2009). Whether these signs of oxidative damage are a downstream consequence of neurodegeneration or if they play a causal role in the pathogenesis of the disease is not known. As the disease and its neuropathology progresses, the loss of inhibitory interneurons and Purkinje cells becomes apparent (Shannon et al., 2002), which is not observed in younger (≤6 months) animals.

2.4.3 Other CSTB-deficient models in EPM1 research

In addition to the *Cstb*$^{-/-}$ mouse, also other experimental models have been generated for EPM1 research. During the past years, several research groups have reported the generation of induced pluripotent stem cells (iPSCs) from EPM1 patient cells (Di Matteo et al., 2020; Lucchino et al., 2022; Singh et al., 2023; Tegelberg, manuscript in preparation). These have also been further differentiated into human cerebral organoids (hCOs) (Penna et al., 2019; Di Matteo et al., 2020; Pizzella et al., 2023). Animal models have included mice in which null mutations and overexpression of CSTB have been induced by *in utero* plasmid electroporation (Di Matteo et al., 2020) and mice with trisomy of the *Cstb* gene (Brault et al., 2011;

Trstenjak-Prebanda et al., 2023). Cell models have mainly been derived from the *Cstb*$^{-/-}$ mouse and include cultured neural stem and progenitor cells (NPCs) (Daura et al., 2021, 2022), primary neurons (Lehtinen et al., 2009; Joensuu et al., 2014), microglia (Okuneva et al., 2015; Korber et al., 2016), astrocytes (Polajnar et al., 2014), and bone marrow-derived macrophages (BMDMs) (Maher et al., 2014; Trstenjak Prebanda et al., 2019; Trstenjak-Prebanda et al., 2023). Findings from these experimental models are broadly consistent with previously reported disease processes in the *Cstb*$^{-/-}$ mouse but have provided more detailed insights about the underlying mechanisms.

2.4.4 Pathophysiological findings of CSTB-deficiency at the cellular and molecular level

In cell and organoid models of embryonic and early brain development, CSTB-deficiency manifests as altered neurogenesis and mitochondrial respiration in neural progenitor cells from *Cstb*$^{-/-}$ mice (Daura et al., 2021) and altered interneuron migration, neuronal morphology, and synaptic physiology in human cerebral organoids (Penna et al., 2019; Di Matteo et al., 2020; Pizzella et al., 2023). In cells from postnatal *Cstb*$^{-/-}$ mouse brain, alterations in GABAergic signaling are observed prior to EPM1-symptom onset in the expression levels of genes and proteins and in the electrophysiological properties of Purkinje cells (Joensuu et al., 2014). Signs of pathological neuroinflammation are observed in several cell models: cultured microglia from *Cstb*$^{-/-}$ mice display widespread alterations in inflammatory signaling (Korber et al., 2016), which is also detected in inflammasomes from CSTB-deficient bone marrow-derived macrophages that are more susceptible to activation (Maher et al., 2014; Trstenjak-Prebanda et al., 2023). Impaired phagocytic capacity has been reported in microglia from *Cstb*$^{-/-}$ mice (Sierra-Torre et al., 2020). The protective role of CSTB in oxidative stress has been implied both in neurons (Lehtinen et al., 2009) and macrophages (Trstenjak Prebanda et al., 2019; Trstenjak-Prebanda et al., 2023).

3 AIMS OF THE STUDY

The general aim of this doctoral dissertation was to get insight into the synaptic physiology in the cerebellum of *Cstb*$^{-/-}$ mice modeling EPM1 using omics approaches, and to understand the early molecular pathology of EPM1 disease onset.

The specific aims were as follows:

1. To identify key mechanisms affecting synaptic pathophysiology and symptom onset in the presymptomatic and early symptomatic *Cstb*$^{-/-}$ mouse.

2. To determine the role of the GABAergic signaling pathway in disease onset and early progression in presymptomatic and early symptomatic *Cstb*$^{-/-}$ mice.

3. To evaluate the functional and structural properties of synaptic mitochondria in the *Cstb*$^{-/-}$ mouse during disease onset and early progression.

4 MATERIALS AND METHODS

4.1 MATERIALS

4.1.1 Ethics statement (I, II, unpublished)

All the animal work presented in this doctoral dissertation was approved by the Animal Ethics Committee of the State Provincial Office of Southern Finland and carried out under the following project licenses: ESAVI/10765/2015 and ESAVI/471/2019. The experiments were performed in accordance with good practice for the handling of laboratory animals.

4.1.2 Animal model (I, II, unpublished)

4.1.2.1 The *Cstb*$^{-/-}$ mouse

The *Cstb*$^{-/-}$ mouse model was generated by targeted disruption of exon 1 of the mouse cystatin B gene (Pennacchio et al., 1998). The mouse strain was obtained from the Jackson Laboratory (Bar Harbor, ME; 129-*Cstb*^{tm1Rm}/SvJ; stock #003486). To maintain the *Cstb*$^{-/-}$ mouse line and expand the colony from heterozygous littermates, heterozygous *Cstb*$^{+/-}$ males were backcrossed with inbred wild type females. The genetic background of the mouse colony was refreshed annually with wild type females, and F1-F3 generations were used for experimental procedures. Wild type mice of same genetic background were used as controls. Both male and female mice were used for the experimental procedures.

4.1.2.2 Housing and genotyping

All animals were housed under standard conditions applied by the University of Helsinki Laboratory Animal Center with ad libitum feeding and a 12 + 12 hour light/dark cycle.

DNA was extracted from mouse ear punches using the DNeasy Blood & Tissue Kit (Qiagen, Venlo, Netherlands) according to the manufacturer's instructions and

genotyped for the *Cstb* gene by polymerase chain reaction (PCR) and agarose gel electrophoresis. The primers for genotyping are listed in **Table 3**.

4.1.3 Primer sequences (I, II, unpublished)

Table 3 Primer sequences used in studies of this doctoral dissertation

Target	Primers	Used in
Cstb	F: 5'-TCCGTGCTACCCCGACTACTG-3' R: 5'-GCTCAGACTGGCCTGACCT-3'	I, II, unpublished
Mt-Rnr1	F: 5′-AGGAGCCTGTTCTATAATCGATAAA-3′ R: 5′-GATGGCGGTATATAGGCTGAA-3′	II

F=forward; R=reverse

4.1.4 Antibodies (I, II)

Table 4 Antibodies used in studies of this doctoral dissertation

Target	Host species	Cat no	Supplier	RRID	Clonality	Used in
ATPB	rabbit	17247-1-AP	Proteintech	AB_2061878	polyclonal	II
CDK-5	mouse	05-364	Upstate	AB_11213993	monoclonal	I, II
HDAC2	mouse	05-814	Millipore	AB_310022	monoclonal	I, II
mtCO1	mouse	ab14705	Abcam	AB_2084810	monoclonal	II
OPA1	mouse	612606	BD Biosciences	AB_399888	monoclonal	II
PSD-95	mouse	610495	Transduction Laboratories	AB_397861	monoclonal	I, II
SDHA	mouse	ab14715	Abcam	AB_301433	monoclonal	II
SYP	mouse	M0776	DAKO	AB_2199013	monoclonal	I, II
TOM20	rabbit	11802-1-AP	Proteintech	AB_2207530	polyclonal	II
Tom40	rabbit	sc-11414	Santa Cruz	AB_793274	polyclonal	II
VDAC1	mouse	ab14734	Abcam	AB_443084	monoclonal	II
Vinculin	rabbit	ab129002	Abcam	AB_11144129	monoclonal	II
beta-tubulin	mouse	T4026	Sigma	AB_477577	monoclonal	I, II

4.2 METHODS

The methods used in this doctoral dissertation are presented in detail in the original publications (I-II) and summarized in **Table 5**. In addition, unpublished details are presented below.

Table 5 Methods used in studies of this doctoral dissertation

Method	Used in
Synaptosome isolation	I, II, unpublished
Liquid chromatography-tandem mass spectrometry (LC-MS/MS)	I, II
Analysis of omics data (proteomics/transcriptomics)	I, II, unpublished
Electrophysiological recordings	I
High-resolution respirometry	II
Protein extraction	I, II
Immunoblot analysis	I, II
Nucleic acid extraction (DNA/RNA)	I, II, unpublished
Mitochondrial DNA copy number determination	II
Electron microscopy	II
Statistical analyses	I, II
RNA sequencing	unpublished

4.2.1 Synaptosome isolation (I, II, unpublished)

Cerebellar synaptosomes were isolated from mice using sucrose and Percoll (Cytiva, MA, USA) based fractionations. Young mice (<21 days of age) were euthanized by cervical dislocation and adolescent mice (≥21 days) by inhalation of excess carbon dioxide followed by cervical dislocation. Synaptosome preparations for mass spectrometry analyses were isolated using sucrose with a protocol adapted from Nolt (Nolt et al., 2011). As this method was not suitable for isolation of functional mitochondria, samples for follow-up analyses in study II were isolated using Percoll, modifying the protocols of Dunkley and Tenreiro (Dunkley et al., 2008; Tenreiro et al., 2017). Synaptosome preparations for RNA isolation (unpublished, see 4.2.6.1) were isolated using Percoll.

4.2.2 Analysis of omics data (I, II, unpublished)

Principal component analyses (PCA) of proteomic and transcriptomic data were performed using the web-tool ClustVis (Metsalu and Vilo, 2015), using singular value decomposition.

Synaptic genes and proteins were identified using the SynGO knowledgebase (Koopmans et al., 2019).

To identify mitochondrial proteins and genes, proteomics and transcriptomics data were annotated against Mitocarta3.0 (Rath et al., 2021).

DAVID functional annotation clustering was performed on statistically significant proteomics and transcriptomics data using version 2021 (Huang et al., 2009b, 2009a), medium classification stringency and EASE scoring, followed by Benjamini-Hochberg correction (false discovery rate; FDR) for multiple testing, considering FDR <0.05 statistically significant.

Biological relationships between differentially expressed transcripts were investigated using Gene Ontology (GO) classification (Ashburner et al., 2000; Gene Ontology Consortium, 2021).

To produce more consistent data for this doctoral dissertation, the proteomic datasets from studies I and II were re-analysed using updated versions of the bioinformatics tools listed above.

4.2.3 High-resolution respirometry (II)

Oxidative phosphorylation was measured from synaptosome preparations using high-resolution respirometry (Oroboros). Recordings were performed with freshly isolated synaptosome preparations from *Cstb*$^{-/-}$ and control samples in parallel.

4.2.4 Mitochondrial DNA copy number determination (II)

Mitochondrial DNA (mtDNA) copy number was determined from synaptosomal DNA by reverse transcription-quantitative PCR (RT-qPCR). A standard-curve based method was used for copy number quantification, as the conventionally used relative measure (copies of mitochondrial gene/copies of nuclear gene) is not suitable for synaptosome preparations that lack nuclear DNA.

4.2.5 Statistical analyses (I, II)

Quantitative comparisons of the data presented in this doctoral dissertation were performed using the GraphPad Prism version 9 software. Student's t-test was used to analyse differences between two experimental groups, and one-way ANOVA with the Šídák correction was used for comparisons between more than two experimental groups. P-values <0.05 were considered statistically significant. The details of the comparisons discussed in studies I and II are specified in the relevant publications.

All data sets were tested for normality prior to use of parametric statistic tests. When the data did not follow a normal distribution or the sample size was considered small (<10 replicates), the non-parametric Mann-Whitney U-test was used. Outlier analysis was performed using GraphPad Prism's ROUT method (Q=1%).

4.2.6 RNA sequencing (unpublished)

4.2.6.1 RNA extraction, library preparation and sequencing

RNA was extracted from freshly isolated synaptosome preparations using Trizol, chloroform and the RNA Clean & Concentrator-5 kit (Zymo Research, CA, USA). Prior to using the kit, the synaptosome preparations were suspended in 300 µl Trizol and incubated for 5 min at room temperature. Next, 60 µl chloroform was added and the samples were vigorously vortexed for 15 seconds, followed by incubation for 2-3 min at room temperature. Samples were centrifuged at 12 000 xg for 15 min at +4°C and the upper aqueous phase was transferred to a Zymo-Spin IC Column. The RNA was bound to the spin column by centrifugation according to the manufacturer's instructions and the sample was washed twice with RNA wash buffer. DNase I treatment and subsequent washes were performed according to the manufacturer's instructions. RNA was eluted in 10 µl DNase/RNase-free water. RNA concentration was measured using a Qubit 2 fluorometer (Invitrogen) and a Qubit RNA Assay Kit (Thermo Fisher Scientific). The quality of the RNA was assessed using the TapeStation RNA High Sensitivity Assay (Agilent). RNA samples were stored at -80°C until further used.

The RNA sequencing was carried out by the Biomedicum Functional Genomics Unit at the Helsinki Institute of Life Science and Biocenter Finland at the University of Helsinki. The sequencing method used was 3'-RNA sequencing "Bulkseq", based on the previously published Drop-seq protocol (Macosko et al., 2015; Freitag et al., 2020). Briefly, 10 ng of RNA was mixed with Indexing Oligonucleotides (Integrated

DNA Technologies, Coralville, IA). After 5 min of incubation at ambient temperature, RNA was combined with reverse transcriptase (RT) mix, containing 1x Maxima RT buffer, 1 µmol/ml deoxynucleoside triphosphate, 10 U/µl Maxima H-RTase (all Thermo Fisher Scientific), 1 U/µl RNase inhibitor (Lucigen, WI, USA), and 2.5 µmol/l Template Switch Oligo (Integrated DNA Technologies, IA, USA). Samples were incubated in a T100 thermal cycler (BioRad, CA, USA) for 30 min at 22°C and 90 min at 42°C. The constructed complementary DNA was amplified by PCR in a volume of 15 µl using 5 µl of RT mix as template, 1x HiFi HotStart Readymix (Kapa Biosystems, MA, USA), and 0.8 µmol/l SMART PCR primer. The samples were thermocycled in the T100 thermocycler (BioRad) as follows: 95°C for 3 min; then 4 cycles of 98°C for 20 sec, 65°C for 45 sec, 72°C for 3 min; then 16 cycles of 98°C for 20 sec, 67°C for 20 sec, 72°C for 3 min; and a final 5 min extension step at 72°C. PCR products were pooled into sets of 12 samples containing different indexing oligos and purified with 0.6x Agencourt AMPure XP Beads (Beckman Coulter, CA, USA) according to the manufacturer's instructions and eluted in 10 µl of molecular grade water. The 3'-end complementary DNA fragments for sequencing were prepared using the Nextera XT (Illumina) tagmentation reaction, with 600 pg of each PCR product as input. The reaction was performed according to the manufacturer's instructions, except for the P5 SMART primer, which was used instead of the S5xx Nextera primer. Each set of samples pooled after the PCR reaction was tagmented with a different Nextera N7xx index. Subsequently, the samples were PCR amplified as follows: 95°C for 30 sec, 12 cycles of 95°C for 10 sec, 55°C for 30 sec, and 72°C for 30 sec, with a final extension step of 5 min at 72°C. Samples were purified twice using 0.6x and 1.0x Agencourt AMPure Beads (Beckman Coulter) and eluted in 10 µl molecular-grade water. The concentration of the libraries was measured using a Qubit 2 fluorometer (Invitrogen) and a Qubit DNA HS Assay Kit (Thermo Fisher Scientific). The quality of the sequencing libraries was assessed using the TapeStation DNA High Sensitivity Assay (Agilent). The samples were stored at -70°C until further used.

The libraries were sequenced on an Illumina NextSeq 500 (Illumina, CA, USA) with a custom primer producing read 1 of 20 base pairs (bp) and read 2 (paired end) of 62 bp.

4.2.6.2 RNA data preprocessing and analysis

The raw sequence data was inspected using FastQC and multiQC to ensure the quality of sequencing results (Andrews, 2010; Ewels et al., 2016). Reads were filtered to remove low-quality reads and reads shorter than 20 bp using Trimmomatic software (Bolger et al., 2014) with its default settings: ILLUMINACLIP:TruSeq3-SE.fa:2:30:10 LEADING:3 TRAILING:3

SLIDINGWINDOW:4:15 MINLEN:20. Reads passing the filter were further processed using Drop-seq tools and the pipeline originally described in the Drop-seq publication (Macosko et al., 2015). Briefly, the raw, filtered read libraries were converted to sorted, unaligned BAM files using Picard tools (v2.10.10), and the reads were tagged with sample-specific barcodes and unique molecular identifiers (UMIs). Tagged reads were trimmed for 5' adapters and 3' poly A tails. Alignment-ready reads were converted from BAM format files to FASTQ files and used as input for STAR aligner (Dobin et al., 2013). Alignments were performed using GENCODE Mouse Release M27 as reference genome (GRCm39) and comprehensive gene annotation files (Frankish et al., 2019) with STAR default settings. Aligned reads were sorted and merged with the previous unaligned tagged BAM file to recover barcodes and UMIs lost during the alignment step. Annotation tags were added to the aligned and barcoded tagged BAM files to complete the alignment process. Finally, Drop-seq tools were used to detect and correct systematic synthesis errors in sample barcode sequences. Digital expression matrices were generated by counting the total number of UMI sequences, merging sequences differing only by a single base, for each transcript.

Differential expression statistics from the RNA sequencing count data were calculated using the DESeq2 software (Love et al., 2014) in the R environment. Three control and five *Cstb*$^{-/-}$ samples were compared from P30-aged mice, and the corresponding sample numbers from P45-aged mice were five and five. Normalization of count values between samples was performed using a geometric mean and estimation of sample-specific factors to correct for variation. Gene-specific dispersions, such as variance and scatter, were estimated between experimental conditions, and possible sample outliers were visually inspected from PCA plots. P-values were generated using a negative binomial linear model and the Wald test to detect differentially expressed genes in the data. To optimize p-value adjustment, Cook's distance was used to detect genes with insufficient expression levels or extreme count outliers. Multiple testing adjustment of p-values was performed using the Benjamini-Hochberg procedure. Genes with an adjusted p-value <0.05 were considered as significantly differentially expressed.

5 RESULTS

In this doctoral dissertation, synaptic alterations were investigated in the cerebellum of the *Cstb*$^{-/-}$ mouse model at three different stages of CSTB deficiency-associated disease progression using omics approaches and complementary functional analyses (**Figure 10**). The first proteomic and electrophysiological analyses were performed from mice in the postnatal period at P14, when the cerebellar development is not yet complete, but the first signs of disease pathology are observed. The following proteomic and transcriptomic-level analyses were performed at the times of symptom onset and at the early symptomatic phase, at P30 and P45, when the neural networks of the cerebellum are mainly developed. These analyses were complemented by electrophysiological, respirometry, and molecular level analyses. Together, our data provided new insights into synaptic physiology at different stages of development and disease in CSTB deficiency.

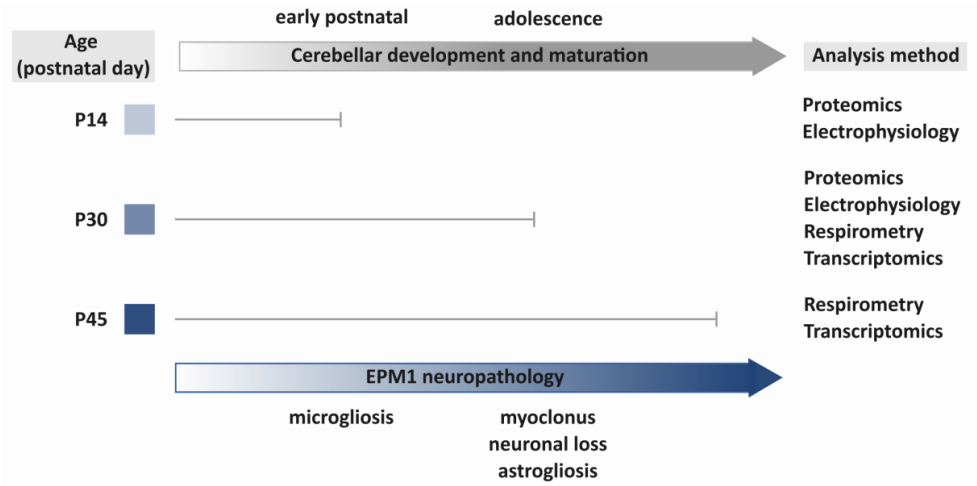

Figure 10 Graphical summary of the analyses performed in this doctoral dissertation and their relationship to postnatal cerebellar development and maturation and pathological changes occurring in the cerebellum of *Cstb*$^{-/-}$ mice.

All results presented here are reported in detail in the original publications. Unpublished data is also presented.

5.1 Detection of disease-related proteome alterations in synaptosomes (I, II)

CSTB deficiency results in epigenetic, transcriptional and functional changes in the *Cstb*$^{-/-}$ mouse brain already during embryonic neural stem cell differentiation (Daura et al., 2021), although the first clinical symptoms of CSTB deficiency do not manifest until the postnatal age of one month (Pennacchio et al., 1998; Pollari et al., 2023). To investigate whether synapse-level pathology is an early feature of CSTB deficiency, we isolated and purified cerebellar synaptosome fractions from P14 and P30-aged *Cstb*$^{-/-}$ and control mice, representing the presymptomatic and early symptomatic phases of the disease, and performed independent quantitative mass spectrometry analyses to map alterations in the synaptic proteomes.

PCA of the two proteomics datasets showed a clear difference between *Cstb*$^{-/-}$ and control samples at both time points, indicating that already during early disease pathogenesis, synaptosomes from *Cstb*$^{-/-}$ mice exhibit proteome characteristics different from those in control mice (**Figure 11A** and **B**). We also identified individual proteomic features associated with CSTB deficiency at both age points. At P14, 128 differentially abundant proteins (DAPs) were identified between *Cstb*$^{-/-}$ and control mice. Of these, 92 proteins were significantly increased and 36 were significantly decreased (reproducibility-optimized test statistic (ROTS); FDR <0.05) in synaptosomes of *Cstb*$^{-/-}$ mice (**Figure 11C**; **S. Table S2** in **I**). At P30, 349 differentially abundant proteins between genotypes were identified. Of these, 188 were significantly increased and 161 significantly decreased (Student's t-test; FDR <0.05) in *Cstb*$^{-/-}$ mice (**Figure 11D**; **S. Table 1_sheet2** in **II**). Among these proteins were previously identified CSTB-interactors, including cathepsin B (Green et al., 1984), SOD1 (Ulbrich et al., 2014) and beta-spectrin (Giaimo et al., 2002). In addition, protein families that have been associated with CSTB deficiency, such as ephrins, cadherins and cathepsins (Kaur et al., 2010; Joensuu et al., 2014), as well as several ribosomal and mitochondrial proteins (Daura et al., 2021), were identified.

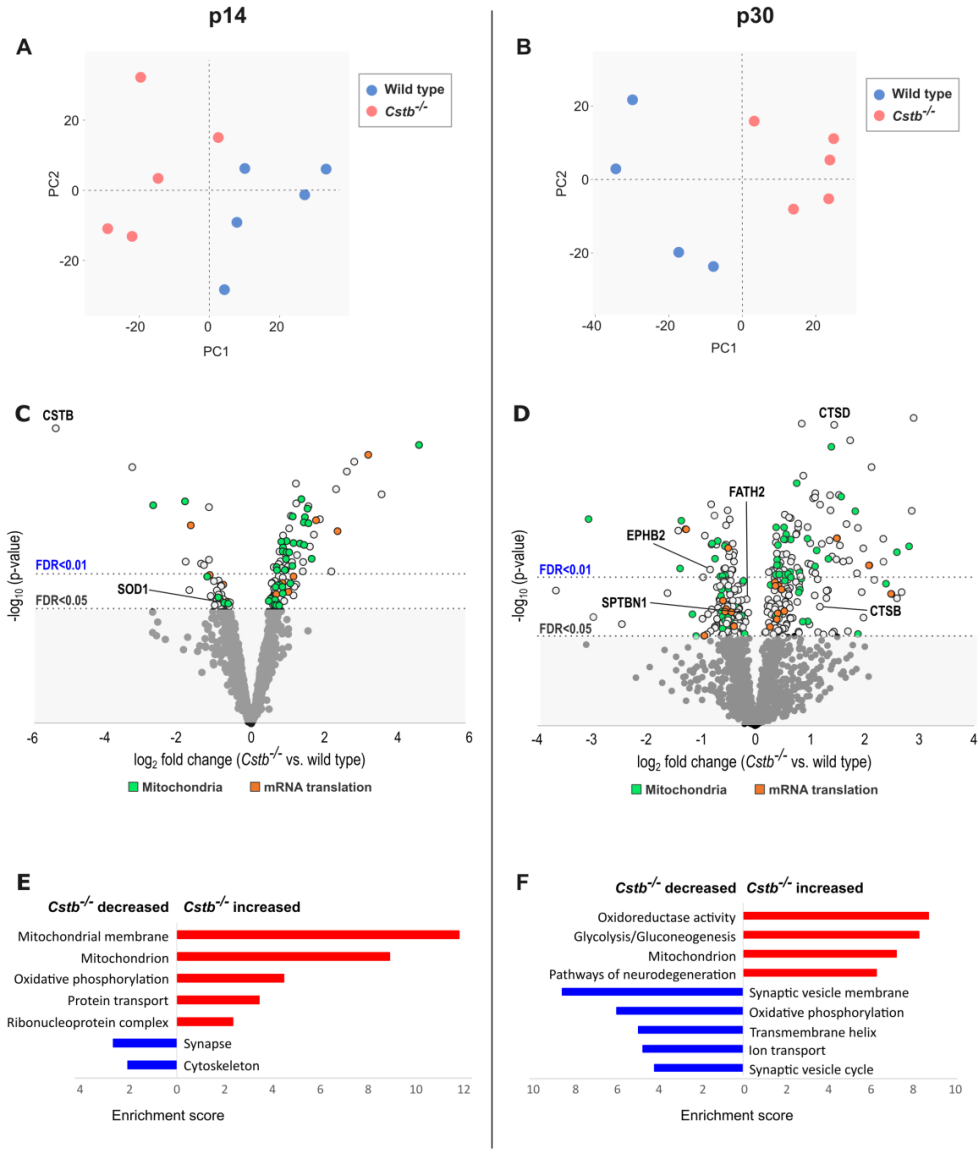

Figure 11 Differences in the synaptic proteome between *Cstb*$^{-/-}$ and control mice at P14 (left) and P30 (right). (A-B) Principal component analysis (PCA) of proteins in synaptosomes from P14 (A) and P30 (B) aged mice. Control samples are shown in blue and *Cstb*$^{-/-}$ in red. (C-D) Volcano plot of quantified proteins as $-\log_{10}$-transformed p-value vs. $\log_2$ fold change protein abundance at P14 (C) and P30 (D). Significantly different mitochondrial proteins and proteins involved in mRNA translation are plotted in green and orange, respectively. Previously identified interactors and proteins associated with CSTB have been marked (CSTB=cystatin B; SOD1=superoxide dismutase 1; SPTBN1=neuronal beta-II spectrin; EPHB2=ephrin type-B receptor 2; FATH2=cadherin 2; CTSD=cathepsin D; CTSB=cathepsin B). Proteins with non-significant q-values (FDR ≥0.05) are plotted in the grey area below the threshold limit of FDR <0.05. (E-F) Enriched DAVID functional annotation clusters of DAPs with increased (red) and decreased (blue) abundance at P14 (E) and P30 (F). The image contains summarized data from Supplementary Table S1 in I and Supplementary table 1_sheet1 in II.

To further investigate the altered proteomic profiles in *Cstb*$^{-/-}$ synaptosomes, we annotated the significantly differing proteins in both groups using DAVID functional annotation clustering and identified biological processes affected by CSTB deficiency. In the P14 group, the 92 increased proteins in *Cstb*$^{-/-}$ synaptosomes were associated with mitochondrial structure and energy production, protein transport, and cytosolic mRNA translation (**Figure 11E**). In the P30 group, the 188 increased proteins in *Cstb*$^{-/-}$ synaptosomes were associated with mitochondrial structure and function, glucose metabolism, and known pathways of neurodegeneration (**Figure 11F**). In contrast, the 36 decreased proteins from P14 *Cstb*$^{-/-}$ mice were associated with the synapse and the cytoskeletal structure (**Figure 11E**). In the P30 group, the 161 decreased proteins were associated with synaptic vesicles and oxidative phosphorylation (**Figure 11F**).

Between the P14 and P30 groups, 21 differentially abundant proteins common for both groups were identified (**Table 6**). The direction of change was consistent for most proteins, with the majority being increased in abundance. Of the 21 proteins, a substantial number were mitochondrial.

Collectively, proteomic data from P14 and P30 *Cstb*$^{-/-}$ mice show that CSTB deficiency results in synaptic changes that are detected prior to the onset of symptoms and suggest that mitochondrial changes occur in the early stages of the disease.

Table 6 Differentially abundant proteins common at P14 and P30

Protein	Gene		Abundance (*Cstb*$^{-/-}$ vs. wt)	
			P14	P30
Cytochrome c oxidase subunit 6B1	*Cox6b1*	M	increased	increased
Hemoglobin subunit alpha	*Hba*		increased	increased
Hemoglobin subunit beta-1	*Hbb-b1*		increased	increased
Cytochrome c, somatic	*Cycs*	M	decreased	decreased
ATPase family AAA domain-containing protein 1	*Atad1*	M	increased	decreased
Ubiquitin-40S ribosomal protein S27a	*Rps27a*		decreased	decreased
Mitochondrial import inner membrane translocase subunit Tim13	*Timm13*	M	increased	increased
Dihydropteridine reductase	*Qdpr*	M	increased	increased
Vesicle-associated membrane protein 1	*Vamp1*		decreased	decreased
Dynein light chain 2, cytoplasmic	*Dynll2*		decreased	increased
Ornithine aminotransferase, mitochondrial	*Oat*	M	increased	increased
Tenascin-R	*Tnr*		increased	decreased
60S ribosomal protein L4	*Rpl4*		increased	increased
Malate dehydrogenase, cytoplasmic	*Mdh1*		increased	increased
Tubulin alpha-1A chain	*Tuba1a*		increased	increased
BTB/POZ domain-containing protein 17	*Btbd17*		increased	increased
High mobility group protein B1	*Hmgb1*		increased	increased
V-type proton ATPase subunit D	*Atp6v1d*		decreased	increased
NADH dehydrogenase [ubiquinone] 1alpha subcomplex subunit 6	*Ndufa6*	M	increased	increased
Sodium- and chloride-dependent GABA transporter 1	*Slc6a1*		decreased	decreased
Phosphoglucomutase-1	*Pgm1*		decreased	increased

M = mitochondrial

5.2 Differential protein abundance and functional changes in synaptic mitochondria of *Cstb*$^{-/-}$ mice (I, II)

5.2.1 Proteomic profiling reveals early signs of mitochondrial dysfunction in *Cstb*$^{-/-}$ mice (I, II)

Primary data analysis of differentially abundant proteins from P14 and P30 *Cstb*$^{-/-}$ synaptosomes showed that alterations in the mitochondrial proteome are early and profound. To study these changes further, we identified and grouped the differentially abundant mitochondrial proteins according to their key processes (**Appendix 1**).

Among the differentially abundant proteins at P14 and P30, 40 and 66 were mitochondrial, respectively. Of these, nine and nineteen were associated with the respiratory chain, spanning all five protein complexes, while three and fourteen were involved in carbohydrate and lipid metabolism. These processes have previously been associated with CSTB deficiency (Daura et al., 2021). Additional functions of the differentially abundant proteins included ROS metabolism, which has been shown to contribute to cell death in granule neurons of *Cstb*$^{-/-}$ mice (Lehtinen et al., 2009); two and four proteins were associated with this function, respectively. Furthermore, two and three proteins were involved in the central maintenance of mitochondrial structure and dynamics, a process disrupted in primary bone marrow-derived macrophages from *Cstb*$^{-/-}$ mice (Maher et al., 2014). Other identified proteins were involved in mitochondrial trafficking, calcium signaling, protein and small molecule import and homeostasis, and amino acid metabolism. In the P14 dataset, most proteins showed increased abundance, whereas in the P30 group, the ratio of proteins with increased to decreased ratio was approximately equal.

5.2.2 Mitochondrial respiratory decline in *Cstb*$^{-/-}$ mice during disease progression (II)

To assess the functional consequences of mitochondrial proteome re-organization, we performed high-resolution respirometry to evaluate oxidative phosphorylation in cerebellar synaptosomes. Given that impairment of mitochondrial respiration had already been reported to occur during *Cstb*$^{-/-}$ mice neural stem cell differentiation (Daura et al., 2021), we also aimed to determine whether this developmental mitochondrial dysfunction continues into adulthood.

To examine mitochondrial oxygen consumption rates (OCRs), we plotted concentration and consumption over time as synaptosome samples were applied with oxidative phosphorylation substrates and inhibitors following a previously established substrate-uncoupler-inhibitor-titration (SUIT) protocol (Awadhpersad

and Jackson, 2021). OCRs were measured in synaptosomes from *Cstb*$^{-/-}$ and control mice at symptom onset at P30 and during the early progression at P45 to evaluate possible changes associated with the onset and progression of clinical symptoms.

At P30, no differences in OCRs were observed between genotypes in any of the respiration states examined (**Figures 4B-D** in **II**), suggesting that synaptic mitochondrial respiration is not compromised at the onset of myoclonus or neuronal death. However, at P45, during the early stages of disease progression, the overall respiratory rate was significantly reduced in *Cstb*$^{-/-}$ mice (**Figure 12**), indicating that mitochondrial function is affected as the disease progresses. Impaired OCRs were observed across all respiration states examined (**Figures 4B-D** in **II**), indicative of a general respiratory dysfunction. Leak respiration was not elevated in *Cstb*$^{-/-}$ samples (**Supplementary figure 4** in **II**), which in turn would have indicated damage to the mitochondrial inner membrane. Further analysis of individual OXPHOS complexes II, IV, and V by immunoblotting revealed no differences between genotypes (**Figures 4E-H** in **II**).

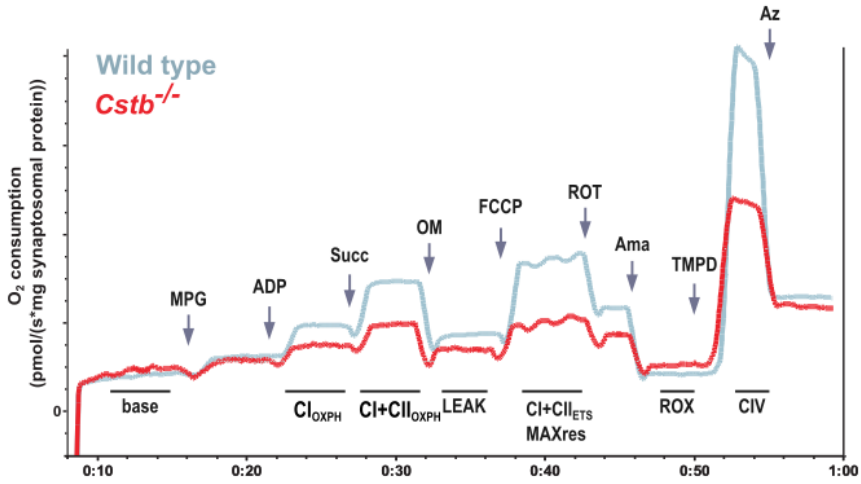

Figure 12 Mitochondrial respiration traces in *Cstb*$^{-/-}$ (red) and control (blue) synaptosomes at P45, examined using a SUIT-protocol showing oxygen consumption (pmol/(s*mg synaptosomal protein); y-axis) during substrate and coupling states (x-axis). MPG = malate/pyruvate/glutamate; ADP = adenosine diphosphate; Succ = succinate; OM = oligomycin; FCCP = carbonyl cyanide-*p*-trifluoromethoxyphenylhydrazone; ROT = rotenone; Ama = antimycin A; TMPD = *N,N,N,N*-tetramethyl-*p*-phenylenediamine; Az = azide; CI_{OXPH} = phosphorylating respiration (OXPHOS) in presence of CI substrates; $CI + CII_{OXPH}$ = OXPHOS respiration in presence of CI and CII substrates; LEAK = oligomycin-inhibited non-phosphorylating basal respiration; $CI + CII_{ETS}$ MAX_{res} = maximal capacity of the electron transport system; ROX = residual oxygen consumption; CIV = complex IV activity. Image reproduced from Figure 4 in II.

In conclusion, mitochondrial respiration rates are not altered in *Cstb*$^{-/-}$ synaptosomes at symptom onset at P30 but are drastically reduced early in disease progression at P45, making mitochondrial dysfunction an early phenotype in CSTB deficiency.

5.2.3 Synaptic mitochondria in *Cstb*$^{-/-}$ mice show no evidence of primary defects (II)

Mitochondrial dysfunction is often associated with changes in dynamics and membrane morphology (Bertholet et al., 2016). To investigate whether impaired respiration in *Cstb*$^{-/-}$ synaptosomes was associated with alterations in mitochondrial phenotype, we examined mitochondrial membrane ultrastructure by transmission electron microscopy (TEM) in cerebellar tissue samples from *Cstb*$^{-/-}$ and control mice at multiple age points, starting at the presymptomatic age of P14, continuing to the early symptomatic phases at P30 and P45, and to fully symptomatic phases at P70 and P120. The results were in line with those previously reported (Pennacchio et al., 1998; Tegelberg et al., 2012): the number of granule neurons with dense nuclei indicative of apoptotic cells increased with age in *Cstb*$^{-/-}$ samples, and these were often associated with swollen mitochondria in vicinity. However, at the presymptomatic and early symptomatic stages of the disease (P14-P45), such changes in ultrastructure were not observed (**Figures 5B-C** in **II**), thus no morphological differences between genotypes were detected.

Given that no morphological changes were observed, we next investigated molecular level markers that could indicate primary mitochondrial defects leading to early mitochondrial dysfunction. Consistent with the TEM results, the proteomics data showed no changes in key factors coordinating mitochondrial membrane fusion and fission. Additionally, no differences were found in early indicators of cellular stress (**Figure 5D-E** in **II**). This was evaluated by examining the percentage of the short isoforms of the mitochondrial protein Dynamin-like GTPase OPA1 (S-OPA1) relative to total OPA1. Furthermore, no significant differences in mtDNA copy number were detected in synaptosome samples from *Cstb*$^{-/-}$ and control mice at P30 or P45 (**Figure 5A** in **II**). Taken together, these findings suggest that the mitochondrial respiratory decline observed in early CSTB deficiency is not due to a primary mitochondrial defect.

5.3 Characterization of synaptic function in *Cstb*$^{-/-}$ mice (I, II)

5.3.1 Molecular-level changes in GABAergic signaling in *Cstb*$^{-/-}$ mice (I, II)

Our research group had previously identified differences in the mediation of GABAergic inhibitory currents and the expression of $GABA_A$ receptor subunits in the cerebella between *Cstb*$^{-/-}$ and control mice (Joensuu et al., 2014), indicating alterations in the excitation-inhibition balance. To identify synaptic proteins with differential abundance relevant for the GABAergic signaling pathway, we next annotated the differentially abundant proteins -datasets to the SynGO database.

The SynGO database identified six GABA-associated proteins in the proteomics datasets whose abundance was significantly altered (**Figure 13**). These proteins have previously been associated with presynaptic neurotransmitter uptake (GABA transporter-1, GAT-1) and with $GABA_A$ receptor-mediated phasic and tonic activities (GAT-1; Contactin-associated protein-like 2, CNTNAP2; Acyl-CoA-binding protein, DBI; GTPase KRas, KRAS; Neuroligin-2, NLGN2; Protein kinase C epsilon, PRKCE) (Jensen et al., 2003; Proctor et al., 2003; Poulopoulos et al., 2009; Bridi et al., 2017; Papale et al., 2017; Alquier et al., 2021). The abundance level of all the proteins was decreased in *Cstb*$^{-/-}$ synaptosomes, with the exception of PRKCE, which was increased by 4.5-fold in *Cstb*$^{-/-}$ samples. Only the GAT-1 protein was consistently decreased at both age points, whereas the remaining five proteins were only altered at P30.

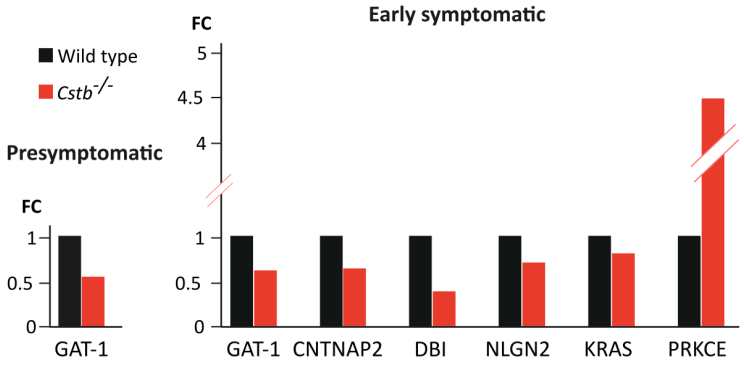

Figure 13 Relative abundance levels of significantly altered GABA related proteins in cerebellar synaptosomes from presymptomatic (P14; left) and early symptomatic (P30; right) *Cstb*$^{-/-}$ (red) and control (black) mice. Fold changes (FC) are presented as abundance level *Cstb*$^{-/-}$ in relation to control. n=4-5/genotype/age group.

5.3.2 Unaltered GAT-1 activity in cerebellar granule neurons from *Cstb*$^{-/-}$ mice (I)

Given that the abundance level of the GAT-1 protein was reduced, we investigated its functional effects and possible implications for disturbed GABAergic signaling. In mature neurons, GAT-1 terminates GABAergic neurotransmission by removing GABA from the synaptic cleft (Guastella et al., 1990), and genetic depletion or pharmacological inhibition of GAT-1 results in elevated ambient GABA levels and increased $GABA_A$ receptor-mediated tonic conductance (Wall and Usowicz, 1997; Rossi et al., 2003). During the early postnatal period, GAT-1 is abundant and functional in presynaptic GABAergic terminals (Sipilä et al., 2004; Safiulina et al., 2006), but its role is somewhat unclear as GABAergic neurons are still maturing. Fine-tuning of developmental neural circuits has been proposed, but evidence of this is limited (Sipilä et al., 2004).

To assess whether proteome-level alterations in GAT-1 abundance were associated with changes in neurotransmission, we performed whole-cell voltage clamp electrophysiology in cerebellar granule cells from P14 presymptomatic and P30 early symptomatic *Cstb*$^{-/-}$ and control mice (**Figure 14A**). GAT-1 was inhibited using its antagonist NNC-711 (Suzdak et al., 1992), and the resulting increase in tonic $GABA_A$ receptor-mediated currents was used as a readout of GAT-1 activity. At the end of all experiments, $GABA_A$ receptor-mediated tonic currents were completely blocked by application of picrotoxin (Korpi et al., 2002).

Electrophysiological currents between granule cells from *Cstb*$^{-/-}$ and control mice did not differ at any of the examined conditions at either age point. NNC-711-mediated inhibition of GAT-1 caused an increase in the amplitude of tonic $GABA_A$ receptor-mediated currents (**Figure 14B**), implying that the GAT-1 protein is functional at both developmental ages. The increase was evident in all sample groups and no differences were detected between genotypes (**Figure 14C**). A complete block of the tonic current using picrotoxin (**Figure 14B**) was seen in all sample groups, showing no genotype-specific differences (**Figure 14D**). Together, these results indicate that despite the proteome-level reduction of GAT-1 in *Cstb*$^{-/-}$ synaptosomes, its activity as a GABA transporter in the synapse is sufficient to preserve the electrophysiological properties of cerebellar granule neurons in *Cstb*$^{-/-}$ mice.

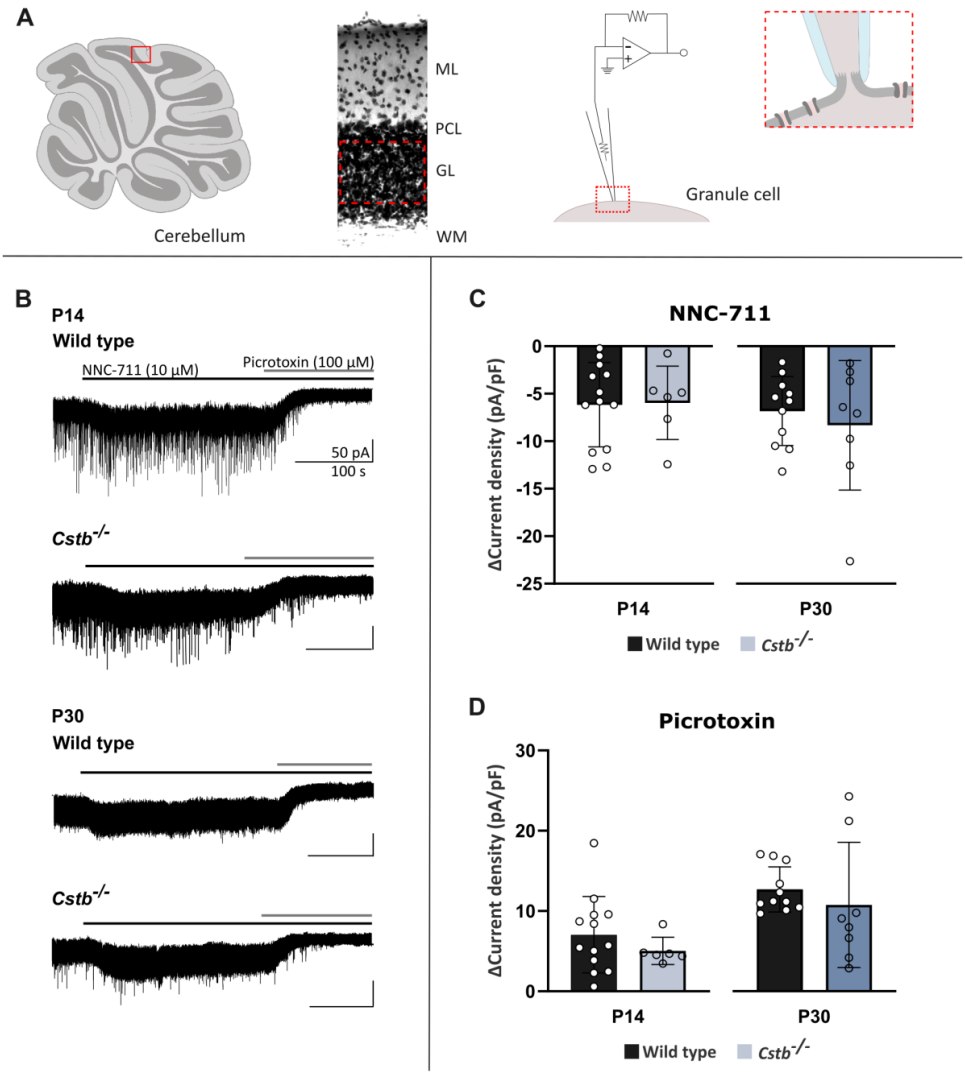

Figure 14 Electrophysiological properties in cerebellar granule cells of *Cstb*$^{-/-}$ mice. (A) Graphical representation of the mouse cerebellum and its different cell layers, and the whole-cell voltage clamp method. ML = molecular layer; PCL = Purkinje cell layer; GL = granule cell layer; WM = white matter. Cell layer image by Saara Tegelberg, Folkhälsan Research Center. (B) Experimental traces of whole-cell voltage clamped cerebellar granule neurons of P14 and P30 *Cstb*$^{-/-}$ and control (wild type) mice. NNC-711 blocks GAT-1 activity and picrotoxin blocks $GABA_A$ receptor -mediated tonic conductance. (C, D) Summary of NNC-711 and picrotoxin application, plotted as mean ±SD (n = 6-13 cells / genotype and age point) of the change (Δ) in current density (pA/pF), induced by drug application. The image contains summarized data from Supplementary Table S6 in I.

5.3.3 Proteome-level alterations in the synaptic vesicle cycle of *Cstb*$^{-/-}$ mice (I, II)

SynGO analysis of differentially abundant proteins showed that CSTB deficiency has a significant impact on members of the synaptic vesicle cycle and its regulators, with a total of 40 proteins being differentially abundant (**Table 7** and **8**). In presymptomatic mice at P14, five members and three regulators were identified. Several of these were also associated with brain development. For example, the protein Epidermal growth factor receptor substrate 15 (EPS15), which showed a nearly 13-fold increase in synaptosomes from P14 *Cstb*$^{-/-}$ mice, regulates synaptic vesicle membrane retrieval in the adult nervous system of *Drosophila* (Majumdar et al., 2006), and is also critical for larval synapse development (Koh et al., 2007). Other developmentally critical synaptic vesicle proteins included protein transcription homolog (SCRIB), reduced to 0.3-fold in *Cstb*$^{-/-}$ mice, and alpha- and beta-soluble NSF attachment proteins (NAPA and NAPB), increased 2.5- and twofold, respectively. Altered expression of these proteins have been linked to disturbances in brain development (Ezan et al., 2021), epileptic seizures and ataxia (Conroy et al., 2016), and embryonic lethality (Chae et al., 2004) in mice, and early-onset epileptic encephalopathy in humans (Conroy et al., 2016).

In early symptomatic mice at P30, 20 and 12 differentially abundant members and regulators of the synaptic vesicle cycle were identified, respectively. Additionally, two regulatory proteins, detected only in one genotype, were identified. The synaptic vesicle proteins that were differentially abundant mainly participate in the localization of synaptic vesicles to the active zone, neurotransmitter fusion and release, and the endocytic retrieval of synaptic vesicles. Most of these proteins were found to be reduced in *Cstb*$^{-/-}$ synaptosomes. The fold differences were generally moderate, except for Syntaxin-1A, which was reduced to 0.1-fold, and alpha-synuclein, which was increased by fivefold compared to control samples. Both proteins have been associated with disease pathology: the loss of Syntaxin-1A with impaired synaptic vesicle priming and fusion, a deficiency partly compensated by Syntaxin-1B (Vardar et al., 2016), while elevated levels of alpha-synuclein have been linked to the inhibition of the synaptic vesicle cycle (Nemani et al., 2010). Among the regulatory proteins, the abundance of Tumor protein p63-regulated gene 1-like protein (also known as Mover), which negatively regulates neurotransmitter release from synaptic vesicles (Körber et al., 2015), was nearly threefold higher in *Cstb*$^{-/-}$ synaptosomes.

Table 7 Differentially abundant synaptic vesicle cycle proteins in cerebellar synaptosomes from *Cstb*$^{-/-}$ mice

Protein	Gene	Fold change (*Cstb*$^{-/-}$ vs. wt)	
		P14	P30
V-type proton ATPase subunit D	*Atp6v1d*	0.68	1.72
Vesicle-associated membrane protein 1	*Vamp1*	0.46	0.67
Alpha-soluble NSF attachment protein	*Napa*	2.47	
Epidermal growth factor receptor substrate 15	*Eps15*	12.97	
Protein scribble homolog	*Scrib*	0.31	
AP-3 complex subunit delta-1	*Ap3d1*		0.77
V-type proton ATPase 116 kDa subunit A isoform 1	*Atp6v0a1*		0.77
V-type proton ATPase subunit B, brain isoform	*Atp6v1b2*		1.16
V-type proton ATPase subunit G 2	*Atp6v1g2*		0.81
Protein bassoon	*Bsn*		0.72
Catenin beta-1	*Ctnnb1*		0.66
Protein piccolo	*Pclo*		0.67
Vesicle-associated membrane protein 2	*Vamp2*		0.75
Regulating synaptic membrane exocytosis protein 1	*Rims1*		0.7
C-terminal-binding protein 2	*Ctbp2*		1.28
Syntaxin-1A	*Stx1a*		0.12
Syntaxin-1B	*Stx1b*		0.59
Amphiphysin	*Amph*		1.33
Dynamin-1	*Dnm1*		1.14
Dynamin-3	*Dnm3*		1.77
Ras-related protein Rab-5A	*Rab5a*		0.64
Clathrin coat assembly protein AP180	*Snap91*		0.75
Alpha-synuclein	*Snca*		5.06

Table 8 Differentially abundant regulators of the synaptic vesicle cycle in cerebellar synaptosomes from *Cstb*$^{-/-}$ mice

Protein	Gene	Fold change (*Cstb*$^{-/-}$ vs. wt)	
		P14	P30
Beta-soluble NSF attachment protein	*Napb*	1.92	
Neuronal calcium sensor 1	*Ncs*	0.57	
DnaJ homolog subfamily C member 5	*Dnajc5*	0.5	not detected in *Cstb*$^{-/-}$
Glyceraldehyde-3-phosphate dehydrogenase	*Gapdh*		1.48
Complexin-2	*Cplx2*		0.81
Proline-rich transmembrane protein 2	*Prrt2*		0.66
Ras-related protein Rab-3A	*Rab3a*		0.8
Voltage-dependent L-type calcium channel subunit beta-4	*Cacnb4*		0.77
Liprin-alpha-2	*Ppfia2*		0.81
Protein kinase C beta type	*Prkcb*		0.77
Tumor protein p63-regulated gene 1-like protein	*Tprg1l*		2.7
Rap guanine nucleotide exchange factor 4	*Rapgef4*		0.69
Synaptogyrin-3	*Syngr3*		0.79
Vesicle-fusing ATPase	*Nsf*		0.89
Transmembrane protein 163	*Tmem163*		0.66
Syntaxin-binding protein 3	*Stxbp3*		not detected in wild type

Together, the data show that CSTB deficiency affects members of the synaptic vesicle cycle and its regulatory proteins, having the largest impact on regulatory proteins linked to pathology.

5.4 Key molecular changes affecting synaptic proteome turnover (I, II, unpublished)

Given that a significant number of differentially abundant proteins were associated with the synaptic vesicle cycle, we aimed at identifying proteins linked to autophagy and the endolysosomal system, as accumulating evidence suggests that these processes are structurally and functionally interconnected (van Niel et al., 2018). In the proteomics and transcriptomics datasets from P14, P30, and P45 *Cstb*$^{-/-}$ synaptosomes, we identified alterations in a total of 22 proteins involved in

autophagic degradation of proteins and organelles (**Table 9**). Of these, five proteins were implicated in autophagosome-lysosome fusion, six in the autophagic vesicle movement, and seven in lysosomal degradation.

Table 9 Differentially abundant proteins in autophagy in cerebellar synaptosomes from *Cstb*$^{-/-}$ mice

Protein	Gene	Proteomics Fold change (*Cstb*$^{-/-}$ vs. wt)		Transcriptomics Fold change (*Cstb*$^{-/-}$ vs. wt)	
		P14	P30	P30	P45
Vesicle-associated membrane protein 1	*Vamp1*	0.46	0.67		
Coatomer subunit alpha	*Copa*	1.6			
Coatomer subunit beta	*Copb1*	1.6			
Coatomer subunit delta	*Arcn1*	1.8			
Dynactin subunit 2	*Dctn2*		1.41		
Dynactin subunit 3	*Dctn3*	2.0			
Alpha-soluble NSF attachment protein	*Napa*	2.47			
Cathepsin D	*Ctsd*		2.71	1.8	1.99
Cathepsin B	*Ctsb*		2.26		
Cathepsin E	*Ctse*			3.72	7.63
Cathepsin H	*Ctsh*			1.94	
Cathepsin Z	*Ctsz*				1.72
V-type proton ATPase subunit D	*Atp6v1d*	0.68	1.72		
V-type proton ATPase subunit B, brain isoform	*Atp6v1b2*		1.16		
Ras-related protein Rab-3A	*Rab3a*		0.8		
Ras-related protein Rab-18	*Rab18*		0.71		
Ras-related protein Rab-5A	*Rab5a*		0.64		
Ras-related protein Rab-11B	*Rab11b*		0.77		
Ras-related protein Rab-14	*Rab14*		0.78		
Ras-related protein Rab-24	*Rab24*				0.72
Bcl-2-related protein A1	*Bcl2a1a*			14.05	
Bcl-2 homology region 1-3 domain-containing protein	*Bcl2a1d*			4.71	

At P14, the majority of differentially abundant proteins were increased in abundance, for example coatomer subunits alpha, beta and delta, along with the alpha-soluble NSF attachment protein (**Table 9**). Coatomer proteins are critical for endosome transport and the maturation of autophagic vesicles (Razi et al., 2009), while the alpha-soluble NSF attachment protein is essential for the fusion of autophagosomes with lysosomes (Abada et al., 2017). The upregulation of these proteins suggests enhanced autophagy in developing synaptosomes of P14-aged *Cstb*$^{-/-}$ mice.

In P30 mice, we observed a reduction in five Ras-associated binding (Rab)-proteins: Rab3a, Rab5a, Rab11b, Rab14, and Rab18, which are key regulators of intracellular vesicle transport and are involved in the formation of autophagosomes and their fusion with lysosomes (Pfeffer, 2013). Conversely, lysosomal cathepsins B and D, as well as vacuolar-type ATPase (v-ATPase) proton pump subunits B and D, responsible for proteolysis and acidification, were significantly increased. Notably, defects in the V-type proton ATPase subunit B have previously been associated with clinical conditions such as epilepsy and neurodegeneration (Rousseau et al., 2023). Additionally, differentially expressed local transcripts, including cathepsins D, E, H, and Z, were upregulated in P30 and P45 *Cstb*$^{-/-}$ synaptosomes (**Appendix 2**), as well as subunits from the B-cell lymphoma 2 protein family, *Bcl2a1a* and *Bcl2a1d*, which are known negative regulators of autophagy (Pattingre et al., 2005).

We also identified alterations in key transport proteins in the proteomics datasets, affecting both anterograde and retrograde transport (**Table 10**). These proteins operate at both cytoskeletal and adapter-protein levels, suggesting they may influence either global transport mechanisms or the trafficking of specific organelles, proteins, or mRNAs. In P14 mice, the most significant changes were detected in Dynein light chain 2 and Kinesin light chain 1, which are primary mediators for cytoskeletal retrograde and anterograde transport, respectively (Maday et al., 2014). Additionally, mitochondrial Rho GTPase 2, which may be involved in the anchoring of mitochondria to motor proteins (Reis et al., 2009), was altered in P14 mice. In P30 mice, we observed changes in key retrograde transport proteins Dynein light chain 2 and Dynein 1 heavy chain, as well as in the anterograde transport protein Kinesin heavy chain isoform 5c. One Dynactin subunit was altered at both P14 and P30.

Table 10 Differentially abundant key intracellular transport proteins in cerebellar synaptosomes from *Cstb*$^{-/-}$ mice

Protein	Gene	Fold change (*Cstb*$^{-/-}$ vs. wt)	
		P14	P30
Dynein light chain 2, cytoplasmic	*Dynll2*	0.29	3.93
Kinesin light chain 1	*Klc1*	2.24	
Dynactin subunit 3	*Dctn3*	2.0	
Mitochondrial Rho GTPase 2	*Rhot2*	1.91	
Cytoplasmic dynein 1 heavy chain 1	*Dync1h1*		0.79
Kinesin heavy chain isoform 5C	*Kif5c*		1.25
Dynactin subunit 2	*Dctn2*		1.41

Collectively, the data reveal changes in proteins critical for the transport and turnover of synaptic proteins and organelles.

5.5 Altered local translation and inflammatory changes at symptom onset in *Cstb*$^{-/-}$ mice (II, unpublished)

5.5.1 Molecular-level alterations in local translation (I, II)

In the dataset of differentially abundant proteins from presymptomatic mice at P14, we identified twelve members of the local translation machinery (**Supplementary Table S3** in **I**). Most of these were subunits of the large ribosomal subunit, but two key regulatory proteins, detected exclusively in *Cstb*$^{-/-}$ samples, were also found. The altered ribosomal proteins are involved in various processes, including the regulation of global protein translation, maturation of core ribosomal subunits, and the ubiquitination of stalled ribosomes (Fumagalli et al., 2012; Kathjoo and Srivastava, 2022; Oltion et al., 2023). Among the regulatory proteins, nucleophosmin1 (NPM1) serves as a regulator of ribosome biogenesis and intracellular trafficking (Maezawa et al., 2002), while nucleolin is an ribosomal RNA (rRNA) binding adaptor protein that, together with the motor protein kinesin, transports mRNAs regulating cell size to the periphery and modulates their translational regulation in axons (Perry et al., 2016).

In early symptomatic mice at P30, we identified 27 differentially abundant proteins involved in local translation (**Table 11**). The majority of these were ribosomal proteins that function as core subunits and are essential for ribosome maturation, interactions with mRNA, and the initiation of translation (Török et al.,

1999; Pellagatti et al., 2008; Havkin-Solomon et al., 2023). Additionally, several factors that influence translation initiation and elongation were identified, with most showing increased abundance.

Table 11 Differentially abundant proteins in cerebellar synaptosomes of *Cstb*$^{-/-}$ mice at P30 with function in local translation

Protein function	Protein	Gene	Fold change (*Cstb*$^{-/-}$ vs. wt)
Ribosomal subunit	Ubiquitin-40S ribosomal protein S27a	*Rps27a*	0.41
	40S ribosomal protein S17	*Rps17*	0.70
	40S ribosomal protein S19	*Rps19*	2.81
	40S ribosomal protein S14	*Rps14*	0.68
	40S ribosomal protein S9	*Rps9*	1.44
	40S ribosomal protein S3a	*Rps3a*	0.67
	40S ribosomal protein S3	*Rps3*	0.76
	40S ribosomal protein S21	*Rps21*	1.20
	60S ribosomal protein L4	*Rpl4*	1.34
	60S ribosomal protein L12	*Rpl12*	1.39
	60S ribosomal protein L29	*Rpl29*	0.52
	60S ribosomal protein L30	*Rpl30*	not detected in wt
Translation factor	Eukaryotic translation initiation factor 5A-1	*Eif5a*	4.23
	Eukaryotic translation initiation factor 1	*Eif1*	5.61
	Elongation factor 1-alpha2	*Eef1a2*	1.27
	Elongation factor 2	*Eef2*	1.28
	Elongation factor 1-beta	*Eef1b*	0.66
	Elongation factor 1-gamma	*Eef1g*	0.73
	Elongation factor 1-alpha1	*Eef1a1*	1.31
Other	Tryptophan--tRNA ligase, cytoplasmic	*Wars1*	1.32
	Amyloid-beta A4 protein	*App*	2.91
	Hemoglobin subunit beta-1	*Hbb-b1*	6.36
	Rho-associated protein kinase 2	*Rock2*	0.76
	Pyruvate kinase PKM	*Pkm*	1.18
	Glyceraldehyde-3-phosphate dehydrogenase	*Gapdh*	1.48
	Polyadenylate-binding protein 1	*Pabpc1*	0.74
	Calreticulin	*Calr*	1.50

The most significant increases were observed in eukaryotic translation initiation factor 1 (eIF1), which increased nearly sixfold, and eIF-5A1, increased by more than fourfold. eIF1 is a crucial component of the 43S preinitiation complex, essential for translation initiation. It binds to mRNA, scans the 5' untranslated region, and identifies the correct start codon from which translation begins (Hinnebusch, 2014). eIF-5A1 is involved in both the initiation of translation and the promotion of the elongation phase, alongside elongation factor 2 (eEF2) (Saini et al., 2009; Rossi et al., 2016), another critical subunit found to be increased in our dataset. In addition to alterations in translation initiation factors, four of the five members of the eEF1 family of mammalian translation elongation factors (EFs) (eEF1-alpha1, eEF1-alpha2, eEF1-beta and eEF1-gamma), as well as eEF2, were differentially abundant. Among the regulatory proteins, several have previously been associated with neuropathological conditions, for example amyloid-beta A4 protein and Rho-associated protein kinase 2 (ROCK2), both linked to Alzheimer's disease.

5.5.2 Transcriptomic profiling from synaptosomes from *Cstb*$^{-/-}$ mice (unpublished)

Given that several proteins of the local translation machinery were differentially abundant in the synaptosomes from P30 *Cstb*$^{-/-}$ mice, we next profiled the synaptic transcriptome of *Cstb*$^{-/-}$ and control mice at the early symptomatic stages of P30 and P45. PCA of transcriptomic data from both disease stages revealed a difference between genotypes, suggesting that the transcriptomic signatures of synaptosomes in *Cstb*$^{-/-}$ deficient mice differ from those in control mice (**Figure 15A** and **B**).

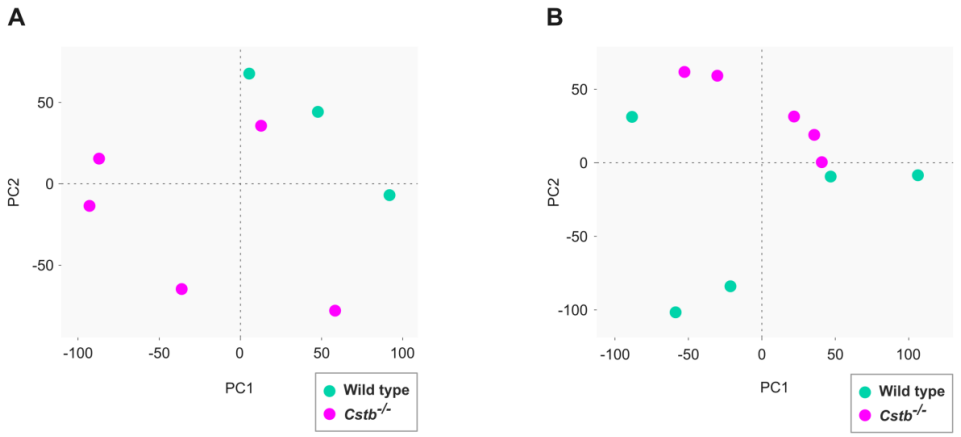

Figure 15 Principal component analysis (PCA) of transcriptomics data of cerebellar synaptosomes from P30 (A) and P45 (B) aged mice. Each dot represents one biological replicate, color coded for genotype: control samples (wild type) are shown in green and *Cstb*$^{-/-}$ in purple.

At P30, we identified 56 differentially expressed genes in the synaptosomes of *Cstb*$^{-/-}$ mice, with 47 transcripts upregulated and 9 downregulated. At P45, a total of 87 genes with differential expression were identified, with 59 upregulated and 28 downregulated. These genes were further grouped by GO annotation (**Appendix 2**). The data showed that the differentially expressed genes (DEGs) in both experimental groups were largely the same or had similar biological functions. This suggests that local transcriptional effects are already present at the onset of clinical symptoms and do not change significantly as symptoms progress.

To identify known transcripts and biological processes associated with CSTB deficiency, we compared the transcriptome data with previously identified CSTB interactors, the proteome data from P30 mice, the SynGO database of synaptic proteins, and performed DAVID functional annotation clustering. Among the differentially expressed transcripts, no previously reported CSTB interactors were identified; however, several proteins involved in immunological signaling, which have previously been linked to CSTB deficiency, were present (Joensuu et al., 2014; Korber et al., 2016; Okuneva et al., 2016) (**Figure 16A** and **B**). Notable common members between the differentially expressed transcripts and differentially abundant proteins were cathepsin D and the mitochondrial phosphate/copper carrier *Slc25a3*, both involved in lysosomal protein degradation and ATP-production (Stoka et al., 2016; Boulet et al., 2018). By examining the SynGO database, we identified three and six differentially expressed genes encoding synaptic proteins at P30 and P45, respectively. These proteins are involved in processes such as immune responses, lysosomal functions, apoptosis, and the synaptic vesicle cycle. DAVID functional annotation clustering revealed that at P30, differentially expressed genes were associated with secreted signal peptides, innate immune responses, and inflammatory responses, while at P45, they were linked to secreted signal peptides, inflammatory responses, innate immunity, and lysosomal functions (**Figure 16C** and **D**).

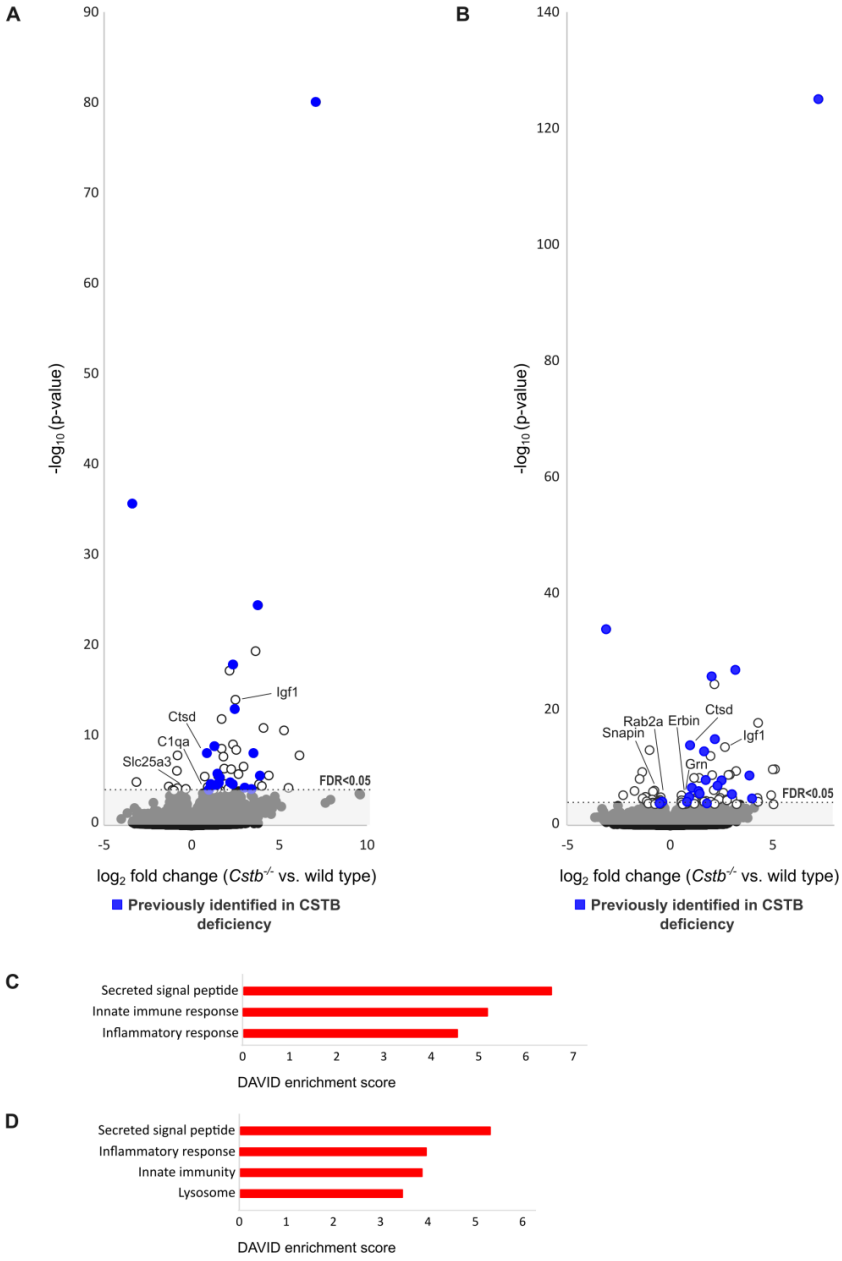

Figure 16 Differences in the synaptic transcriptome between *Cstb*$^{-/-}$ and control mice at P30 and P45. (A-B) Volcano plot of quantified transcripts as -$\log_{10}$-transformed p-value vs. $\log_2$ fold change gene expression at P30 (A) and P45 (B). Significantly different transcripts previously identified in CSTB deficiency are plotted in blue. Transcripts encoding synaptic proteins, and transcripts common with the proteomics data at P30 have been marked with gene symbol. Transcripts with non-significant q-values (FDR ≥0.05) are plotted in the grey area below the threshold limit of FDR <0.05. Fold change is displayed as log2-transformed values to facilitate visualization. (C-D) Enriched DAVID functional annotation clusters of differentially expressed genes at P30 (C) and P45 (D).

5.5.3 Upregulation of inflammatory and apoptosis-related transcripts in *Cstb*$^{-/-}$ mice (unpublished)

Further investigation of the transcriptome data revealed that several inflammatory chemokines (CCL3, CCL4, CCL5, CCL6, CCL12, CXCL10, CXCL13 and CXCL16) were significantly upregulated in the synaptosomes of *Cstb*$^{-/-}$ mice (**Appendix 2**). These chemokines have all been reported to be induced following injury (Ludwig et al., 2005; Coelho et al., 2007; Sorce et al., 2011; Jiang et al., 2016; Popiolek-Barczyk et al., 2020; Watson et al., 2020), and their expression in neurons has been identified (de Haas et al., 2007; Jiang et al., 2016; Simats et al., 2018; Wang et al., 2018; Sowa and Tokarski, 2021). The expression levels of these chemokines varied, with some showing moderate increase (<4 fold; CXCL16) and others exhibiting very high levels (>150 fold; CXCL13), suggesting an ongoing innate immunological response. This has previously been observed at the morphological level in microglia and astrocytes of *Cstb*$^{-/-}$ mice (Tegelberg et al., 2012). Elevated expression of CXCL10 and CXCL13, both at the gene and protein levels, has been reported in cerebellar tissue lysates and serum (Joensuu et al., 2014; Okuneva et al., 2016), as well as CCL5 and CXCL10 expression in microglia from *Cstb*$^{-/-}$ mice (Korber et al., 2016).

In the transcriptome data, 27 of a total of 29 apoptosis-associated genes were upregulated in *Cstb*$^{-/-}$ synaptosomes (**Appendix 2**). These included anti-apoptotic B-cell lymphoma-2 (*Bcl-2*) family members, complement component 3 (*C3*), a critical mediator of synaptic remodeling after injury (Rahpeymai et al., 2006; Maier et al., 2008), and insulin-like growth factor-1 (*Igf1*), a promoter of repair processes in damaged tissue (Kooijman et al., 2009). Several of these proteins are predicted to be secreted or lysosomal in location (**Appendix 2**), including the inflammatory chemokines presented above, as well as lysosomal cathepsins, which are effector molecules of apoptosis (Repnik et al., 2012).

Taken together, the proteome and transcriptome data imply altered local protein translation in synaptosomes from P30 and P45 *Cstb*$^{-/-}$ mice, with immunity and apoptosis-related pathways activated.

6 DISCUSSION

EPM1 is a neurological disorder with progressive brain-specific manifestations. The underlying cause is explained by pathogenic variants of the CSTB gene, but pathological functions that could explain the onset and progression of the disease on cellular level have not been demonstrated.

When this doctoral dissertation was initiated, little was known about the CSTB-dependent cellular and molecular mechanisms of EPM1. CSTB is a known inhibitor of lysosomal cathepsins B, S, and L (Green et al., 1984; Rinne et al., 2002), and a pathological cathepsin B-mediated signaling mechanism in CSTB deficiency had been proposed based on four factors: first, the lysosome-associated localization of cytoplasmic CSTB (Alakurtti et al., 2005) suggested that CSTB inhibits the proteolytic activity of cathepsins as they leak into the cytoplasm (Turk et al., 2002); second, loss of CSTB results in increased cathepsin B activity in lymphoblastoid cells from EPM1 patients (Rinne et al., 2002) and in cerebellar granule neurons (Lehtinen et al., 2009) and neural progenitor cells (Daura et al., 2021) from *Cstb*$^{-/-}$ mice; third, cathepsin B overexpression sensitizes cerebellar granule neurons to oxidative stress -induced death in *Cstb*$^{-/-}$ mice, whereas its knockdown reduces oxidative stress -induced death (Lehtinen et al., 2009); and fourth, CSTB and cathepsin B double knockout mice exhibit less neurodegeneration compared to *Cstb*$^{-/-}$ mice (Houseweart et al., 2003a). Increased cathepsin B expression and activity have been reported in several neurodegenerative diseases that manifest diverse clinical symptoms and pathology, suggesting that cathepsin B has one or more functions that contribute to neurodegeneration and brain dysfunction (Hook et al., 2020). By contrast, cathepsin S expression is predominantly restricted to mature macrophages and microglial cells both in the brain and in the periphery (Liuzzo et al., 1999; Takayama et al., 2017), and its increased activity has been associated with elevated cytokine expression and microglial activation (Liuzzo et al., 1999; Wendt et al., 2008; Liu et al., 2025). Although upregulation of cathepsin S expression has been observed in brains of 8-month-old *Cstb*$^{-/-}$ mice (Lieuallen et al., 2001), coinciding with an advanced disease phenotype and widespread inflammation in the brain (Pennacchio et al., 1998; Tegelberg et al., 2012), cathepsin S likely contributes to CSTB deficiency through immune-mediated mechanisms rather than direct synaptic effects. Similarly, cathepsin L plays a

critical role in brain development through proteolytic processing of nuclear proteins involved in chromatin remodeling (Ceru et al., 2010; Daura et al., 2021). Cathepsin L acitivity is increased in chromatin-associated fractions from *Cstb*$^{-/-}$ brains, representing nuclear proteins, but not in whole-tissue lysates (Daura et al., 2021). Neither cathepsin S nor L were detected in the proteomic data of this study, suggesting that they contribute to disease pathogenesis through mechanisms distinct from those at the synapses.

Synapses are known to be particularly vulnerable to a broad range of stimuli, partly due to the compartmentalized structure of neurons (Wishart et al., 2006), but also to region-specific differences in organelles (Brown et al., 2006). Many neurodegenerative diseases are associated with disturbances in synaptic function that precede their structural degeneration (Gillingwater and Wishart, 2013), and such dysfunction has also been previously demonstrated in presymptomatic *Cstb*$^{-/-}$ mice (Joensuu et al., 2014). These observations prompted us to further investigate the characteristics of cerebellar synaptosomes of *Cstb*$^{-/-}$ mice in the early stages of disease pathology.

6.1 Linking early mitochondrial disruptions to disease pathogenesis in *Cstb*$^{-/-}$ mice

6.1.1 Impact of CSTB deficiency on synaptic mitochondria: Early alterations and delayed respiratory dysfunction

Synaptic mitochondria are morphologically, molecularly, and functionally distinct from non-synaptic mitochondria, exhibiting smaller size, unique proteomic profiles, and distinct enzymatic, antioxidant and calcium buffering properties (Lai et al., 1977; Bertoni-Freddari et al., 1993; Brown et al., 2006; Yarana et al., 2012; Graham et al., 2017). Our proteomic data revealed extensive alterations in synaptic mitochondria of both presymptomatic and early symptomatic *Cstb*$^{-/-}$ mice, suggesting that the impact of CSTB deficiency on synaptic mitochondria is both early and profound. The altered mitochondrial proteins were associated with processes critical for synaptic function (Tang et al., 2019), including ATP production, ROS metabolism, mitochondrial trafficking, and calcium signaling. Mitochondrial dysfunction has previously been linked to CSTB deficiency in neural progenitor cells from *Cstb*$^{-/-}$ mice, where mitochondrial gene expression and respiration were altered (Daura et al., 2021), and in primary bone marrow-derived macrophages from *Cstb*$^{-/-}$ mice, where mitochondrial membrane potential was unstable and mitochondrial ROS production increased (Maher et al., 2014).

Respirometry studies of synaptosomes showed that the respiratory capacity of synaptic mitochondria does not differ between *Cstb*$^{-/-}$ and wild type mice at

symptom onset but is significantly reduced in *Cstb*$^{-/-}$ mice shortly thereafter. This is of particular interest, as impaired mitochondrial respiration has been reported in neural progenitor cells from *Cstb*$^{-/-}$ mice during cell differentiation *in vitro*, which was preceded by a delayed activation of nuclear-encoded mitochondrial genes (Daura et al., 2021). Primary mitochondrial dysfunction has since been a potential candidate for the brain pathology associated with CSTB deficiency, although its status in differentiated cells has remained unclear. Neurons are known to survive dysfunction for prolonged periods of time, as evidence has been presented for a temporal discrepancy between the loss of mitochondrial gene expression, alterations in mitochondrial morphology, and the apparent onset of neurodegeneration (Sörensen et al., 2001; Ignatenko et al., 2018; Motori et al., 2020). Our data presented here demonstrate that although synaptic mitochondrial proteome remodeling occurs early, respiratory impairment is evident only after onset of clinical symptoms and neuronal apoptosis. Thus, the mitochondrial dysfunction likely contributes to neuronal loss, but it is unlikely that mitochondrial respiratory failure alone triggers the pathogenesis in CSTB deficiency.

Mitochondrial dysfunction is often associated with alterations in membrane dynamics or morphology, such as swelling (Fiskum et al., 2003; Bertholet et al., 2016). Despite a significant respiratory decline, we did not observe phenotypic alterations in the mitochondrial membrane ultrastructure, mtDNA copy number, or proteolytic cleavage of long isoforms of the regulatory protein OPA1, which would have been indications of primary mitochondrial dysfunction or early cellular stress (Duvezin-Caubet et al., 2006; Baker et al., 2014; Filograna et al., 2021). Proteome-level abundance of key factors coordinating mitochondrial membrane fission and fusion also showed no indications for changes in dynamics or integrity. Alterations in the abundance levels of proteins involved in OXPHOS and fatty acid metabolism were identified, which, in other experimental disease models, have been interpreted as metabolic adaptations compensating for impaired ATP production (Fukushima et al., 2015; Zabielski et al., 2016; Völgyi et al., 2017; Wang et al., 2022). As neuronal mitochondria have a low capacity to generate energy from fatty acids (Schönfeld and Reiser, 2013), such metabolic adaptations are however unlikely. Similar proteome-level alterations in crucial enzymes and transporters of carbohydrates, lipids, and amino acids have been previously reported in the early stages of Alzheimer's disease and Huntington's disease (Reiman et al., 2005; Powers et al., 2007). These findings collectively suggest that neurodegenerative disorders may involve a rewiring of mitochondrial metabolism during their early pathogenesis.

6.1.2 Integrating oxidative damage and metabolic alterations to CSTB deficiency

Beyond impairing cellular energy production, mitochondrial dysfunction is often associated with a phenotype caused by the accumulation of ROS-induced damage (Guo et al., 2013). Of these, increased lipid peroxidation and antioxidant depletion have been observed in the brains of older, symptomatic *Cstb*$^{-/-}$ mice (Lehtinen et al., 2009). Our proteomics data showed that ROS scavengers superoxide dismutase, glutathione peroxidase, catalase, and thioredoxin are altered in synaptosomes of presymptomatic mice, linking already the early pathology of CSTB deficiency to altered ROS metabolism.

ROS are known to damage the integrity of cell and organelle membranes, including lysosomes (Su et al., 2019). Lysosomal membrane permeabilization leads to the release of cathepsins and other proteases into the cytoplasm (Yang et al., 1998; Kurz et al., 2006; Boya and Kroemer, 2008), which, depending on the extent of the damage, can result in controlled proteolysis at specific subcellular sites (Stahl-Meyer et al., 2021) or trigger apoptosis (Yang et al., 1997). Recent findings have demonstrated that lysosomal membrane disruption leads to the release of cathepsins B and L, triggering metabolic reprogramming characterized by mitochondrial proteome remodeling, metabolic alterations, and OXPHOS impairment in a human iPSC-derived macrophage model (Bussi et al., 2022). These observations are highly relevant to our study, as elevated lysosomal cathepsin activity is a predicted consequence of CSTB loss and has been detected in lymphoblastoid cells from EPM1 patients (Rinne et al., 2002), as well as in cerebellar granule neurons (Lehtinen et al., 2009) and neural progenitor cells (Daura et al., 2021) from *Cstb*$^{-/-}$ mice. In our experiments, we identified comparable proteomic, metabolic, and functional alterations in synaptosomes from *Cstb*$^{-/-}$ mice. Notably, these changes occurred in the absence of morphological pathology, suggesting that they may arise from metabolic reprogramming rather than degenerative processes. It is well-known that macrophages undergo metabolic reprogramming when activating immune responses or releasing cytokines in the brain (Bernier et al., 2020). Given that the expression levels of neuronal cytokines, having functions that remain incompletely understood (Rostène et al., 2007; Sowa and Tokarski, 2021), were significantly elevated in our transcriptome data, we cannot exclude their potential contribution to the observed metabolic alterations.

6.2 Inflammatory changes in *Cstb*$^{-/-}$ mice: Implications for synaptic pathology

6.2.1 The role of inflammatory signaling and autophagy impairment in CSTB-deficiency

Neuroinflammation is a common finding in neurodegenerative disorders and their animal models (Ransohoff, 2016), including EPM1 (Pennacchio et al., 1998; Shannon et al., 2002; Tegelberg et al., 2012; Okuneva et al., 2016). Widespread alterations in inflammatory signaling have been identified in several CSTB-deficient models, such as cultured microglia from *Cstb*$^{-/-}$ mice (Korber et al., 2016), serum of adult, symptomatic *Cstb*$^{-/-}$ mice after peripheral LPS injection (Maher et al., 2014), and here in synaptosomes from *Cstb*$^{-/-}$ mice cerebella (**Appendix II**). Our transcriptome data show a significant upregulation of immunological cytokines and chemokines at the early symptomatic phases of CSTB deficiency, for example in the expression level of the chemokine CXCL13, which was more than 150-fold higher in *Cstb*$^{-/-}$ mice than in controls. Increased CXCL13 levels have previously been reported in cerebellar tissue lysates and serum of *Cstb*$^{-/-}$ mice at both the transcript and protein levels (Joensuu et al., 2014; Okuneva et al., 2016; Gumusgoz et al., 2023). The data presented here suggest that CXCL13 is also synthetized and secreted from *Cstb*$^{-/-}$ neurons. Previously, CXCL13 expression has been observed following pathological injury in spinal neurons and sensory neurons of the dorsal root ganglia (Jiang et al., 2016; Zhou et al., 2022), where it activates astrocytes and inhibits axonal regeneration (Jiang et al., 2016; Zhou et al., 2022). These results suggest that neuronal immune factors also contribute to the development and progression of CSTB deficiency-induced pathology in the brain.

Cells from *Cstb*$^{-/-}$ mice are more sensitive to oxidative stress-induced events compared to control cells. For example, hydrogen peroxide increases the susceptibility of cerebellar granule neurons to cell death (Lehtinen et al., 2009), and LPS causes increased mitochondrial membrane instability, elevated ROS levels, increased expression of antioxidant proteins, and activation of the nucleotide-binding domain, leucine-rich–containing family, pyrin domain–containing-3 (NLRP3) inflammasome in bone marrow-derived macrophages from *Cstb*$^{-/-}$ mice (Maher et al., 2014; Trstenjak Prebanda et al., 2019). The NLRP3 inflammasome induces inflammation and pyroptotic cell death, and its activation has been identified as a cause of chronic inflammation in several common diseases, including Alzheimer's and Parkinson's diseases (Bruchard et al., 2013; Stahl-Meyer et al., 2021). The mechanism of NLRP3 activation is controversial, but two partially overlapping models have been described: a lysosomal and a mitochondrial model. The mitochondrial model proposes that activation is mediated by mitochondrial ROS, while the lysosomal model suggests that activation is mediated by cathepsin

B, released from damaged lysosomes (Bruchard et al., 2013; Stahl-Meyer et al., 2021; Xie et al., 2023), which proteolytically activates nuclear factor kappa-B (NF-kappa-B), a key activator of inflammation (Biasizzo and Kopitar-Jerala, 2020). The lysosomal model is particularly relevant, as cathepsin B is a target of CSTB inhibition and its increased activity has been observed in various CSTB-deficient cells (Rinne et al., 2002; Lehtinen et al., 2009; Daura et al., 2021). This model is further supported by the fact that cathepsin B inhibition has shown protective effects in animal models of neurodegenerative diseases, such as reduction in brain cytokine levels (Hoegen et al., 2011), linking cathepsin B activity to a broader immunological response in the brain.

The role of NF-kappa-B in inflammation is complex. It functions as a key activator of autophagy, one of the major protein and organelle degradation mechanisms in cells (Hara et al., 2006; Komatsu et al., 2006; Kuijpers et al., 2021). Autophagy, among others, prevents NLRP3 inflammasome activation and excess inflammation (Zhong et al., 2016) by removing inflammasome components, cytokines, and ROS (Biasizzo and Kopitar-Jerala, 2020; Deretic, 2021). However, NF-kappa-B also induces the expression of Bcl-2 family genes, which are negative regulators of autophagy (Pattingre et al., 2005). Impairments in autophagic flux, a measure of degradation activity, have been associated with CSTB deficiency (Polajnar et al., 2014) as well as several other neurodegenerative disorders (Klionsky et al., 2021). Consistent with these findings, the proteomic and transcriptomic data presented here suggest that autophagy disruption is also present in synaptosomes of *Cstb*$^{-/-}$ mice. Such dysfunction can cause pathological accumulation of proteins and organelles (Guo et al., 2018), leading, among others, to the progressive impairment of mitochondrial function presented in study II, due to slower mitochondrial turnover and ultimately less functional mitochondria (Wang et al., 2023). Dysfunctional autophagy can also lead to diseases with hyperinflammation and excessive activation of the NLPR3 inflammasome (Biasizzo and Kopitar-Jerala, 2020), possibly through cathepsin B, which is a negative regulator of lysosome and autophagosome dynamics (Man and Kanneganti, 2016; Qi et al., 2016). A further association between CSTB and autophagy has been demonstrated in macrophages from mice with trisomy of the *Cstb* gene, in which autophagy is upregulated and inflammatory responses are reduced upon LPS-induced inflammation (Trstenjak-Prebanda et al., 2023). This effect may be mediated by CSTB-dependent inhibition of the mechanistic target of rapamycin (mTOR) signaling pathway, whose activity is reduced in this model (Trstenjak-Prebanda et al., 2023) and which also promotes NLRP3 inflammasome activation.

6.2.2 Early-stage inflammation and its effects on neuronal plasticity in CSTB deficiency

The inflammatory phenotype of microglia and astrocytes, along with the presence of inflammatory mediators, is notably higher in the brains of *Cstb*$^{-/-}$ mice during development and the early stages of CSTB deficiency, compared to the more advanced stages of the disease, when signs of inflammation appear to be reduced (Tegelberg et al., 2012; Okuneva et al., 2015, 2016; Gumusgoz et al., 2023). An early presence of inflammatory mediators in the developing brain is known to impact intracellular metabolic pathways in neurons and glia, shifting energy production between glycolysis, OXPHOS, amino acid, and/or fatty acid metabolism (Bernier et al., 2020; Mitra et al., 2022). This raises the question of whether such metabolic shifts could as a consequence alter neural circuits, contributing to the clinical symptoms and neuropathological findings observed in EPM1 patients and *Cstb*$^{-/-}$ mice. Early inflammation is known to affect synaptic plasticity at both the morphological and physiological levels (Citri and Malenka, 2008; Mottahedin et al., 2017), but these have not been investigated in the *Cstb*$^{-/-}$ mouse.

Microglial activation and the release of inflammatory mediators during postnatal development can impact fundamental physiological processes of the neurons, including axonal growth, intracellular transport, and autophagy (Monje et al., 2003; Alirezaei et al., 2008; Favrais et al., 2011). We found proteome-level indications of alterations in these processes in presymptomatic *Cstb*$^{-/-}$ mice. The presence of immunological mediators at various stages of brain development is known to trigger different long-term responses: for example, an immunological response induced during a critical postnatal neurodevelopmental period can predispose rats to increased susceptibility to seizures, cytokine release, and neuronal degeneration in adulthood (Galic et al., 2008; Somera-Molina et al., 2009; Zipp et al., 2023). Furthermore, early postnatal infections in rats have been shown to prime the brain for a second immune challenge in adulthood, leading to altered cytokine responses, persistent microglial activation, transient proliferation of activated microglia, dysregulated neurogenesis, and adverse brain development (Bilbo et al., 2005; Du et al., 2011; Smith et al., 2014). Many of these effects have been described in patients and disease models of CSTB deficiency (Lehesjoki and Kälviäinen, 2020; Pennacchio et al., 1998; Tegelberg et al., 2012; Joensuu et al., 2014; Okuneva et al., 2015; Körber, 2016; Mancini et al., 2016; O'Brien et al., 2017; Di Matteo et al., 2020; Daura et al., 2021; Pizzella et al., 2023; Pollari et al., 2023). This makes early-life neuron-glia interactions in CSTB deficiency a particularly intriguing area for further investigation.

6.3 Implications of synaptic dysfunction in *Cstb*$^{-/-}$ mice

6.3.1 Exploring the basis for GABAergic changes in *Cstb*$^{-/-}$ mice

At the time of the initiation of this thesis work, available evidence from EPM1 patients and *Cstb*$^{-/-}$ mice suggested that disturbances in inhibitory GABAergic signaling could be a contributing factor to the clinical symptoms of EPM1 (Airaksinen and Leino, 1982; Franceschetti et al., 2007; Buzzi et al., 2012; Joensuu et al., 2014; Silvennoinen et al., 2023), a known dysfunction in epilepsy (Treiman, 2001). Early changes affecting the inhibitory GABAergic signaling pathway have been previously described on multiple levels in the presymptomatic and early symptomatic *Cstb*$^{-/-}$ mouse cerebellum, including reduced postsynaptic GABAergic currents and completely absent GABAergic bursts in Purkinje cells, reduced immunostaining of GABAergic synapse markers, increased expression of extrasynaptic $GABA_A$ receptor genes, and reduced ligand binding to $GABA_A$ receptors (Joensuu et al., 2014). Dysfunction of this signaling pathway has since been considered a potential candidate for the seizure phenotype, particularly since GABA-related changes, with a progressive loss of GABAergic interneurons, hyperexcitability, and increased susceptibility to kainate-induced seizures, has also been described in the brains of older *Cstb*$^{-/-}$ mice with an advanced disease phenotype (Franceschetti et al., 2007; Buzzi et al., 2012).

Previous studies have not determined whether GABAergic disturbances in *Cstb*$^{-/-}$ mice are a result of (i) transient alterations in the maturation of GABAergic synapses and subsequent changes in GABA activity that evolve over time, or (ii) persistent developmental changes in the formation of GABAergic neural networks that continue into adulthood. In our proteomic data from synaptosomes of presymptomatic and early symptomatic *Cstb*$^{-/-}$ mice, we observed a consistent depletion of the GABA transporter protein GAT-1, which in a GAT-1-deficient mouse model has similar clinical, electrophysiological, and cellular manifestations as reported in *Cstb*$^{-/-}$ mice (Pennacchio et al., 1998; Chiu et al., 2005; Joensuu et al., 2014). GAT-1-deficient mice show increased $GABA_A$ receptor-mediated tonic conductance in cerebellar Purkinje and granule cells due to impaired GABA uptake and elevated extracellular GABA levels (Chiu et al., 2005), an electrophysiological feature not previously studied in *Cstb*$^{-/-}$ mice. Our electrophysiological recordings of GAT-1 function were conducted in cerebellar granule neurons from presymptomatic and early symptomatic *Cstb*$^{-/-}$ mice, reflecting different stages of cerebellar maturation and disease progression. The data revealed no changes in the functional activity of GAT-1 at either age point. Persistently reduced GABAergic postsynaptic currents would typically be reflected in ambient GABA concentrations and tonic conduction in both Purkinje and granule cells (Kaneda et al., 1995; Brickley et al., 1996; Wall and Usowicz, 1997; Chiu et al., 2005; Guo et al., 2016).

Thus, our results suggest that the previously observed electrophysiological changes in Purkinje cells of developing *Cstb*$^{-/-}$ mice are not permanent. Our observations are further supported by previous findings showing reduced immunostaining of GABAergic synapse markers during cerebellar development in *Cstb*$^{-/-}$ mice, as these markers reach control levels by one month of age (Joensuu et al., 2014). On a functional level, however, the reduced GABAergic currents and bursts during synapse formation, strengthening, and elimination likely influence the emergence and decay of neural network connections (Peerboom and Wierenga, 2021), as for example, loss of GABAergic inputs leads to autophagic $GABA_A$ receptor turnover at the postsynapse (Rowland et al., 2006).

6.3.2 Unraveling the mechanisms for synaptic dysfunction in CSTB deficiency

Neural progenitor cells from *Cstb*$^{-/-}$ mice and EPM1 patient-derived cerebral organoids differentiate prematurely (Di Matteo et al., 2020; Daura et al., 2021; Pizzella et al., 2023), but the development and maturation of physiological functions in synapses appear to be delayed (Pizzella et al., 2023). CSTB deficiency has been associated with early synaptic and cytoskeletal alterations at both the transcriptome and morphological levels (Joensuu et al., 2014; Pizzella et al., 2023). In EPM1 patient-derived neurons, this exhibits as longer and more branched neurites, with more intersections and nodes (Pizzella et al., 2023).

Our studies in (i) presymptomatic, (ii) early symptomatic, and (iii) symptomatic *Cstb*$^{-/-}$ mice were performed at different stages of postnatal development. At the presymptomatic stage, cerebellar maturation is incomplete, with neuronal axons growing, synaptic contacts forming, and excess synapses being eliminated (Ackerman, 1992; Schafer and Stevens, 2010), representing a phase critical for establishing neural circuits. By the early symptomatic and symptomatic stages, cerebellar maturation is considered complete in terms of development and electrophysiological spike firing patterns (Arancillo et al., 2015; Leto et al., 2016; Sathyanesan et al., 2019).

Our findings are consistent with previous studies (Joensuu et al., 2014; Polajnar et al., 2014; Pizzella et al., 2023), showing alterations in several proteins related to the microtubule-based axonal protein and organelle transport systems, local protein synthesis, endolysosomes and autophagy, extracellular vesicle-mediated export, and the synaptic vesicle cycle. These processes are pivotal for the maintenance of synaptic protein homeostasis and plasticity, and deficiencies can not only lead to pathological accumulation of dysfunctional proteins and organelles, but also to morphological and functional deficits (Deng et al., 2017; Glock et al., 2017; Berth and Lloyd, 2023). For example, elevated autophagy in neuronal precursor cells has been linked to reduced neuron number, suppressed axon

growth, and inhibition of neurite outgrowth (Ban et al., 2013; Chen et al., 2013; Ka et al., 2017), demonstrating the regulatory effects of autophagy on axonal morphogenesis and cytoskeletal structures. Particularly notable is the association between CSTB deficiency and synaptic vesicles, extracellular vesicles, and endolysosomes, as these organelles physiologically originate from the same endosomal system (van Niel et al., 2018) and have been linked to CSTB deficiency in previous independent studies (Joensuu et al., 2014; Polajnar et al., 2014; Pizzella et al., 2023).

6.4 Strengths and limitations of the research

While the research presented in this thesis provides valuable insights into the synaptic physiology of CSTB deficiency, it is crucial to acknowledge both its strengths and limitations. These affect the robustness of the conclusions and the interpretation and generalization of the findings, respectively, to fully understand its contribution to the field and its implications for future research.

Strengths:

1. **Comprehensive experimental design:** The research employs a combination of *in silico* and *in vitro* methodologies, including proteomics, transcriptomics, electrophysiology, respirometry, and molecular biology methods to investigate synaptic function. This multi-method approach enhances the robustness of findings, allowing for a thorough evaluation of synaptic physiology from multiple angles.

2. **Cutting-edge techniques:** The application of state-of-the-art techniques significantly reduces the risk of interpretation biases and provides unprecedented insight into physiological and pathological states of CSTB deficiency: mass spectrometry and transcriptomics provides in-depth information on protein and gene abundance, and their molecular processes; electron microscopy enables high-resolution visualization of mitochondrial morphology and dynamics; respirometry enables detailed analysis of mitochondrial bioenergetics; and electrophysiological recordings facilitate detailed capture of neuronal activity with high temporal and spatial resolution.

3. **Proteomic and transcriptomic profiling:** Using quantitative proteomics and transcriptomics, this research provides a comprehensive and unbiased analysis of synaptic protein and transcript expression in CSTB deficiency. This approach not only identifies previously known proteins and

transcripts, but also uncovers novel candidates involved in synaptic dysfunction and neurodegeneration, thereby advancing our understanding of synaptic physiology.

4. **Time-point analysis:** The longitudinal design of the research's functional experiments, which includes multiple time points across different stages of disease progression, provides valuable insight into the temporal dynamics of disease progression.

5. **Reproducibility:** The research was conducted using standardized or thoroughly reported protocols and strict quality control measures to ensure that the findings are reproducible by other researchers or in other experimental models.

Limitations:

1. **Sample size:** Although the research includes multiple experimental conditions, the sample size was limited due to the availability of the animal model. *Cstb*$^{-/-}$ mice presents significant breeding challenges, as the mice typically produce small litters and maternal infanticide is frequently observed, further reducing the number of viable offspring available for experimentation. A larger cohort would increase the statistical power of the analysis and provide a more accurate representation of the variability in the data. However, while the small sample size is a limitation, it is important to note that the results still provide novel insights into CSTB deficiency, and future studies with larger cohorts are needed to validate these findings and establish their broader relevance.

2. **Temporal resolution:** Although the research spans multiple time points, the earliest time point captures cerebellar development, which poses challenges for studying disease progression. Sampling frequency could be increased both during cerebellar development and later stages of the disease to provide more detailed information on, for example, aberrant mitochondrial function. This would provide a clearer picture of the early progression of mitochondrial dysfunction and its impact on synaptic physiology.

3. **Data interpretation and technical limitations:** The transcriptomic analysis performed in this thesis provides valuable insights of local protein synthesis. However, the research is limited to the transcript level, which may lead to misinterpretation of local protein production, which was not

investigated here. Furthermore, although attempt was made to isolate pure synaptosomal preparations for RNA extraction, the presence of contaminating RNA from glial cells cannot be excluded. This is evidenced by the detection of the oligodendrocyte marker *Plp1* in the transcriptome data from P45 mice. However, the general trends observed in our transcriptomic findings are in line with previous literature, suggesting that the results are robust. Future studies may alleviate these limitations by employing ribosomal footprinting analysis, which would allow the identification of actively translated synaptic genes and provide a deeper understanding of translation efficiency and dynamics in CSTB-deficient synaptosomes.

4. **Generalizability of findings:** Much of the data in this dissertation is observational, and further functional studies would be needed to understand their physiological relevance. Furthermore, although the use of the *Cstb*$^{-/-}$ mouse model offers valuable insights of CSTB deficiency-associated pathology, the findings may not fully translate to human disease. Further studies using human-derived cell lines or post-mortem brain tissue would be necessary to confirm whether similar alterations occur in EPM1.

In conclusion, while there are some limitations related to sample size and methodological constraints, the strengths of this research, particularly the innovative approach and comprehensive data collection, provide a strong foundation for future studies on CSTB deficiency.

7 CONCLUSIONS AND FUTURE PROSPECTS

In this dissertation, we identified early and novel roles for synaptic physiology in CSTB deficiency-related disease. Our findings provide new insights into the onset and development of neuronal pathology and demonstrate that early mitochondrial proteomic alterations can result in organelle dysfunction at the synapse. Previous studies have reported early molecular and biological changes during cerebellar maturation despite symptom onset occurring around one month of age, our study supporting and extending these observations of early changes and providing further information on their effects.

Traditionally, mitochondrial dysfunction has been associated with genetic, structural, or biochemical defects. While this remains true for many mitochondrial diseases, our findings demonstrate that early proteomic alterations may predict later-onset mitochondrial impairment. This dysfunction is likely to compromise key energy-demanding synaptic processes, including the synaptic vesicle cycle and protein turnover. Mitochondrial gene expression is altered already in neuronal progenitor cells of *Cstb*$^{-/-}$ mice, accompanied by reduced mitochondrial respiration during cell differentiation, a critical developmental window when OXPHOS capacity increases under physiological conditions. Our data indicate that the previously detected developmental mitochondrial dysfunction is not a persistent primary defect: mitochondrial respiration levels appear comparable to control levels at the time of symptom onset at one month of age but declines thereafter. Understanding the progression and potential triggers of this dysfunction, such as lysosomal cathepsins or inflammatory cytokines, both for example promoting ROS production, will be essential to clarify the role of mitochondria in *Cstb*$^{-/-}$ pathology. Moreover, given the sensitivity of the postnatal cerebellar development to metabolic disruption, it will be important to investigate how transient developmental mitochondrial impairment may affect neuronal maturation.

Neuroinflammation emerges as the earliest detectable pathophysiological change in brains of presymptomatic *Cstb*$^{-/-}$ mice, initiated with microglial activation from postnatal day 14 (P14), followed by astrocyte activation and increased expression of proinflammatory markers from one month of age. This dissertation further reveals that *Cstb*$^{-/-}$ neurons themselves express inflammatory mediators, contributing to the neuroinflammation. The expression levels of cytokines are comparable to those previously reported, with CXCL13 being the most highly

expressed. While the upstream triggers and downstream functions of neuronal cytokine expression remain unresolved, further research is needed to determine how these mediators contribute to disease progression. Understanding neuroinflammation in CSTB deficiency requires a dual perspective: its role during development and in the mature brain. In the mature brain, questions remain regarding the physiological consequences of neuronal cytokines: for example, do they influence synaptic function through modulation of physiological functions including metabolism, local protein synthesis, or protein/organelle turnover? Are there receptor-mediated interactions between neurons and glial that drive further pathology? Although this dissertation did not investigate developmental neuroinflammation, future research should explore its potential impact on cerebellar development, neuronal migration, synaptic plasticity, and network formation. Such studies could also address whether early-life inflammation in CSTB deficiency contributes to long-term outcomes, as observed in other models of developmental infection or immune activation.

Integrating proteomic, transcriptomic, and functional analyses, this dissertation highlights alterations in mitochondrial function, the synaptic vesicle cycle, protein turnover, and expression of neuronal inflammatory mediators. Notably, one of the central aims of this dissertation was to further investigate GABAergic signaling in CSTB deficiency, as reduced GABAergic currents had previously been reported in Purkinje cells from *Cstb*$^{-/-}$ mice at P7. From the proteomics analyses, the GABA transporter protein GAT-1 emerged as a potential candidate for further investigation. However, electrophysiological recordings at P14 and P30 showed no significant differences in GABAergic properties between *Cstb*$^{-/-}$ and control mice. These findings suggest that the previously observed GABAergic deficits are transient and related to development, although their impact on cerebellar maturation warrants further investigation.

While many open questions remain, this work suggests an early interplay between mitochondrial dysfunction, neuroinflammation, and synaptic physiology in *Cstb*$^{-/-}$ mice, providing a foundation for future studies that aim to understand how early molecular disturbances give rise to the complex neurodegenerative phenotype associated with CSTB deficiency. Future directions should focus on dissecting the temporal progression of mitochondrial and inflammatory alterations, exploring neuron-glia interactions, and determining how these early changes influence long-term neuronal health and network function.

Acknowledgements

This thesis work was carried out at Folkhälsan Research Center and the department of Medical Genetics, University of Helsinki. Professor Anna-Elina Lehesjoki, Head of the Research Center, is acknowledged for providing excellent research facilities and resources. The work was financially supported by Folkhälsan Research Foundation, the Doctoral Programme in Biomedicine (DPBM) of the Doctoral School in Health Sciences, the Finnish Concordia Fund, Epilepsiatutkimussäätiö, the Chancellors travel fund of the University of Helsinki, and grants to the research group from the Sigrid Jusélius Foundation and Medicinska Understödsföreningen Liv och Hälsa r.f.

I wish to express my sincerest gratitude to my supervisors, Professor Anna-Elina Lehesjoki, Adjunct Professor Brendan Battersby, and the late Adjunct Professor Outi Kopra. Anna-Elina, your wide knowledge and enthusiasm for EPM1 research are admirable, as is your commitment to keeping the scientific focus on patients. I thank you for welcoming me into your group, for trusting me with the challenging projects that ultimately formed this dissertation, and for the freedom to pursue my own research paths. Your support, openness to discussion, and availability have meant a great deal. Brendan, your never-ending enthusiasm for science is inspiring, as are your kindness, patience, and support. I thank you for providing new and exciting insight into the projects that evolved into central elements of this dissertation. I admire your wide-ranging knowledge, your practical advice, and your "just-do-it" attitude. But above all, I am deeply grateful for your guidance and encouragement during the most difficult time: after Outi's passing, you took on the challenge of diving into the complex world of EPM1 and my unfinished projects. And for that, I am eternally thankful. Outi, you were the spark behind this journey. Your brave, curious, and direct approach to science was inspirational, as well as your kindness and outspoken nature. I thank you for your ideas, support, and hands-on help isolating those very first synaptosome samples. I hope this work makes you proud, even though it did not focus on your favorite topics, calcium signaling or cathepsin inhibition. Cheers to you, wherever you may be.

I warmly thank Professor Sara Mole for accepting the role of official opponent, and Professor Annakaisa Haapasalo and Adjunct Professor Nataša Kopitar-Jerala for

their valuable time and thoughtful evaluation as thesis reviewers. Your encouraging comments and thoughts meant a lot and have left a meaningful mark on the final work. Professor Katariina Öörni is thanked for serving as Custos and for her advice on the public examination. I also wish to thank thesis committee members Aija Kyttälä and Claudio Rivera for their helpful advice and critical-yet-supporting comments during follow-up meetings. I have truly enjoyed the vivid discussions and enthusiastic atmosphere in those sessions.

I warmly thank all co-authors and collaborators for their invaluable contributions as this dissertation would not have been possible without your collective expertise. Chris Jackson, I admire your optimism, skills, and drive. In moments of doubt (there were many of them), you believed in the data and convinced me to do the same. I will never forget the excitement of receiving the respirometry data showing mitochondrial dysfunction in *Cstb*$^{-/-}$ mice. Tuula Nyman, I thank you for the seamless collaboration throughout the projects. Your kindness and patience amazed me every time I came to you with a technical proteomics-related question, and collaboration with you has truly been a joy. Albert Spoljaric, your enthusiasm, dedication, and expertise in the electrophysiological experiments in Study I were invaluable. I appreciate these, as well as the entertaining and educational electrophysiology recordings in Viikki. Professor Kai Kaila, I thank you for your guidance and expertise in GABAergic signaling, which was critical for interpreting the results and shaping the conceptual framework in Study I. Veronika Rezov, I am grateful for your skilled help in Study II. It was a great relief to pass on part of the project to such capable hands. I also thank Anne Rokka from the Turku Proteomic center and the staff at the Laboratory Animal Centre of University of Helsinki for their flexible, always kind, and professional cooperation.

I also wish to acknowledge collaborators from projects that did not make it until submission but were meaningful parts of this journey. Thank you, Martyn James (FuGu) and Anni Laari (Biosite), for your invaluable assistance in isolating synaptosomal RNA. Juho Väänänen (FuGu), thank you for performing and explaining the data analysis for the synaptosomal RNA sequencing project, whose results are published in this thesis. Esa Korpi and Elena de Miguel, thank you for the collaboration on the GABA study. I am sorry that the efforts did not make it to submission, although the results were highly interesting. Additionally, I thank Tiina and Hanna (Fugu) for assistance in the lentivirus project; Carina von Schanz-Fant (FIMM) for the chemical screening project; Susanna Narkilahti for the MEA project; and Maciej Lalowski and Rabah Soliymani for the initial proteomics analyses.

To all past and present members of the Lehesjoki group, thank you for your support and inspiration throughout these years. Saara Tegelberg, I want to express my special gratitude to you, as you always found the time for scientific and nonscientific discussions and spent countless hours helping me with immunostainings, microscopy, mouse brain preparations, vector graphics, adobe software, antibodies, wedding invitations, and so much more. Tarja Joensuu, thank you for sharing your extensive knowledge on the molecular biology of EPM1, all the discussions in your office, and the smooth management of administrative matters. Paula Hakala, thank you for all the technical help, advice on various laboratory methods, being the official pimp of *Cstb*$^{-/-}$ mice, and for inspirational discussions. Eduard Daura Sarroca, thank you for the shared journey towards a doctoral degree, for your technical assistance, and your kind and encouraging words. I hope to have absorbed some of your never-ending ideas and enthusiasm during these years. Carina Lund, thank you for your friendship, scientific and nonscientific discussions, and joint frustration on proteomics data. I also warmly thank past group members Inken Körber, Olesya Okuneva, Mervi Kuronen, Otto Manninen, Anni Laari, Henna Kallo, Erika Kuosa, Katri Aksentjeff, Julia Eriksson, Joska Pulkki, Marina Díaz, Iuliia Savenko, and Francesca Simonetti for your help on technical issues, scientific conversations, and helping hands.

My warmest thanks go to Sonja Jansson, Jaakko Sarparanta, pH Jonson, Ann-Liz Träskelin, Marjatta Valkama, Vilma-Lotta Lehtokari, Peter Hackman, Uwe Richter, Brendan Battersby, Carolina Courage, Joni Turunen, Teija Toivonen, Helena Luque, Pauliina Repo, Mira Aronen, Katri Aksentjeff, Taru Hilander, Paula Marttinen, Johanna Lehtonen, Janne Purhonen, Jukka Kallijärvi, Minna Pekkinen, Mari Tervaniemi, Outi Elomaa, Sampo Koivunen, Mridul Johari, my dear office mates Kirsi Määttä, Sandra Barck, Sabita Kawan, and Annamari Immonen, and many more, for help on technical issues, scientific conversations, lunch company, reagents, helping hands, much needed hugs, and friendship. I also wish to thank all past and present members of Folkhälsan Research Center for the supportive workplace atmosphere, as well as a bunch of people who, in one way or another, made a difference: Vanessa Fuller, Juha Voipio, Heidi Repo, Liisa Kauppi, and the staff at the Viikki PhD office.

My dear friends Pauliina Repo, Mira Aronen, Carolina Courage, and Riikka Mäkitie, your friendship and support throughout the years have been invaluable. Pauliina and Mira, you make every day at work brighter. Thank you for sharing discussions, lunches, coffee breaks, Zoom calls, gardening fairs, pastry baking, motherhood, and life in general. Caro, thank you for the many special discussions we have had, I hold them close to my heart. I admire your kindness, quirky humor, and professionalism in science, and I appreciate the time shared with you. Riikka, it was a privilege to

share an office, early mornings, and the journey towards a PhD with you. Your excitement for science and drive to success is admirable, and your friendship is no less important.

To past colleagues from the Battersby and Wartiovaara groups, Saara Forsström, Joni Nikkanen, Sofia Ahola, Uwe Richter, Mervi Kuronen, Olesia Ignatenko, Chris Carroll, Riikka Jokinen, Paula Marttinen, Maarit Myöhänen, Antti Muranen and many more: thank you for your friendship and for being inspirational role models throughout these years. It still amazes me how many wonderful people worked under the same roof at the same time.

To my dear friends outside academia, Michelle Sahal-Estimé, Karen Ahlnäs, Carina Lund, Emilie Kvist, Aura Lindeberg, and Minea Berg: thank you for your continued support, perspectives, and the much-needed distraction to the sometimes very overwhelming PhD life. I am lucky to have you.

Finally, I wish to thank my family for their support throughout these years. To my parents, siblings, and extended families, thank you for your encouragement and interest. To my partner and children, the patience, perspective, and joy you have brought to my life have meant more than words can express.

Helsinki, October
2025

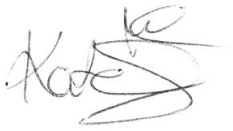

References

Abada, A., Levin-Zaidman, S., Porat, Z., Dadosh, T., and Elazar, Z. (2017). SNARE priming is essential for maturation of autophagosomes but not for their formation. *Proc. Natl. Acad. Sci. U. S. A.* 114, 12749–12754. doi: 10.1073/pnas.1705572114

Abdel-Hamid, M. S., Abdel-Ghafar, S. F., Sayed, I. S. M., Zaki, M. S., and Abdel-Salam, G. M. H. (2025). Delineating the Clinical and Brain Imaging Characteristics of the Neonatal Form of CSTB -Related Neurodevelopmental Disorders. *Clin. Genet.* 108, 184–193. doi: 10.1111/cge.14720

Ackerman, S. (1992). *Discovering the brain*. Washington, D.C: National Academy Press.

Aebersold, R., and Mann, M. (2003). Mass spectrometry-based proteomics. *Nature* 422, 198–207. doi: 10.1038/nature01511

Aebersold, R., and Mann, M. (2016). Mass-spectrometric exploration of proteome structure and function. *Nature* 537, 347–355. doi: 10.1038/nature19949

Airaksinen, E. M., and Leino, E. (1982). Decrease of GABA in the cerebrospinal fluid of patients with progressive myoclonus epilepsy and its correlation with the decrease of 5HIAA and HVA. *Acta Neurol. Scand.* 66, 666–672. doi: 10.1111/j.1600-0404.1982.tb04531.x

Alakurtti, K., Virtaneva, K., Joensuu, T., Palvimo, J. J., and Lehesjoki, A. E. (2000). Characterization of the cystatin B gene promoter harboring the dodecamer repeat expanded in progressive myoclonus epilepsy, EPM1. *Gene* 242, 65–73. doi: S0378-1119(99)00550-8%20%5Bpii%5D

Alakurtti, K., Weber, E., Rinne, R., Theil, G., Haan, G.-J. de, Lindhout, D., et al. (2005). Loss of lysosomal association of cystatin B proteins representing progressive myoclonus epilepsy, EPM1, mutations. *Eur. J. Hum. Genet. EJHG* 13, 208–215. doi: 10.1038/sj.ejhg.5201300

Alirezaei, M., Kiosses, W. B., Flynn, C. T., Brady, N. R., and Fox, H. S. (2008). Disruption of neuronal autophagy by infected microglia results in neurodegeneration. *PloS One* 3, e2906. doi: 10.1371/journal.pone.0002906

Alquier, T., Christian-Hinman, C. A., Alfonso, J., and Færgeman, N. J. (2021). From benzodiazepines to fatty acids and beyond: revisiting the role of ACBP/DBI. *Trends Endocrinol. Metab. TEM* 32, 890–903. doi: 10.1016/j.tem.2021.08.009

Amunts, K., and Zilles, K. (2015). Architectonic Mapping of the Human Brain beyond Brodmann. *Neuron* 88, 1086–1107. doi: 10.1016/j.neuron.2015.12.001

Anadolu, M. N., Sun, J., Kailasam, S., Chalkiadaki, K., Krimbacher, K., Li, J. T.-Y., et al. (2023). Ribosomes in RNA Granules Are Stalled on mRNA Sequences That Are Consensus Sites for FMRP Association. *J. Neurosci. Off. J. Soc. Neurosci.* 43, 2440–2459. doi: 10.1523/JNEUROSCI.1002-22.2023

Anderson, B. W., Kortz, M. W., Black, A. C., and Al Kharazi, K. A. (2023). "Anatomy, Head and Neck, Skull," in *StatPearls*, (Treasure Island (FL): StatPearls Publishing). Available at: http://www.ncbi.nlm.nih.gov/books/NBK499834/ (Accessed October 31, 2023).

Andrews, S. (2010). *FastQC: a quality control tool for high throughput sequence data*. Babraham Bioinformatics, Babraham Institute, Cambridge, United Kingdom.

Arancillo, M., White, J. J., Lin, T., Stay, T. L., and Sillitoe, R. V. (2015). In vivo analysis of Purkinje cell firing properties during postnatal mouse development. *J. Neurophysiol.* 113, 578–591. doi: 10.1152/jn.00586.2014

Araque, A., Parpura, V., Sanzgiri, R. P., and Haydon, P. G. (1999). Tripartite synapses: glia, the unacknowledged partner. *Trends Neurosci.* 22, 208–215. doi: 10.1016/s0166-2236(98)01349-6

Ashburner, M., Ball, C. A., Blake, J. A., Botstein, D., Butler, H., Cherry, J. M., et al. (2000). Gene ontology: tool for the unification of biology. The Gene Ontology Consortium. *Nat. Genet.* 25, 25–29. doi: 10.1038/75556

Ashrafi, G., Schlehe, J. S., LaVoie, M. J., and Schwarz, T. L. (2014). Mitophagy of damaged mitochondria occurs locally in distal neuronal axons and requires PINK1 and Parkin. *J. Cell Biol.* 206, 655–670. doi: 10.1083/jcb.201401070

Ashutosh, null, Kou, W., Cotter, R., Borgmann, K., Wu, L., Persidsky, R., et al. (2011). CXCL8 protects human neurons from amyloid-β-induced neurotoxicity: relevance to Alzheimer's disease. *Biochem. Biophys. Res. Commun.* 412, 565–571. doi: 10.1016/j.bbrc.2011.07.127

Assenza, G., Benvenga, A., Gennaro, E., Tombini, M., Campana, C., Assenza, F., et al. (2017). A novel c132-134del mutation in Unverricht-Lundborg disease and the review of literature of heterozygous compound patients. *Epilepsia* 58, e31–e35. doi: 10.1111/epi.13626%20%5Bdoi%5D

Attwell, D., and Laughlin, S. B. (2001). An energy budget for signaling in the grey matter of the brain. *J. Cereb. Blood Flow Metab. Off. J. Int. Soc. Cereb. Blood Flow Metab.* 21, 1133–1145. doi: 10.1097/00004647-200110000-00001

Awadhpersad, R., and Jackson, C. B. (2021). High-Resolution Respirometry to assess Bioenergetics in Cells and Tissues using Chamber- and Plate-Based Respirometers. *J. Vis. Exp.*, 63000. doi: 10.3791/63000

Bai, F., and Witzmann, F. A. (2007). Synaptosome proteomics. *Subcell. Biochem.* 43, 77–98. doi: 10.1007/978-1-4020-5943-8_6

Baker, M. J., Lampe, P. A., Stojanovski, D., Korwitz, A., Anand, R., Tatsuta, T., et al. (2014). Stress-induced OMA1 activation and autocatalytic turnover regulate OPA1-dependent mitochondrial dynamics. *EMBO J.* 33, 578–593. doi: 10.1002/embj.201386474

Ban, B.-K., Jun, M.-H., Ryu, H.-H., Jang, D.-J., Ahmad, S. T., and Lee, J.-A. (2013). Autophagy negatively regulates early axon growth in cortical neurons. *Mol. Cell. Biol.* 33, 3907–3919. doi: 10.1128/MCB.00627-13

Banisadr, G., Gosselin, R.-D., Mechighel, P., Kitabgi, P., Rostène, W., and Parsadaniantz, S. M. (2005). Highly regionalized neuronal expression of monocyte chemoattractant protein-1 (MCP-1/CCL2) in rat brain: evidence for its colocalization with neurotransmitters and neuropeptides. *J. Comp. Neurol.* 489, 275–292. doi: 10.1002/cne.20598

Bernier, L.-P., York, E. M., and MacVicar, B. A. (2020). Immunometabolism in the Brain: How Metabolism Shapes Microglial Function. *Trends Neurosci.* 43, 854–869. doi: 10.1016/j.tins.2020.08.008

Berth, S. H., and Lloyd, T. E. (2023). Disruption of axonal transport in neurodegeneration. *J. Clin. Invest.* 133, e168554. doi: 10.1172/JCI168554

Bertholet, A. M., Delerue, T., Millet, A. M., Moulis, M. F., David, C., Daloyau, M., et al. (2016). Mitochondrial fusion/fission dynamics in neurodegeneration and neuronal plasticity. *Neurobiol. Dis.* 90, 3–19. doi: 10.1016/j.nbd.2015.10.011

Bertoni-Freddari, C., Fattoretti, P., Casoli, T., Spagna, C., Meier-Ruge, W., and Ulrich, J. (1993). Morphological plasticity of synaptic mitochondria during aging. *Brain Res.* 628, 193–200. doi: 10.1016/0006-8993(93)90955-m

Bhattacharyya, B. J., Banisadr, G., Jung, H., Ren, D., Cronshaw, D. G., Zou, Y., et al. (2008). The chemokine stromal cell-derived factor-1 regulates GABAergic inputs to neural progenitors in the postnatal dentate gyrus. *J. Neurosci. Off. J. Soc. Neurosci.* 28, 6720–6730. doi: 10.1523/JNEUROSCI.1677-08.2008

Biasizzo, M., and Kopitar-Jerala, N. (2020). Interplay Between NLRP3 Inflammasome and Autophagy. *Front. Immunol.* 11, 591803. doi: 10.3389/fimmu.2020.591803

Bilbo, S. D., Levkoff, L. H., Mahoney, J. H., Watkins, L. R., Rudy, J. W., and Maier, S. F. (2005). Neonatal infection induces memory impairments following an immune challenge in adulthood. *Behav. Neurosci.* 119, 293–301. doi: 10.1037/0735-7044.119.1.293

Bolger, A. M., Lohse, M., and Usadel, B. (2014). Trimmomatic: a flexible trimmer for Illumina sequence data. *Bioinforma. Oxf. Engl.* 30, 2114–2120. doi: 10.1093/bioinformatics/btu170

Boulet, A., Vest, K. E., Maynard, M. K., Gammon, M. G., Russell, A. C., Mathews, A. T., et al. (2018). The mammalian phosphate carrier SLC25A3 is a mitochondrial copper transporter required for cytochrome c oxidase biogenesis. *J. Biol. Chem.* 293, 1887–1896. doi: 10.1074/jbc.RA117.000265

Boya, P., and Kroemer, G. (2008). Lysosomal membrane permeabilization in cell death. *Oncogene* 27, 6434–6451. doi: 10.1038/onc.2008.310

Bradford, H. F., Docherty, M., Wu, J. Y., Cash, C. D., Ehret, M., Maitre, M., et al. (1989). The immunolysis, isolation, and properties of subpopulations of mammalian brain synaptosomes. *Neurochem. Res.* 14, 301–310. doi: 10.1007/BF01000031

Brault, V., Martin, B., Costet, N., Bizot, J.-C., and Hérault, Y. (2011). Characterization of PTZ-induced seizure susceptibility in a down syndrome mouse model that overexpresses CSTB. *PloS One* 6, e27845. doi: 10.1371/journal.pone.0027845

Brickley, S. G., Cull-Candy, S. G., and Farrant, M. (1996). Development of a tonic form of synaptic inhibition in rat cerebellar granule cells resulting from persistent activation of GABAA receptors. *J. Physiol.* 497 (Pt 3), 753–759. doi: 10.1113/jphysiol.1996.sp021806

Bridi, M. S., Park, S. M., and Huang, S. (2017). Developmental Disruption of GABA $_{A}$ R-Meditated Inhibition in Cntnap2 KO Mice. *eneuro* 4, ENEURO.0162-17.2017. doi: 10.1523/ENEURO.0162-17.2017

Brömme, D., Rinne, R., and Kirschke, H. (1991). Tight-binding inhibition of cathepsin S by cystatins. *Biomed. Biochim. Acta* 50, 631–635.

Brown, M. R., Sullivan, P. G., and Geddes, J. W. (2006). Synaptic Mitochondria Are More Susceptible to Ca2+Overload than Nonsynaptic Mitochondria. *J. Biol. Chem.* 281, 11658–11668. doi: 10.1074/jbc.M510303200

Bruchard, M., Mignot, G., Derangère, V., Chalmin, F., Chevriaux, A., Végran, F., et al. (2013). Chemotherapy-triggered cathepsin B release in myeloid-derived suppressor cells activates the Nlrp3 inflammasome and promotes tumor growth. *Nat. Med.* 19, 57–64. doi: 10.1038/nm.2999

Bussi, C., Heunis, T., Pellegrino, E., Bernard, E. M., Bah, N., Dos Santos, M. S., et al. (2022). Lysosomal damage drives mitochondrial proteome remodelling and reprograms macrophage immunometabolism. *Nat. Commun.* 13, 7338. doi: 10.1038/s41467-022-34632-8

Buzzi, A., Chikhladze, M., Falcicchia, C., Paradiso, B., Lanza, G., Soukupova, M., et al. (2012). Loss of cortical GABA terminals in Unverricht-Lundborg disease. *Neurobiol. Dis.* 47, 216–224. doi: 10.1016/j.nbd.2012.04.005

Cabras, T., Manconi, B., Iavarone, F., Fanali, C., Nemolato, S., Fiorita, A., et al. (2012). RP-HPLC-ESI-MS evidenced that salivary cystatin B is detectable in adult human whole saliva mostly as S-modified derivatives: S-Glutathionyl, S-cysteinyl and S-S 2-mer. *J. Proteomics* 75, 908–913. doi: 10.1016/j.jprot.2011.10.006

Cagnetta, R., Frese, C. K., Shigeoka, T., Krijgsveld, J., and Holt, C. E. (2018). Rapid Cue-Specific Remodeling of the Nascent Axonal Proteome. *Neuron* 99, 29-46.e4. doi: 10.1016/j.neuron.2018.06.004

Cai, Q., Davis, M. L., and Sheng, Z.-H. (2011). Regulation of axonal mitochondrial transport and its impact on synaptic transmission. *Neurosci. Res.* 70, 9–15. doi: 10.1016/j.neures.2011.02.005

Cajigas, I. J., Tushev, G., Will, T. J., tom Dieck, S., Fuerst, N., and Schuman, E. M. (2012). The local transcriptome in the synaptic neuropil revealed by deep sequencing and high-resolution imaging. *Neuron* 74, 453–466. doi: 10.1016/j.neuron.2012.02.036

Callewaere, C., Fernette, B., Raison, D., Mechighel, P., Burlet, A., Calas, A., et al. (2008). Cellular and subcellular evidence for neuronal interaction between the chemokine stromal cell-

derived factor-1/CXCL 12 and vasopressin: regulation in the hypothalamo-neurohypophysial system of the Brattleboro rats. *Endocrinology* 149, 310–319. doi: 10.1210/en.2007-1097

Canafoglia, L., Gennaro, E., Capovilla, G., Gobbi, G., Boni, A., Beccaria, F., et al. (2012). Electroclinical presentation and genotype-phenotype relationships in patients with Unverricht-Lundborg disease carrying compound heterozygous CSTB point and indel mutations. *Epilepsia* 53, 2120–2127. doi: 10.1111/j.1528-1167.2012.03718.x

Carey, M. R. (2024). The cerebellum. *Curr. Biol. CB* 34, R7–R11. doi: 10.1016/j.cub.2023.11.048

Ceru, S., Konjar, S., Maher, K., Repnik, U., Krizaj, I., Bencina, M., et al. (2010). Stefin B interacts with histones and cathepsin L in the nucleus. *J. Biol. Chem.* 285, 10078–10086. doi: 10.1074/jbc.M109.034793

Chae, T. H., Kim, S., Marz, K. E., Hanson, P. I., and Walsh, C. A. (2004). The hyh mutation uncovers roles for alpha Snap in apical protein localization and control of neural cell fate. *Nat. Genet.* 36, 264–270. doi: 10.1038/ng1302

Chandramouli, K., and Qian, P.-Y. (2009). Proteomics: challenges, techniques and possibilities to overcome biological sample complexity. *Hum. Genomics Proteomics HGP* 2009, 239204. doi: 10.4061/2009/239204

Changeux, J. P., and Danchin, A. (1976). Selective stabilisation of developing synapses as a mechanism for the specification of neuronal networks. *Nature* 264, 705–712. doi: 10.1038/264705a0

Che, X., Ye, W., Panga, L., Wu, D. C., and Yang, G. Y. (2001). Monocyte chemoattractant protein-1 expressed in neurons and astrocytes during focal ischemia in mice. *Brain Res.* 902, 171–177. doi: 10.1016/s0006-8993(01)02328-9

Chen, J.-X., Sun, Y.-J., Wang, P., Long, D.-X., Li, W., Li, L., et al. (2013). Induction of autophagy by TOCP in differentiated human neuroblastoma cells lead to degradation of cytoskeletal components and inhibition of neurite outgrowth. *Toxicology* 310, 92–97. doi: 10.1016/j.tox.2013.05.012

Chen, Y., and Sheng, Z.-H. (2013). Kinesin-1-syntaphilin coupling mediates activity-dependent regulation of axonal mitochondrial transport. *J. Cell Biol.* 202, 351–364. doi: 10.1083/jcb.201302040

Chiu, C.-S., Brickley, S., Jensen, K., Southwell, A., Mckinney, S., Cull-Candy, S., et al. (2005). GABA transporter deficiency causes tremor, ataxia, nervousness, and increased GABA-induced tonic conductance in cerebellum. *J. Neurosci. Off. J. Soc. Neurosci.* 25, 3234–3245. doi: 10.1523/JNEUROSCI.3364-04.2005

Chu, Y., Jin, X., Parada, I., Pesic, A., Stevens, B., Barres, B., et al. (2010). Enhanced synaptic connectivity and epilepsy in C1q knockout mice. *Proc. Natl. Acad. Sci. U. S. A.* 107, 7975–7980. doi: 10.1073/pnas.0913449107

Chung, W.-S., Allen, N. J., and Eroglu, C. (2015). Astrocytes Control Synapse Formation, Function, and Elimination. *Cold Spring Harb. Perspect. Biol.* 7, a020370. doi: 10.1101/cshperspect.a020370

Cioni, J.-M., Koppers, M., and Holt, C. E. (2018). Molecular control of local translation in axon development and maintenance. *Curr. Opin. Neurobiol.* 51, 86–94. doi: 10.1016/j.conb.2018.02.025

Cipollini, E., Riccio, M., Di Giaimo, R., Dal Piaz, F., Pulice, G., Catania, S., et al. (2008). Cystatin B and its EPM1 mutants are polymeric and aggregate prone in vivo. *Biochim. Biophys. Acta* 1783, 312–322. doi: 10.1016/j.bbamcr.2007.08.007

Citri, A., and Malenka, R. C. (2008). Synaptic plasticity: multiple forms, functions, and mechanisms. *Neuropsychopharmacol. Off. Publ. Am. Coll. Neuropsychopharmacol.* 33, 18–41. doi: 10.1038/sj.npp.1301559

Classification of progressive myoclonus epilepsies and related disorders. Marseille Consensus Group (1990). *Ann. Neurol.* 28, 113–116. doi: 10.1002/ana.410280129

Coelho, A. L., Schaller, M. A., Benjamim, C. F., Orlofsky, A. Z., Hogaboam, C. M., and Kunkel, S. L. (2007). The chemokine CCL6 promotes innate immunity via immune cell activation and recruitment. *J. Immunol. Baltim. Md 1950* 179, 5474–5482. doi: 10.4049/jimmunol.179.8.5474

Cohen, L. D., Zuchman, R., Sorokina, O., Müller, A., Dieterich, D. C., Armstrong, J. D., et al. (2013). Metabolic turnover of synaptic proteins: kinetics, interdependencies and implications for synaptic maintenance. *PloS One* 8, e63191. doi: 10.1371/journal.pone.0063191

Cohen, N. R., Hammans, S. R., Macpherson, J., and Nicoll, J. A. R. (2011). New neuropathological findings in Unverricht-Lundborg disease: neuronal intranuclear and cytoplasmic inclusions. *Acta Neuropathol. (Berl.)* 121, 421–427. doi: 10.1007/s00401-010-0738-2

Cohen-Cory, S., Kidane, A. H., Shirkey, N. J., and Marshak, S. (2010). Brain-derived neurotrophic factor and the development of structural neuronal connectivity. *Dev. Neurobiol.* 70, 271–288. doi: 10.1002/dneu.20774

Conroy, J., Allen, N. M., Gorman, K. M., Shahwan, A., Ennis, S., Lynch, S. A., et al. (2016). NAPB - a novel SNARE-associated protein for early-onset epileptic encephalopathy. *Clin. Genet.* 89, 1. doi: 10.1111/cge.12648

Corti, E., and Duarte, C. B. (2023). The role of post-translational modifications in synaptic AMPA receptor activity. *Biochem. Soc. Trans.* 51, 315–330. doi: 10.1042/BST20220827

Cox, L. J., Hengst, U., Gurskaya, N. G., Lukyanov, K. A., and Jaffrey, S. R. (2008). Intra-axonal translation and retrograde trafficking of CREB promotes neuronal survival. *Nat. Cell Biol.* 10, 149–159. doi: 10.1038/ncb1677

Dalla Costa, I., Buchanan, C. N., Zdradzinski, M. D., Sahoo, P. K., Smith, T. P., Thames, E., et al. (2021). The functional organization of axonal mRNA transport and translation. *Nat. Rev. Neurosci.* 22, 77–91. doi: 10.1038/s41583-020-00407-7

D'Amato, E., Kokaia, Z., Nanobashvili, A., Reeben, M., Lehesjoki, A. E., Saarma, M., et al. (2000). Seizures induce widespread upregulation of cystatin B, the gene mutated in progressive myoclonus epilepsy, in rat forebrain neurons. *Eur. J. Neurosci.* 12, 1687–1695. doi: ejn058%20%5Bpii%5D

Danner, N., Julkunen, P., Khyuppenen, J., Hukkanen, T., Könönen, M., Säisänen, L., et al. (2009). Altered cortical inhibition in Unverricht-Lundborg type progressive myoclonus epilepsy (EPM1). *Epilepsy Res.* 85, 81–88. doi: 10.1016/j.eplepsyres.2009.02.015

Dansereau, M.-A., Gosselin, R.-D., Pohl, M., Pommier, B., Mechighel, P., Mauborgne, A., et al. (2008). Spinal CCL2 pronociceptive action is no longer effective in CCR2 receptor antagonist-treated rats. *J. Neurochem.* 106, 757–769. doi: 10.1111/j.1471-4159.2008.05429.x

Daura, E., Tegelberg, S., Hakala, P., Lehesjoki, A.-E., and Joensuu, T. (2022). Cystatin B deficiency results in sustained histone H3 tail cleavage in postnatal mouse brain mediated by increased chromatin-associated cathepsin L activity. *Front. Mol. Neurosci.* 15, 1069122. doi: 10.3389/fnmol.2022.1069122

Daura, E., Tegelberg, S., Yoshihara, M., Jackson, C., Simonetti, F., Aksentjeff, K., et al. (2021). Cystatin B-deficiency triggers ectopic histone H3 tail cleavage during neurogenesis. *Neurobiol. Dis.* 156, 105418. doi: 10.1016/j.nbd.2021.105418

Davies, M. E., and Barrett, A. J. (1984). Immunolocalization of human cystatins in neutrophils and lymphocytes. *Histochemistry* 80, 373–377. doi: 10.1007/BF00495420

Davis, C. O., Kim, K.-Y., Bushong, E. A., Mills, E. A., Boassa, D., Shih, T., et al. (2014). Transcellular degradation of axonal mitochondria. *Proc. Natl. Acad. Sci. U. S. A.* 111, 9633–9638. doi: 10.1073/pnas.1404651111

de Haas, A. H., van Weering, H. R. J., de Jong, E. K., Boddeke, H. W. G. M., and Biber, K. P. H. (2007). Neuronal chemokines: versatile messengers in central nervous system cell interaction. *Mol. Neurobiol.* 36, 137–151. doi: 10.1007/s12035-007-0036-8

de Jong, E. K., Dijkstra, I. M., Hensens, M., Brouwer, N., van Amerongen, M., Liem, R. S. B., et al. (2005). Vesicle-mediated transport and release of CCL21 in endangered neurons: a possible explanation for microglia activation remote from a primary lesion. *J. Neurosci. Off. J. Soc. Neurosci.* 25, 7548–7557. doi: 10.1523/JNEUROSCI.1019-05.2005

Deng, J., Koutras, C., Donnelier, J., Alshehri, M., Fotouhi, M., Girard, M., et al. (2017). Neurons Export Extracellular Vesicles Enriched in Cysteine String Protein and Misfolded Protein Cargo. *Sci. Rep.* 7, 956. doi: 10.1038/s41598-017-01115-6

Deretic, V. (2021). Autophagy in inflammation, infection, and immunometabolism. *Immunity* 54, 437–453. doi: 10.1016/j.immuni.2021.01.018

Di Matteo, F., Pipicelli, F., Kyrousi, C., Tovecci, I., Penna, E., Crispino, M., et al. (2020). Cystatin B is essential for proliferation and interneuron migration in individuals with EPM 1 epilepsy. *EMBO Mol. Med.* 12. doi: 10.15252/emmm.201911419

Dictenberg, J. B., Swanger, S. A., Antar, L. N., Singer, R. H., and Bassell, G. J. (2008). A direct role for FMRP in activity-dependent dendritic mRNA transport links filopodial-spine morphogenesis to fragile X syndrome. *Dev. Cell* 14, 926–939. doi: 10.1016/j.devcel.2008.04.003

Dienel, G. A. (2012). Fueling and imaging brain activation. *ASN Neuro* 4, e00093. doi: 10.1042/AN20120021

Dienel, G. A. (2017). Lack of appropriate stoichiometry: Strong evidence against an energetically important astrocyte-neuron lactate shuttle in brain. *J. Neurosci. Res.* 95, 2103–2125. doi: 10.1002/jnr.24015

Dobin, A., Davis, C. A., Schlesinger, F., Drenkow, J., Zaleski, C., Jha, S., et al. (2013). STAR: ultrafast universal RNA-seq aligner. *Bioinforma. Oxf. Engl.* 29, 15–21. doi: 10.1093/bioinformatics/bts635

Docherty, M., Bradford, H. F., and Wu, J. Y. (1987). The preparation of highly purified GABAergic and cholinergic synaptosomes from mammalian brain. *Neurosci. Lett.* 81, 232–238. doi: 10.1016/0304-3940(87)91004-4

Dodd, P., Hardy, J. A., Oakley, A. E., and Strong, A. J. (1981). Synaptosomes prepared from fresh human cerebral cortex; morphology, respiration and release of transmitter amino acids. *Brain Res.* 224, 419–425. doi: 10.1016/0006-8993(81)90871-4

Domon, B., and Aebersold, R. (2006). Mass spectrometry and protein analysis. *Science* 312, 212–217. doi: 10.1126/science.1124619

Dörrbaum, A. R., Alvarez-Castelao, B., Nassim-Assir, B., Langer, J. D., and Schuman, E. M. (2020). Proteome dynamics during homeostatic scaling in cultured neurons. *eLife* 9, e52939. doi: 10.7554/eLife.52939

Dörrbaum, A. R., Kochen, L., Langer, J. D., and Schuman, E. M. (2018). Local and global influences on protein turnover in neurons and glia. *eLife* 7, e34202. doi: 10.7554/eLife.34202

Doyle, M., and Kiebler, M. A. (2011). Mechanisms of dendritic mRNA transport and its role in synaptic tagging. *EMBO J.* 30, 3540–3552. doi: 10.1038/emboj.2011.278

Du, X., Fleiss, B., Li, H., D'angelo, B., Sun, Y., Zhu, C., et al. (2011). Systemic stimulation of TLR2 impairs neonatal mouse brain development. *PloS One* 6, e19583. doi: 10.1371/journal.pone.0019583

Dunkley, P. R., Jarvie, P. E., and Robinson, P. J. (2008). A rapid Percoll gradient procedure for preparation of synaptosomes. *Nat. Protoc.* 3, 1718–1728. doi: 10.1038/nprot.2008.171

Duvezin-Caubet, S., Jagasia, R., Wagener, J., Hofmann, S., Trifunovic, A., Hansson, A., et al. (2006). Proteolytic processing of OPA1 links mitochondrial dysfunction to alterations in mitochondrial morphology. *J. Biol. Chem.* 281, 37972–37979. doi: 10.1074/jbc.M606059200

Edelmann, E., Lessmann, V., and Brigadski, T. (2014). Pre- and postsynaptic twists in BDNF secretion and action in synaptic plasticity. *Neuropharmacology* 76 Pt C, 610–627. doi: 10.1016/j.neuropharm.2013.05.043

Eldridge, R., Iivanainen, M., Stern, R., Koerber, T., and Wilder, B. J. (1983). "Baltic" myoclonus epilepsy: hereditary disorder of childhood made worse by phenytoin. *Lancet Lond. Engl.* 2, 838–842. doi: 10.1016/s0140-6736(83)90749-3

Elvira, G., Wasiak, S., Blandford, V., Tong, X.-K., Serrano, A., Fan, X., et al. (2006). Characterization of an RNA granule from developing brain. *Mol. Cell. Proteomics MCP* 5, 635–651. doi: 10.1074/mcp.M500255-MCP200

Ewels, P., Magnusson, M., Lundin, S., and Käller, M. (2016). MultiQC: summarize analysis results for multiple tools and samples in a single report. *Bioinforma. Oxf. Engl.* 32, 3047–3048. doi: 10.1093/bioinformatics/btw354

Ezan, J., Moreau, M. M., Mamo, T. M., Shimbo, M., Decroo, M., Richter, M., et al. (2021). Early loss of Scribble affects cortical development, interhemispheric connectivity and psychomotor activity. *Sci. Rep.* 11, 9106. doi: 10.1038/s41598-021-88147-1

Favrais, G., van de Looij, Y., Fleiss, B., Ramanantsoa, N., Bonnin, P., Stoltenburg-Didinger, G., et al. (2011). Systemic inflammation disrupts the developmental program of white matter. *Ann. Neurol.* 70, 550–565. doi: 10.1002/ana.22489

Ferlazzo, E., Magaudda, A., Striano, P., Vi-Hong, N., Serra, S., and Genton, P. (2007). Long-term evolution of EEG in Unverricht-Lundborg disease. *Epilepsy Res.* 73, 219–227. doi: 10.1016/j.eplepsyres.2006.10.006

Fernandez, L., Rogasch, N. C., Do, M., Clark, G., Major, B. P., Teo, W.-P., et al. (2020). Cerebral Cortical Activity Following Non-invasive Cerebellar Stimulation-a Systematic Review of Combined TMS and EEG Studies. *Cerebellum Lond. Engl.* 19, 309–335. doi: 10.1007/s12311-019-01093-7

Filograna, R., Mennuni, M., Alsina, D., and Larsson, N. (2021). Mitochondrial DNA copy number in human disease: the more the better? *FEBS Lett.* 595, 976–1002. doi: 10.1002/1873-3468.14021

Fiskum, G., Starkov, A., Polster, B. M., and Chinopoulos, C. (2003). Mitochondrial mechanisms of neural cell death and neuroprotective interventions in Parkinson's disease. *Ann. N. Y. Acad. Sci.* 991, 111–119. doi: 10.1111/j.1749-6632.2003.tb07469.x

Fornasiero, E. F., Mandad, S., Wildhagen, H., Alevra, M., Rammner, B., Keihani, S., et al. (2018). Precisely measured protein lifetimes in the mouse brain reveal differences across tissues and subcellular fractions. *Nat. Commun.* 9, 4230. doi: 10.1038/s41467-018-06519-0

Franceschetti, S., Antozzi, C., Binelli, S., Carrara, F., Nardocci, N., Zeviani, M., et al. (1993). Progressive myoclonus epilepsies: an electroclinical, biochemical, morphological and molecular genetic study of 17 cases. *Acta Neurol. Scand.* 87, 219–223. doi: 10.1111/j.1600-0404.1993.tb04105.x

Franceschetti, S., Sancini, G., Buzzi, A., Zucchini, S., Paradiso, B., Magnaghi, G., et al. (2007). A pathogenetic hypothesis of Unverricht-Lundborg disease onset and progression. *Neurobiol. Dis.* 25, 675–685. doi: 10.1016/j.nbd.2006.11.006

Frankish, A., Diekhans, M., Ferreira, A.-M., Johnson, R., Jungreis, I., Loveland, J., et al. (2019). GENCODE reference annotation for the human and mouse genomes. *Nucleic Acids Res.* 47, D766–D773. doi: 10.1093/nar/gky955

Frappier, T., Stetzkowski-Marden, F., and Pradel, L. A. (1991). Interaction domains of neurofilament light chain and brain spectrin. *Biochem. J.* 275 (Pt 2), 521–527. doi: 10.1042/bj2750521

Freitag, T. L., Podojil, J. R., Pearson, R. M., Fokta, F. J., Sahl, C., Messing, M., et al. (2020). Gliadin Nanoparticles Induce Immune Tolerance to Gliadin in Mouse Models of Celiac Disease. *Gastroenterology* 158, 1667-1681.e12. doi: 10.1053/j.gastro.2020.01.045

Fuertes, G., Villarroya, A., and Knecht, E. (2003). Role of proteasomes in the degradation of short-lived proteins in human fibroblasts under various growth conditions. *Int. J. Biochem. Cell Biol.* 35, 651–664. doi: 10.1016/s1357-2725(02)00382-5

Fukushima, A., Milner, K., Gupta, A., and Lopaschuk, G. D. (2015). Myocardial Energy Substrate Metabolism in Heart Failure : from Pathways to Therapeutic Targets. *Curr. Pharm. Des.* 21, 3654–3664. doi: 10.2174/1381612821666150710150445

Fumagalli, S., Ivanenkov, V. V., Teng, T., and Thomas, G. (2012). Suprainduction of p53 by disruption of 40S and 60S ribosome biogenesis leads to the activation of a novel G2/M checkpoint. *Genes Dev.* 26, 1028–1040. doi: 10.1101/gad.189951.112

Galic, M. A., Riazi, K., Heida, J. G., Mouihate, A., Fournier, N. M., Spencer, S. J., et al. (2008). Postnatal inflammation increases seizure susceptibility in adult rats. *J. Neurosci. Off. J. Soc. Neurosci.* 28, 6904–6913. doi: 10.1523/JNEUROSCI.1901-08.2008

Garber, K. B., Visootsak, J., and Warren, S. T. (2008). Fragile X syndrome. *Eur. J. Hum. Genet. EJHG* 16, 666–672. doi: 10.1038/ejhg.2008.61

Garner, J. A., and Mahler, H. R. (1987). Biogenesis of presynaptic terminal proteins. *J. Neurochem.* 49, 905–915. doi: 10.1111/j.1471-4159.1987.tb00979.x

Gene Ontology Consortium (2021). The Gene Ontology resource: enriching a GOld mine. *Nucleic Acids Res.* 49, D325–D334. doi: 10.1093/nar/gkaa1113

Gerevich, Z., Kovács, R., Liotta, A., Hasam-Henderson, L. A., Weh, L., Wallach, I., et al. (2023). Metabolic implications of axonal demyelination and its consequences for synchronized network activity: An in silico and in vitro study. *J. Cereb. Blood Flow Metab. Off. J. Int. Soc. Cereb. Blood Flow Metab.* 43, 1571–1587. doi: 10.1177/0271678X231170746

Giaimo, R. D., Riccio, M., Santi, S., Galeotti, C., Ambrosetti, D. C., and Melli, M. (2002). New insights into the molecular basis of progressive myoclonus epilepsy: a multiprotein complex with cystatin B. *Hum. Mol. Genet.* 11, 2941–2950. doi: 10.1093/hmg/11.23.2941

Gillingwater, T. H., and Wishart, T. M. (2013). Mechanisms underlying synaptic vulnerability and degeneration in neurodegenerative disease. *Neuropathol. Appl. Neurobiol.* 39, 320–334. doi: 10.1111/nan.12014

Glock, C., Biever, A., Tushev, G., Nassim-Assir, B., Kao, A., Bartnik, I., et al. (2021). The translatome of neuronal cell bodies, dendrites, and axons. *Proc. Natl. Acad. Sci. U. S. A.* 118, e2113929118. doi: 10.1073/pnas.2113929118

Glock, C., Heumüller, M., and Schuman, E. M. (2017). mRNA transport & local translation in neurons. *Curr. Opin. Neurobiol.* 45, 169–177. doi: 10.1016/j.conb.2017.05.005

Graham, L. C., Eaton, S. L., Brunton, P. J., Atrih, A., Smith, C., Lamont, D. J., et al. (2017). Proteomic profiling of neuronal mitochondria reveals modulators of synaptic architecture. *Mol. Neurodegener.* 12, 77. doi: 10.1186/s13024-017-0221-9

Green, G. D., Kembhavi, A. A., Davies, M. E., and Barrett, A. J. (1984). Cystatin-like cysteine proteinase inhibitors from human liver. *Biochem. J.* 218, 939–946.

Greer, J. M., and Lees, M. B. (2002). Myelin proteolipid protein--the first 50 years. *Int. J. Biochem. Cell Biol.* 34, 211–215. doi: 10.1016/s1357-2725(01)00136-4

Grønborg, M., Pavlos, N. J., Brunk, I., Chua, J. J. E., Münster-Wandowski, A., Riedel, D., et al. (2010). Quantitative comparison of glutamatergic and GABAergic synaptic vesicles unveils selectivity for few proteins including MAL2, a novel synaptic vesicle protein. *J. Neurosci. Off. J. Soc. Neurosci.* 30, 2–12. doi: 10.1523/JNEUROSCI.4074-09.2010

Guastella, J., Nelson, N., Nelson, H., Czyzyk, L., Keynan, S., Miedel, M. C., et al. (1990). Cloning and expression of a rat brain GABA transporter. *Science* 249, 1303–1306. doi: 10.1126/science.1975955

Guedes-Dias, P., and Holzbaur, E. L. F. (2019). Axonal transport: Driving synaptic function. *Science* 366, eaaw9997. doi: 10.1126/science.aaw9997

Gumusgoz, E., Kasiri, S., Verma, M., Wu, J., Villarreal Acha, D., Marriam, U., et al. (2023). CSTB gene replacement improves neuroinflammation, neurodegeneration and ataxia in murine type 1 progressive myoclonus epilepsy. *Gene Ther.* doi: 10.1038/s41434-023-00433-x

Guo, C., Sun, L., Chen, X., and Zhang, D. (2013). Oxidative stress, mitochondrial damage and neurodegenerative diseases. *Neural Regen. Res.* 8, 2003–2014. doi: 10.3969/j.issn.1673-5374.2013.21.009

Guo, C., Witter, L., Rudolph, S., Elliott, H. L., Ennis, K. A., and Regehr, W. G. (2016). Purkinje Cells Directly Inhibit Granule Cells in Specialized Regions of the Cerebellar Cortex. *Neuron* 91, 1330–1341. doi: 10.1016/j.neuron.2016.08.011

Guo, F., Liu, X., Cai, H., and Le, W. (2018). Autophagy in neurodegenerative diseases: pathogenesis and therapy. *Brain Pathol. Zurich Switz.* 28, 3–13. doi: 10.1111/bpa.12545

Gylys, K. H., Fein, J. A., and Cole, G. M. (2000). Quantitative characterization of crude synaptosomal fraction (P-2) components by flow cytometry. *J. Neurosci. Res.* 61, 186–192. doi: 10.1002/1097-4547(20000715)61:2%3C186::AID-JNR9%3E3.0.CO;2-X

Hall, C. N., Klein-Flügge, M. C., Howarth, C., and Attwell, D. (2012). Oxidative phosphorylation, not glycolysis, powers presynaptic and postsynaptic mechanisms underlying brain information processing. *J. Neurosci. Off. J. Soc. Neurosci.* 32, 8940–8951. doi: 10.1523/JNEUROSCI.0026-12.2012

Haltia, M., Kristensson, K., and Sourander, P. (1969). Neuropathological studies in three Scandinavian cases of progressive myoclonus epilepsy. *Acta Neurol. Scand.* 45, 63–77.

Hanus, C., and Schuman, E. M. (2013). Proteostasis in complex dendrites. *Nat. Rev. Neurosci.* 14, 638–648. doi: 10.1038/nrn3546

Hanz, S., Perlson, E., Willis, D., Zheng, J.-Q., Massarwa, R., Huerta, J. J., et al. (2003). Axoplasmic importins enable retrograde injury signaling in lesioned nerve. *Neuron* 40, 1095–1104. doi: 10.1016/s0896-6273(03)00770-0

Hara, T., Nakamura, K., Matsui, M., Yamamoto, A., Nakahara, Y., Suzuki-Migishima, R., et al. (2006). Suppression of basal autophagy in neural cells causes neurodegenerative disease in mice. *Nature* 441, 885–889. doi: 10.1038/nature04724

Harris, J. J., Jolivet, R., and Attwell, D. (2012). Synaptic Energy Use and Supply. *Neuron* 75, 762–777. doi: 10.1016/j.neuron.2012.08.019

Harrison, J. K., Jiang, Y., Chen, S., Xia, Y., Maciejewski, D., McNamara, R. K., et al. (1998). Role for neuronally derived fractalkine in mediating interactions between neurons and CX3CR1-expressing microglia. *Proc. Natl. Acad. Sci. U. S. A.* 95, 10896–10901. doi: 10.1073/pnas.95.18.10896

Havkin-Solomon, T., Itzhaki, E., Joffe, N., Reuven, N., Shaul, Y., and Dikstein, R. (2023). Selective translational control of cellular and viral mRNAs by RPS3 mRNA binding. *Nucleic Acids Res.* 51, 4208–4222. doi: 10.1093/nar/gkad269

Hayakawa, K., Esposito, E., Wang, X., Terasaki, Y., Liu, Y., Xing, C., et al. (2016). Transfer of mitochondria from astrocytes to neurons after stroke. *Nature* 535, 551–555. doi: 10.1038/nature18928

Hebb, C. O., and Whittaker, V. P. (1958). Intracellular distributions of acetylcholine and choline acetylase. *J. Physiol.* 142, 187–196. doi: 10.1113/jphysiol.1958.sp006008

Herculano-Houzel, S. (2009). The human brain in numbers: a linearly scaled-up primate brain. *Front. Hum. Neurosci.* 3, 31. doi: 10.3389/neuro.09.031.2009

Hinnebusch, A. G. (2014). The scanning mechanism of eukaryotic translation initiation. *Annu. Rev. Biochem.* 83, 779–812. doi: 10.1146/annurev-biochem-060713-035802

Hodge, R. D., Bakken, T. E., Miller, J. A., Smith, K. A., Barkan, E. R., Graybuck, L. T., et al. (2019). Conserved cell types with divergent features in human versus mouse cortex. *Nature* 573, 61–68. doi: 10.1038/s41586-019-1506-7

Hoegen, T., Tremel, N., Klein, M., Angele, B., Wagner, H., Kirschning, C., et al. (2011). The NLRP3 inflammasome contributes to brain injury in pneumococcal meningitis and is activated through ATP-dependent lysosomal cathepsin B release. *J. Immunol. Baltim. Md 1950* 187, 5440–5451. doi: 10.4049/jimmunol.1100790

Holt, C. E., Martin, K. C., and Schuman, E. M. (2019). Local translation in neurons: visualization and function. *Nat. Struct. Mol. Biol.* 26, 557–566. doi: 10.1038/s41594-019-0263-5

Hook, V., Yoon, M., Mosier, C., Ito, G., Podvin, S., Head, B. P., et al. (2020). Cathepsin B in neurodegeneration of Alzheimer's disease, traumatic brain injury, and related brain disorders. *Biochim. Biophys. Acta BBA - Proteins Proteomics* 1868, 140428. doi: 10.1016/j.bbapap.2020.140428

Houseweart, M. K., Pennacchio, L. A., Vilaythong, A., Peters, C., Noebels, J. L., and Myers, R. M. (2003a). Cathepsin B but not cathepsins L or S contributes to the pathogenesis of Unverricht-Lundborg progressive myoclonus epilepsy (EPM1). *J. Neurobiol.* 56, 315–327. doi: 10.1002/neu.10253

Houseweart, M. K., Vilaythong, A., Yin, X.-M., Turk, B., Noebels, J. L., and Myers, R. M. (2003b). Apoptosis caused by cathepsins does not require Bid signaling in an in vivo model of progressive myoclonus epilepsy (EPM1). *Cell Death Differ.* 10, 1329–1335. doi: 10.1038/sj.cdd.4401309

Hu, X., Viesselmann, C., Nam, S., Merriam, E., and Dent, E. W. (2008). Activity-dependent dynamic microtubule invasion of dendritic spines. *J. Neurosci. Off. J. Soc. Neurosci.* 28, 13094–13105. doi: 10.1523/JNEUROSCI.3074-08.2008

Huang, D. W., Sherman, B. T., and Lempicki, R. A. (2009a). Bioinformatics enrichment tools: paths toward the comprehensive functional analysis of large gene lists. *Nucleic Acids Res.* 37, 1–13. doi: 10.1093/nar/gkn923

Huang, D. W., Sherman, B. T., and Lempicki, R. A. (2009b). Systematic and integrative analysis of large gene lists using DAVID bioinformatics resources. *Nat. Protoc.* 4, 44–57. doi: 10.1038/nprot.2008.211

Hypponen, J., Aikia, M., Joensuu, T., Julkunen, P., Danner, N., Koskenkorva, P., et al. (2015). Refining the phenotype of Unverricht-Lundborg disease (EPM1): a population-wide Finnish study. *Neurology* 84, 1529–1536. doi: 10.1212/WNL.0000000000001466%20%5Bdoi%5D

Ignatenko, O., Chilov, D., Paetau, I., de Miguel, E., Jackson, C. B., Capin, G., et al. (2018). Loss of mtDNA activates astrocytes and leads to spongiotic encephalopathy. *Nat. Commun.* 9, 70. doi: 10.1038/s41467-017-01859-9

Imai, Y., Ibata, I., Ito, D., Ohsawa, K., and Kohsaka, S. (1996). A novel gene iba1 in the major histocompatibility complex class III region encoding an EF hand protein expressed in a monocytic lineage. *Biochem. Biophys. Res. Commun.* 224, 855–862. doi: 10.1006/bbrc.1996.1112

Ismail, F. Y., Fatemi, A., and Johnston, M. V. (2017). Cerebral plasticity: Windows of opportunity in the developing brain. *Eur. J. Paediatr. Neurol. EJPN Off. J. Eur. Paediatr. Neurol. Soc.* 21, 23–48. doi: 10.1016/j.ejpn.2016.07.007

Jahn, O., Tenzer, S., and Werner, H. B. (2009). Myelin proteomics: molecular anatomy of an insulating sheath. *Mol. Neurobiol.* 40, 55–72. doi: 10.1007/s12035-009-8071-2

Jähne, S., Mikulasch, F., Heuer, H. G. H., Truckenbrodt, S., Agüi-Gonzalez, P., Grewe, K., et al. (2021). Presynaptic activity and protein turnover are correlated at the single-synapse level. *Cell Rep.* 34, 108841. doi: 10.1016/j.celrep.2021.108841

Järvinen, M., and Rinne, A. (1982). Human spleen cysteineproteinase inhibitor. Purification, fractionation into isoelectric variants and some properties of the variants. *Biochim. Biophys. Acta* 708, 210–217.

Jensen, K., Chiu, C.-S., Sokolova, I., Lester, H. A., and Mody, I. (2003). GABA transporter-1 (GAT1)-deficient mice: differential tonic activation of GABAA versus GABAB receptors in the hippocampus. *J. Neurophysiol.* 90, 2690–2701. doi: 10.1152/jn.00240.2003

Ji, B., Zhang, Z., Zhang, M., Zhu, H., Zhou, K., Yang, J., et al. (2009). Differential expression profiling of the synaptosome proteome in a rat model of antipsychotic resistance. *Brain Res.* 1295, 170–178. doi: 10.1016/j.brainres.2009.07.097

Jiang, B.-C., Cao, D.-L., Zhang, X., Zhang, Z.-J., He, L.-N., Li, C.-H., et al. (2016). CXCL13 drives spinal astrocyte activation and neuropathic pain via CXCR5. *J. Clin. Invest.* 126, 745–761. doi: 10.1172/JCI81950

Joensuu, T., Kuronen, M., Alakurtti, K., Tegelberg, S., Hakala, P., Aalto, A., et al. (2007). Cystatin B: mutation detection, alternative splicing and expression in progressive myclonus epilepsy of Unverricht-Lundborg type (EPM1) patients. *Eur. J. Hum. Genet. EJHG* 15, 185–193. doi: 5201723%20%5Bpii%5D

Joensuu, T., Tegelberg, S., Reinmaa, E., Segerstrale, M., Hakala, P., Pehkonen, H., et al. (2014). Gene expression alterations in the cerebellum and granule neurons of Cstb(-/-) mouse are associated with early synaptic changes and inflammation. *PloS One* 9, e89321. doi: 10.1371/journal.pone.0089321%20%5Bdoi%5D

Jonckheere, A. I., Smeitink, J. A. M., and Rodenburg, R. J. T. (2012). Mitochondrial ATP synthase: architecture, function and pathology. *J. Inherit. Metab. Dis.* 35, 211–225. doi: 10.1007/s10545-011-9382-9

Julkunen, P., Säisänen, L., Könönen, M., Vanninen, R., Kälviäinen, R., and Mervaala, E. (2013). TMS-EEG reveals impaired intracortical interactions and coherence in Unverricht-Lundborg type progressive myoclonus epilepsy (EPM1). *Epilepsy Res.* 106, 103–112. doi: 10.1016/j.eplepsyres.2013.04.001

Jung, H., Gkogkas, C. G., Sonenberg, N., and Holt, C. E. (2014). Remote control of gene function by local translation. *Cell* 157, 26–40. doi: 10.1016/j.cell.2014.03.005

Jung, H., Yoon, B. C., and Holt, C. E. (2012). Axonal mRNA localization and local protein synthesis in nervous system assembly, maintenance and repair. *Nat. Rev. Neurosci.* 13, 308–324. doi: 10.1038/nrn3210

Juraska, J. M., and Drzewiecki, C. M. (2020). Cortical reorganization during adolescence: What the rat can tell us about the cellular basis. *Dev. Cogn. Neurosci.* 45, 100857. doi: 10.1016/j.dcn.2020.100857

Ka, M., Smith, A. L., and Kim, W.-Y. (2017). MTOR controls genesis and autophagy of GABAergic interneurons during brain development. *Autophagy* 13, 1348–1363. doi: 10.1080/15548627.2017.1327927

Kaasik, A., Kuum, M., Aonurm, A., Kalda, A., Vaarmann, A., and Zharkovsky, A. (2007). Seizures, ataxia, and neuronal loss in cystatin B heterozygous mice. *Epilepsia* 48, 752–757. doi: 10.1111/j.1528-1167.2007.00985.x

Kälviäinen, R., Khyuppenen, J., Koskenkorva, P., Eriksson, K., Vanninen, R., and Mervaala, E. (2008). Clinical picture of EPM1-Unverricht-Lundborg disease. *Epilepsia* 49, 549–556. doi: 10.1111/j.1528-1167.2008.01546.x

Kaneda, M., Farrant, M., and Cull-Candy, S. G. (1995). Whole-cell and single-channel currents activated by GABA and glycine in granule cells of the rat cerebellum. *J. Physiol.* 485 (Pt 2), 419–435. doi: 10.1113/jphysiol.1995.sp020739

Kang, J.-S., Tian, J.-H., Pan, P.-Y., Zald, P., Li, C., Deng, C., et al. (2008). Docking of axonal mitochondria by syntaphilin controls their mobility and affects short-term facilitation. *Cell* 132, 137–148. doi: 10.1016/j.cell.2007.11.024

Karunadharma, P. P., Basisty, N., Chiao, Y. A., Dai, D.-F., Drake, R., Levy, N., et al. (2015). Respiratory chain protein turnover rates in mice are highly heterogeneous but strikingly conserved across tissues, ages, and treatments. *FASEB J. Off. Publ. Fed. Am. Soc. Exp. Biol.* 29, 3582–3592. doi: 10.1096/fj.15-272666

Kathjoo, M. B., and Srivastava, M. (2022). A link between DNA double-strand breaks and regulation of global translation. *FEBS J.* 289, 3093–3096. doi: 10.1111/febs.16398

Kaur, G., Mohan, P., Pawlik, M., DeRosa, S., Fajiculay, J., Che, S., et al. (2010). Cystatin C Rescues Degenerating Neurons in a Cystatin B-Knockout Mouse Model of Progressive Myoclonus Epilepsy. *Am. J. Pathol.* 177, 2256–2267. doi: 10.2353/ajpath.2010.100461

Kennedy, M. B. (2000). Signal-processing machines at the postsynaptic density. *Science* 290, 750–754. doi: 10.1126/science.290.5492.750

Kiessling, M. C., Büttner, A., Butti, C., Müller-Starck, J., Milz, S., Hof, P. R., et al. (2014). Cerebellar granule cells are generated postnatally in humans. *Brain Struct. Funct.* 219, 1271–1286. doi: 10.1007/s00429-013-0565-z

Kim, I., Rodriguez-Enriquez, S., and Lemasters, J. J. (2007). Selective degradation of mitochondria by mitophagy. *Arch. Biochem. Biophys.* 462, 245–253. doi: 10.1016/j.abb.2007.03.034

Klionsky, D. J., Petroni, G., Amaravadi, R. K., Baehrecke, E. H., Ballabio, A., Boya, P., et al. (2021). Autophagy in major human diseases. *EMBO J.* 40. doi: 10.15252/embj.2021108863

Koh, T.-W., Korolchuk, V. I., Wairkar, Y. P., Jiao, W., Evergren, E., Pan, H., et al. (2007). Eps15 and Dap160 control synaptic vesicle membrane retrieval and synapse development. *J. Cell Biol.* 178, 309–322. doi: 10.1083/jcb.200701030

Komatsu, M., Waguri, S., Chiba, T., Murata, S., Iwata, J., Tanida, I., et al. (2006). Loss of autophagy in the central nervous system causes neurodegeneration in mice. *Nature* 441, 880–884. doi: 10.1038/nature04723

Kooijman, R., Sarre, S., Michotte, Y., and De Keyser, J. (2009). Insulin-like growth factor I: a potential neuroprotective compound for the treatment of acute ischemic stroke? *Stroke* 40, e83-88. doi: 10.1161/STROKEAHA.108.528356

Koopmans, F., van Nierop, P., Andres-Alonso, M., Byrnes, A., Cijsouw, T., Coba, M. P., et al. (2019). SynGO: An Evidence-Based, Expert-Curated Knowledge Base for the Synapse. *Neuron* 103, 217-234.e4. doi: 10.1016/j.neuron.2019.05.002

Körber, C., Horstmann, H., Venkataramani, V., Herrmannsdörfer, F., Kremer, T., Kaiser, M., et al. (2015). Modulation of Presynaptic Release Probability by the Vertebrate-Specific Protein Mover. *Neuron* 87, 521–533. doi: 10.1016/j.neuron.2015.07.001

Körber, I. (2016). Microglial dysfunction in Cstb-/- mice, a model for the neurodegenerative disorder Progressive myoclonus epilepsy of Unverricht-Lundborg type, EPM1. Helsinki: University of Helsinki.

Korber, I., Katayama, S., Einarsdottir, E., Krjutskov, K., Hakala, P., Kere, J., et al. (2016). Gene-Expression Profiling Suggests Impaired Signaling via the Interferon Pathway in Cstb-/- Microglia. *PloS One* 11, e0158195. doi: 10.1371/journal.pone.0158195%20%5Bdoi%5D

Korja, M., Kaasinen, V., Lamusuo, S., Parkkola, R., Någren, K., and Marttila, R. J. (2007). Substantial thalamostriatal dopaminergic defect in Unverricht-Lundborg disease. *Epilepsia* 48, 1768–1773. doi: 10.1111/j.1528-1167.2007.01118.x

Korpi, E. R., Gründer, G., and Lüddens, H. (2002). Drug interactions at GABA(A) receptors. *Prog. Neurobiol.* 67, 113–159. doi: 10.1016/s0301-0082(02)00013-8

Koskenkorva, P., Hyppönen, J., Aikiä, M., Mervaala, E., Kiviranta, T., Eriksson, K., et al. (2011). Severer phenotype in Unverricht-Lundborg disease (EPM1) patients compound heterozygous for the dodecamer repeat expansion and the c.202C>T mutation in the CSTB gene. *Neurodegener. Dis.* 8, 515–522. doi: 10.1159/000323470

Koskenkorva, P., Khyuppenen, J., Niskanen, E., Könönen, M., Bendel, P., Mervaala, E., et al. (2009). Motor cortex and thalamic atrophy in Unverricht-Lundborg disease: voxel-based morphometric study. *Neurology* 73, 606–611. doi: 10.1212/WNL.0b013e3181b3888b

Koskenkorva, P., Niskanen, E., Hyppönen, J., Könönen, M., Mervaala, E., Soininen, H., et al. (2012). Sensorimotor, visual, and auditory cortical atrophy in Unverricht-Lundborg disease mapped with cortical thickness analysis. *AJNR Am. J. Neuroradiol.* 33, 878–883. doi: 10.3174/ajnr.A2882

Koskiniemi, M., Donner, M., Majuri, H., Haltia, M., and Norio, R. (1974a). Progressive myoclonus epilepsy. A clinical and histopathological study. *Acta Neurol. Scand.* 50, 307–332.

Koskiniemi, M., Toivakka, E., and Donner, M. (1974b). Progressive myoclonus epilepsy. Electroencephalographical findings. *Acta Neurol. Scand.* 50, 333–359.

Kowiański, P., Lietzau, G., Czuba, E., Waśkow, M., Steliga, A., and Moryś, J. (2018). BDNF: A Key Factor with Multipotent Impact on Brain Signaling and Synaptic Plasticity. *Cell. Mol. Neurobiol.* 38, 579–593. doi: 10.1007/s10571-017-0510-4

Krichevsky, A. M., and Kosik, K. S. (2001). Neuronal RNA granules: a link between RNA localization and stimulation-dependent translation. *Neuron* 32, 683–696. doi: 10.1016/s0896-6273(01)00508-6

Kuijpers, M., Azarnia Tehran, D., Haucke, V., and Soykan, T. (2021). The axonal endolysosomal and autophagic systems. *J. Neurochem.* 158, 589–602. doi: 10.1111/jnc.15287

Kurz, T., Gustafsson, B., and Brunk, U. T. (2006). Intralysosomal iron chelation protects against oxidative stress-induced cellular damage. *FEBS J.* 273, 3106–3117. doi: 10.1111/j.1742-4658.2006.05321.x

Lai, J. C. K., Walsh, J. M., Dennis, S. C., and Clark, J. B. (1977). SYNAPTIC AND NON-SYNAPTIC MITOCHONDRIA FROM RAT BRAIN: ISOLATION AND CHARACTERIZATION. *J. Neurochem.* 28, 625–631. doi: 10.1111/j.1471-4159.1977.tb10434.x

Lalioti, M. D., Scott, H. S., and Antonarakis, S. E. (1999). Altered spacing of promoter elements due to the dodecamer repeat expansion contributes to reduced expression of the cystatin B gene in EPM1. *Hum. Mol. Genet.* 8, 1791–1798. doi: 10.1093/hmg/8.9.1791

Lalioti, M. D., Scott, H. S., Buresi, C., Rossier, C., Bottani, A., Morris, M. A., et al. (1997). Dodecamer repeat expansion in cystatin B gene in progressive myoclonus epilepsy. *Nature* 386, 847–851. doi: 10.1038/386847a0

Larsell, O. (1952). The morphogenesis and adult pattern of the lobules and fissures of the cerebellum of the white rat. *J. Comp. Neurol.* 97, 281–356. doi: 10.1002/cne.900970204

Larsell, O. (1970). "The comparative anatomy and histology of the cerebellum. 2: From monotremes through apes," (Minneapolis: Univ. of Minnesota Press).

Lee, H.-G., Wheeler, M. A., and Quintana, F. J. (2022). Function and therapeutic value of astrocytes in neurological diseases. *Nat. Rev. Drug Discov.* 21, 339–358. doi: 10.1038/s41573-022-00390-x

Lee, J.-E., Kwon, J., and Baek, M.-C. (2011). A combination method of chemical with enzyme reactions for identification of membrane proteins. *Biochim. Biophys. Acta* 1814, 397–404. doi: 10.1016/j.bbapap.2010.12.001

Lehesjoki, A.-E., and Kälviäinen, R. (1993). "Progressive Myoclonic Epilepsy Type 1," in *GeneReviews®*, eds. M. P. Adam, D. B. Everman, G. M. Mirzaa, R. A. Pagon, S. E. Wallace, L. J. Bean, et al. (Seattle (WA): University of Washington, Seattle). Available at: http://www.ncbi.nlm.nih.gov/books/NBK1142/ (Accessed January 5, 2023).

Lehninger, A. L., Nelson, D. L., and Cox, M. M. (2005). *Lehninger principles of biochemistry*., 4th ed. New York: W.H. Freeman.

Lehtinen, M. K., Tegelberg, S., Schipper, H., Su, H., Zukor, H., Manninen, O., et al. (2009). Cystatin B deficiency sensitizes neurons to oxidative stress in progressive myoclonus epilepsy, EPM1. *J. Neurosci. Off. J. Soc. Neurosci.* 29, 5910–5915. doi: 10.1523/JNEUROSCI.0682-09.2009

Leto, K., Arancillo, M., Becker, E. B. E., Buffo, A., Chiang, C., Ding, B., et al. (2016). Consensus Paper: Cerebellar Development. *Cerebellum Lond. Engl.* 15, 789–828. doi: 10.1007/s12311-015-0724-2

Li, L., Yu, J., and Ji, S.-J. (2021). Axonal mRNA localization and translation: local events with broad roles. *Cell. Mol. Life Sci. CMLS* 78, 7379–7395. doi: 10.1007/s00018-021-03995-4

Li, Q., and Barres, B. A. (2018). Microglia and macrophages in brain homeostasis and disease. *Nat. Rev. Immunol.* 18, 225–242. doi: 10.1038/nri.2017.125

Liao, Y.-C., Fernandopulle, M. S., Wang, G., Choi, H., Hao, L., Drerup, C. M., et al. (2019). RNA Granules Hitchhike on Lysosomes for Long-Distance Transport, Using Annexin A11 as a Molecular Tether. *Cell* 179, 147-164.e20. doi: 10.1016/j.cell.2019.08.050

Lieuallen, K., Pennacchio, L. A., Park, M., Myers, R. M., and Lennon, G. G. (2001). Cystatin B-deficient mice have increased expression of apoptosis and glial activation genes. *Hum. Mol. Genet.* 10, 1867–1871. doi: 10.1093/hmg/10.18.1867

Liu, D., Gao, Y., Liu, J., Huang, Y., Yin, J., Feng, Y., et al. (2021). Intercellular mitochondrial transfer as a means of tissue revitalization. *Signal Transduct. Target. Ther.* 6, 65. doi: 10.1038/s41392-020-00440-z

Liu, P.-P., Liu, X.-H., Ren, M.-J., Liu, X.-T., Shi, X.-Q., Li, M.-L., et al. (2025). Neuronal cathepsin S increases neuroinflammation and causes cognitive decline via CX3CL1-CX3CR1 axis and JAK2-STAT3 pathway in aging and Alzheimer's disease. *Aging Cell* 24, e14393. doi: 10.1111/acel.14393

Liuzzo, J. P., Petanceska, S. S., Moscatelli, D., and Devi, L. A. (1999). Inflammatory mediators regulate cathepsin S in macrophages and microglia: A role in attenuating heparan sulfate interactions. *Mol. Med. Camb. Mass* 5, 320–333.

Love, M. I., Huber, W., and Anders, S. (2014). Moderated estimation of fold change and dispersion for RNA-seq data with DESeq2. *Genome Biol.* 15, 550. doi: 10.1186/s13059-014-0550-8

Lucchino, V., Scaramuzzino, L., Scalise, S., Lo Conte, M., Zannino, C., Benedetto, G. L., et al. (2022). Insights into the Genetic Profile of Two Siblings Affected by Unverricht-Lundborg Disease Using Patient-Derived hiPSCs. *Cells* 11, 3491. doi: 10.3390/cells11213491

Luciano-Montalvo, C., Ciborowski, P., Duan, F., Gendelman, H. E., and Meléndez, L. M. (2008). Proteomic analyses associate cystatin B with restricted HIV-1 replication in placental macrophages. *Placenta* 29, 1016–1023. doi: 10.1016/j.placenta.2008.09.005

Ludwig, A., Schulte, A., Schnack, C., Hundhausen, C., Reiss, K., Brodway, N., et al. (2005). Enhanced expression and shedding of the transmembrane chemokine CXCL16 by reactive astrocytes and glioma cells. *J. Neurochem.* 93, 1293–1303. doi: 10.1111/j.1471-4159.2005.03123.x

Ludwig, P. E., and Das, J. M. (2025). "Histology, Glial Cells," in *StatPearls*, (Treasure Island (FL): StatPearls Publishing). Available at: http://www.ncbi.nlm.nih.gov/books/NBK441945/ (Accessed May 26, 2025).

Ludwig, P. E., Reddy, V., and Varacallo, M. (2023). "Neuroanatomy, Neurons," in *StatPearls*, (Treasure Island (FL): StatPearls Publishing). Available at: http://www.ncbi.nlm.nih.gov/books/NBK441977/ (Accessed October 31, 2023).

Luo, P., Chu, S.-F., Zhang, Z., Xia, C.-Y., and Chen, N.-H. (2019). Fractalkine/CX3CR1 is involved in the cross-talk between neuron and glia in neurological diseases. *Brain Res. Bull.* 146, 12–21. doi: 10.1016/j.brainresbull.2018.11.017

Macioce, P., Gandolfi, N., Leung, C. L., Chin, S. S., Malchiodi-Albedi, F., Ceccarini, M., et al. (1999). Characterization of NF-L and betaIISigma1-spectrin interaction in live cells. *Exp. Cell Res.* 250, 142–154. doi: 10.1006/excr.1999.4479

Macosko, E. Z., Basu, A., Satija, R., Nemesh, J., Shekhar, K., Goldman, M., et al. (2015). Highly Parallel Genome-wide Expression Profiling of Individual Cells Using Nanoliter Droplets. *Cell* 161, 1202–1214. doi: 10.1016/j.cell.2015.05.002

Maday, S., Twelvetrees, A. E., Moughamian, A. J., and Holzbaur, E. L. F. (2014). AXONAL TRANSPORT: CARGO-SPECIFIC MECHANISMS OF MOTILITY AND REGULATION. *Neuron* 84, 292–309. doi: 10.1016/j.neuron.2014.10.019

Maday, S., Wallace, K. E., and Holzbaur, E. L. F. (2012). Autophagosomes initiate distally and mature during transport toward the cell soma in primary neurons. *J. Cell Biol.* 196, 407–417. doi: 10.1083/jcb.201106120

Maezawa, I., Wang, B., Hu, Q., Martin, G. M., Jin, L.-W., and Oshima, J. (2002). Alterations of chaperone protein expression in presenilin mutant neurons in response to glutamate excitotoxicity. *Pathol. Int.* 52, 551–554. doi: 10.1046/j.1440-1827.2002.01398.x

Maher, K., Kokelj, B. J., Butinar, M., Mikhaylov, G., Manček-Keber, M., Stoka, V., et al. (2014). A role for stefin B (cystatin B) in inflammation and endotoxemia. *J. Biol. Chem.* 289, 31736–31750. doi: 10.1074/jbc.M114.609396

Maier, M., Peng, Y., Jiang, L., Seabrook, T. J., Carroll, M. C., and Lemere, C. A. (2008). Complement C3 deficiency leads to accelerated amyloid beta plaque deposition and neurodegeneration and modulation of the microglia/macrophage phenotype in amyloid precursor protein transgenic mice. *J. Neurosci. Off. J. Soc. Neurosci.* 28, 6333–6341. doi: 10.1523/JNEUROSCI.0829-08.2008

Majumdar, A., Ramagiri, S., and Rikhy, R. (2006). Drosophila homologue of Eps15 is essential for synaptic vesicle recycling. *Exp. Cell Res.* 312, 2288–2298. doi: 10.1016/j.yexcr.2006.03.030

Maldonado, K. A., and Alsayouri, K. (2023). "Physiology, Brain," in *StatPearls*, (Treasure Island (FL): StatPearls Publishing). Available at: http://www.ncbi.nlm.nih.gov/books/NBK551718/ (Accessed October 31, 2023).

Man, S. M., and Kanneganti, T.-D. (2016). Regulation of lysosomal dynamics and autophagy by CTSB/cathepsin B. *Autophagy* 12, 2504–2505. doi: 10.1080/15548627.2016.1239679

Mancini, G. M. S., Schot, R., de Wit, M. C. Y., Coo, R. F. de, Oostenbrink, R., Heus, K. B., et al. (2016). CSTB null mutation associated with microcephaly, early developmental delay, and severe dyskinesia. *Neurology* 86, 877–878. doi: 10.1212/WNL.0000000000002422

Manninen, O., Koskenkorva, P., Lehtimaki, K. K., Hypponen, J., Kononen, M., Laitinen, T., et al. (2013). White matter degeneration with Unverricht-Lundborg progressive myoclonus epilepsy: a translational diffusion-tensor imaging study in patients and cystatin B-deficient mice. *Radiology* 269, 232–239. doi: 10.1148/radiol.13122458%20%5Bdoi%5D

Manninen, O., Laitinen, T., Lehtimaki, K. K., Tegelberg, S., Lehesjoki, A. E., Grohn, O., et al. (2014). Progressive volume loss and white matter degeneration in cstb-deficient mice: a diffusion tensor and longitudinal volumetry MRI study. *PloS One* 9, e90709. doi: 10.1371/journal.pone.0090709%20%5Bdoi%5D

Mascalchi, M., Michelucci, R., Cosottini, M., Tessa, C., Lolli, F., Riguzzi, P., et al. (2002). Brainstem involvement in Unverricht-Lundborg disease (EPM1): An MRI and (1)H MRS study. *Neurology* 58, 1686–1689. doi: 10.1212/wnl.58.11.1686

McCommis, K. S., and Finck, B. N. (2015). Mitochondrial pyruvate transport: a historical perspective and future research directions. *Biochem. J.* 466, 443–454. doi: 10.1042/BJ20141171

Mergenthaler, P., Lindauer, U., Dienel, G. A., and Meisel, A. (2013). Sugar for the brain: the role of glucose in physiological and pathological brain function. *Trends Neurosci.* 36, 587–597. doi: 10.1016/j.tins.2013.07.001

Metsalu, T., and Vilo, J. (2015). ClustVis: a web tool for visualizing clustering of multivariate data using Principal Component Analysis and heatmap. *Nucleic Acids Res.* 43, W566–W570. doi: 10.1093/nar/gkv468

Mitchell, P. (1961). Coupling of phosphorylation to electron and hydrogen transfer by a chemi-osmotic type of mechanism. *Nature* 191, 144–148. doi: 10.1038/191144a0

Mitra, S., Banik, A., Saurabh, S., Maulik, M., and Khatri, S. N. (2022). Neuroimmunometabolism: A New Pathological Nexus Underlying Neurodegenerative Disorders. *J. Neurosci. Off. J. Soc. Neurosci.* 42, 1888–1907. doi: 10.1523/JNEUROSCI.0998-21.2022

Monje, M. L., Toda, H., and Palmer, T. D. (2003). Inflammatory blockade restores adult hippocampal neurogenesis. *Science* 302, 1760–1765. doi: 10.1126/science.1088417

Motori, E., Atanassov, I., Kochan, S. M. V., Folz-Donahue, K., Sakthivelu, V., Giavalisco, P., et al. (2020). Neuronal metabolic rewiring promotes resilience to neurodegeneration caused by mitochondrial dysfunction. *Sci. Adv.* 6, eaba8271. doi: 10.1126/sciadv.aba8271

Mottahedin, A., Ardalan, M., Chumak, T., Riebe, I., Ek, J., and Mallard, C. (2017). Effect of Neuroinflammation on Synaptic Organization and Function in the Developing Brain: Implications for Neurodevelopmental and Neurodegenerative Disorders. *Front. Cell. Neurosci.* 11, 190. doi: 10.3389/fncel.2017.00190

Nagappan-Chettiar, S., Yasuda, M., Johnson-Venkatesh, E. M., and Umemori, H. (2023). The molecular signals that regulate activity-dependent synapse refinement in the brain. *Curr. Opin. Neurobiol.* 79, 102692. doi: 10.1016/j.conb.2023.102692

Nemani, V. M., Lu, W., Berge, V., Nakamura, K., Onoa, B., Lee, M. K., et al. (2010). Increased expression of alpha-synuclein reduces neurotransmitter release by inhibiting synaptic vesicle reclustering after endocytosis. *Neuron* 65, 66–79. doi: 10.1016/j.neuron.2009.12.023

Neumann, H., Kotter, M. R., and Franklin, R. J. M. (2009). Debris clearance by microglia: an essential link between degeneration and regeneration. *Brain J. Neurol.* 132, 288–295. doi: 10.1093/brain/awn109

Nolt, M. J., Lin, Y., Hruska, M., Murphy, J., Sheffler-Colins, S. I., Kayser, M. S., et al. (2011). EphB controls NMDA receptor function and synaptic targeting in a subunit-specific manner. *J. Neurosci. Off. J. Soc. Neurosci.* 31, 5353–5364. doi: 10.1523/JNEUROSCI.0282-11.2011

O'Brien, A., Marshall, C. R., Blaser, S., Ray, P. N., and Yoon, G. (2017). Severe neurodegeneration, progressive cerebral volume loss and diffuse hypomyelination associated with a homozygous frameshift mutation in CSTB. *Eur. J. Hum. Genet. EJHG* 25, 775–778. doi: 10.1038/ejhg.2017.39

Okuneva, O., Korber, I., Li, Z., Tian, L., Joensuu, T., Kopra, O., et al. (2015). Abnormal microglial activation in the Cstb(-/-) mouse, a model for progressive myoclonus epilepsy, EPM1. *Glia* 63, 400–411. doi: 10.1002/glia.22760%20%5Bdoi%5D

Okuneva, O., Li, Z., Korber, I., Tegelberg, S., Joensuu, T., Tian, L., et al. (2016). Brain inflammation is accompanied by peripheral inflammation in Cstb (-/-) mice, a model for progressive myoclonus epilepsy. *J. Neuroinflammation* 13, 298–7. doi: 10.1186/s12974-016-0764-7%20%5Bdoi%5D

Oltion, K., Carelli, J. D., Yang, T., See, S. K., Wang, H.-Y., Kampmann, M., et al. (2023). An E3 ligase network engages GCN1 to promote the degradation of translation factors on stalled ribosomes. *Cell* 186, 346-362.e17. doi: 10.1016/j.cell.2022.12.025

O'Rourke, N. A., Weiler, N. C., Micheva, K. D., and Smith, S. J. (2012). Deep molecular diversity of mammalian synapses: why it matters and how to measure it. *Nat. Rev. Neurosci.* 13, 365–379. doi: 10.1038/nrn3170

Palay, S. L. (1956). Synapses in the central nervous system. *J. Biophys. Biochem. Cytol.* 2, 193–202. doi: 10.1083/jcb.2.4.193

Papale, A., d'Isa, R., Menna, E., Cerovic, M., Solari, N., Hardingham, N., et al. (2017). Severe Intellectual Disability and Enhanced Gamma-Aminobutyric Acidergic Synaptogenesis in a Novel Model of Rare RASopathies. *Biol. Psychiatry* 81, 179–192. doi: 10.1016/j.biopsych.2016.06.016

Pathak, D., Shields, L. Y., Mendelsohn, B. A., Haddad, D., Lin, W., Gerencser, A. A., et al. (2015). The Role of Mitochondrially Derived ATP in Synaptic Vesicle Recycling. *J. Biol. Chem.* 290, 22325–22336. doi: 10.1074/jbc.M115.656405

Pattingre, S., Tassa, A., Qu, X., Garuti, R., Liang, X. H., Mizushima, N., et al. (2005). Bcl-2 antiapoptotic proteins inhibit Beclin 1-dependent autophagy. *Cell* 122, 927–939. doi: 10.1016/j.cell.2005.07.002

Paudel, R. R., Lu, D., Roy Chowdhury, S., Monroy, E. Y., and Wang, J. (2023). Targeted Protein Degradation via Lysosomes. *Biochemistry* 62, 564–579. doi: 10.1021/acs.biochem.2c00310

Peerboom, C., and Wierenga, C. J. (2021). The postnatal GABA shift: A developmental perspective. *Neurosci. Biobehav. Rev.* 124, 179–192. doi: 10.1016/j.neubiorev.2021.01.024

Pellagatti, A., Hellström-Lindberg, E., Giagounidis, A., Perry, J., Malcovati, L., Della Porta, M. G., et al. (2008). Haploinsufficiency of RPS14 in 5q- syndrome is associated with deregulation of ribosomal- and translation-related genes. *Br. J. Haematol.* 142, 57–64. doi: 10.1111/j.1365-2141.2008.07178.x

Pellerin, L., Bouzier-Sore, A.-K., Aubert, A., Serres, S., Merle, M., Costalat, R., et al. (2007). Activity-dependent regulation of energy metabolism by astrocytes: an update. *Glia* 55, 1251–1262. doi: 10.1002/glia.20528

Pellerin, L., and Magistretti, P. J. (1994). Glutamate uptake into astrocytes stimulates aerobic glycolysis: a mechanism coupling neuronal activity to glucose utilization. *Proc. Natl. Acad. Sci. U. S. A.* 91, 10625–10629. doi: 10.1073/pnas.91.22.10625

Penna, E., Cerciello, A., Chambery, A., Russo, R., Cernilogar, F. M., Pedone, E. M., et al. (2019). Cystatin B Involvement in Synapse Physiology of Rodent Brains and Human Cerebral Organoids. *Front. Mol. Neurosci.* 12, 195. doi: 10.3389/fnmol.2019.00195

Pennacchio, L. A., Bouley, D. M., Higgins, K. M., Scott, M. P., Noebels, J. L., and Myers, R. M. (1998). Progressive ataxia, myoclonic epilepsy and cerebellar apoptosis in cystatin B-deficient mice. *Nat. Genet.* 20, 251–258. doi: 10.1038/3059%20%5Bdoi%5D

Perry, R. B.-T., Rishal, I., Doron-Mandel, E., Kalinski, A. L., Medzihradszky, K. F., Terenzio, M., et al. (2016). Nucleolin-Mediated RNA Localization Regulates Neuron Growth and Cycling Cell Size. *Cell Rep.* 16, 1664–1676. doi: 10.1016/j.celrep.2016.07.005

Pfeffer, S. R. (2013). Rab GTPase regulation of membrane identity. *Curr. Opin. Cell Biol.* 25, 414–419. doi: 10.1016/j.ceb.2013.04.002

Pines, G., Danbolt, N. C., Bjørås, M., Zhang, Y., Bendahan, A., Eide, L., et al. (1992). Cloning and expression of a rat brain L-glutamate transporter. *Nature* 360, 464–467. doi: 10.1038/360464a0

Pizzella, A., Penna, E., Abate, N., Frenna, E., Canafoglia, L., Ragona, F., et al. (2023). Pathological Deficit of Cystatin B Impairs Synaptic Plasticity in EPM1 Human Cerebral Organoids. *Mol. Neurobiol.* doi: 10.1007/s12035-023-03812-y

Plum, S., Steinbach, S., Abel, L., Marcus, K., Helling, S., and May, C. (2015). Proteomics in neurodegenerative diseases: Methods for obtaining a closer look at the neuronal proteome. *Proteomics Clin. Appl.* 9, 848–871. doi: 10.1002/prca.201400030

Pol, E., and Björk, I. (2003). Contributions of individual residues in the N-terminal region of cystatin B (stefin B) to inhibition of cysteine proteinases. *Biochim. Biophys. Acta* 1645, 105–112. doi: 10.1016/s1570-9639(02)00526-5

Polajnar, M., Zavašnik-Bergant, T., Škerget, K., Vizovišek, M., Vidmar, R., Fonović, M., et al. (2014). Human Stefin B Role in Cell's Response to Misfolded Proteins and Autophagy. *PLoS ONE* 9, e102500. doi: 10.1371/journal.pone.0102500

Pollari, E., Tegelberg, S., Björklund, H., Kälviäinen, R., Lehesjoki, A.-E., and Haapalinna, A. (2023). In depth behavioral phenotyping unravels complex motor disturbances in Cstb−/− mouse, a model for progressive myoclonus epilepsy type 1. *Front. Behav. Neurosci.* 17, 1325051. doi: 10.3389/fnbeh.2023.1325051

Popiolek-Barczyk, K., Ciechanowska, A., Ciapała, K., Pawlik, K., Oggioni, M., Mercurio, D., et al. (2020). The CCL2/CCL7/CCL12/CCR2 pathway is substantially and persistently upregulated in mice after traumatic brain injury, and CCL2 modulates the complement system in microglia. *Mol. Cell. Probes* 54, 101671. doi: 10.1016/j.mcp.2020.101671

Poulopoulos, A., Aramuni, G., Meyer, G., Soykan, T., Hoon, M., Papadopoulos, T., et al. (2009). Neuroligin 2 Drives Postsynaptic Assembly at Perisomatic Inhibitory Synapses through Gephyrin and Collybistin. *Neuron* 63, 628–642. doi: 10.1016/j.neuron.2009.08.023

Powers, W. J., Videen, T. O., Markham, J., McGee-Minnich, L., Antenor-Dorsey, J. V., Hershey, T., et al. (2007). Selective defect of in vivo glycolysis in early Huntington's disease striatum. *Proc. Natl. Acad. Sci. U. S. A.* 104, 2945–2949. doi: 10.1073/pnas.0609833104

Price, J. C., Guan, S., Burlingame, A., Prusiner, S. B., and Ghaemmaghami, S. (2010). Analysis of proteome dynamics in the mouse brain. *Proc. Natl. Acad. Sci. U. S. A.* 107, 14508–14513. doi: 10.1073/pnas.1006551107

Proctor, W. R., Poelchen, W., Bowers, B. J., Wehner, J. M., Messing, R. O., and Dunwiddie, T. V. (2003). Ethanol Differentially Enhances Hippocampal GABA $_A$ Receptor-Mediated Responses in Protein Kinase Cγ (PKCγ) and PKCε Null Mice. *J. Pharmacol. Exp. Ther.* 305, 264–270. doi: 10.1124/jpet.102.045450

Purves, D. ed. (2012). *Neuroscience*., 5. ed. Sunderland, Mass: Sinauer.

Pushpalatha, K. V., and Besse, F. (2019). Local Translation in Axons: When Membraneless RNP Granules Meet Membrane-Bound Organelles. *Front. Mol. Biosci.* 6, 129. doi: 10.3389/fmolb.2019.00129

Qi, X., Man, S. M., Malireddi, R. K. S., Karki, R., Lupfer, C., Gurung, P., et al. (2016). Cathepsin B modulates lysosomal biogenesis and host defense against Francisella novicida infection. *J. Exp. Med.* 213, 2081–2097. doi: 10.1084/jem.20151938

Quirós, P. M., Langer, T., and López-Otín, C. (2015). New roles for mitochondrial proteases in health, ageing and disease. *Nat. Rev. Mol. Cell Biol.* 16, 345–359. doi: 10.1038/nrm3984

Rahpeymai, Y., Hietala, M. A., Wilhelmsson, U., Fotheringham, A., Davies, I., Nilsson, A.-K., et al. (2006). Complement: a novel factor in basal and ischemia-induced neurogenesis. *EMBO J.* 25, 1364–1374. doi: 10.1038/sj.emboj.7601004

Rangaraju, V., Calloway, N., and Ryan, T. A. (2014). Activity-driven local ATP synthesis is required for synaptic function. *Cell* 156, 825–835. doi: 10.1016/j.cell.2013.12.042

Ransohoff, R. M. (2016). How neuroinflammation contributes to neurodegeneration. *Science* 353, 777–783. doi: 10.1126/science.aag2590

Rath, S., Sharma, R., Gupta, R., Ast, T., Chan, C., Durham, T. J., et al. (2021). MitoCarta3.0: an updated mitochondrial proteome now with sub-organelle localization and pathway annotations. *Nucleic Acids Res.* 49, D1541–D1547. doi: 10.1093/nar/gkaa1011

Razi, M., Chan, E. Y. W., and Tooze, S. A. (2009). Early endosomes and endosomal coatomer are required for autophagy. *J. Cell Biol.* 185, 305–321. doi: 10.1083/jcb.200810098

Reiman, E. M., Chen, K., Alexander, G. E., Caselli, R. J., Bandy, D., Osborne, D., et al. (2005). Correlations between apolipoprotein E epsilon4 gene dose and brain-imaging measurements of regional hypometabolism. *Proc. Natl. Acad. Sci. U. S. A.* 102, 8299–8302. doi: 10.1073/pnas.0500579102

Reis, K., Fransson, A., and Aspenström, P. (2009). The Miro GTPases: at the heart of the mitochondrial transport machinery. *FEBS Lett.* 583, 1391–1398. doi: 10.1016/j.febslet.2009.04.015

Repnik, U., Stoka, V., Turk, V., and Turk, B. (2012). Lysosomes and lysosomal cathepsins in cell death. *Biochim. Biophys. Acta* 1824, 22–33. doi: 10.1016/j.bbapap.2011.08.016

Riccio, M., Giaimo, R. D., Pianetti, S., Palmieri, P. P., Melli, M., and Santi, S. (2001). Nuclear localization of cystatin B, the cathepsin inhibitor implicated in myoclonus epilepsy (EPM1). *Exp. Cell Res.* 262, 84–94. doi: 10.1006/excr.2000.5085

Rinne, R., Saukko, P., Järvinen, M., and Lehesjoki, A.-E. (2002). Reduced cystatin B activity correlates with enhanced cathepsin activity in progressive myoclonus epilepsy. *Ann. Med.* 34, 380–385. doi: 10.1080/078538902320772124

Rishal, I., and Fainzilber, M. (2014). Axon-soma communication in neuronal injury. *Nat. Rev. Neurosci.* 15, 32–42. doi: 10.1038/nrn3609

Rivera, L. E., Colon, K., Cantres-Rosario, Y. M., Zenon, F. M., and Melendez, L. M. (2014). Macrophage derived cystatin B/cathepsin B in HIV replication and neuropathogenesis. *Curr. HIV Res.* 12, 111–120. doi: 10.2174/1570162x12666140526120249

Rizzoli, S. O. (2014). Synaptic vesicle recycling: steps and principles. *EMBO J.* 33, 788–822. doi: 10.1002/embj.201386357

Rodriguez, A. J., Czaplinski, K., Condeelis, J. S., and Singer, R. H. (2008). Mechanisms and cellular roles of local protein synthesis in mammalian cells. *Curr. Opin. Cell Biol.* 20, 144–149. doi: 10.1016/j.ceb.2008.02.004

Roostaei, T., Nazeri, A., Sahraian, M. A., and Minagar, A. (2014). The human cerebellum: a review of physiologic neuroanatomy. *Neurol. Clin.* 32, 859–869. doi: 10.1016/j.ncl.2014.07.013

Rossi, D., Barbosa, N. M., Galvão, F. C., Boldrin, P. E. G., Hershey, J. W. B., Zanelli, C. F., et al. (2016). Evidence for a Negative Cooperativity between eIF5A and eEF2 on Binding to the Ribosome. *PloS One* 11, e0154205. doi: 10.1371/journal.pone.0154205

Rossi, D. J., Hamann, M., and Attwell, D. (2003). Multiple modes of GABAergic inhibition of rat cerebellar granule cells. *J. Physiol.* 548, 97–110. doi: 10.1113/jphysiol.2002.036459

Rossi, M. J., and Pekkurnaz, G. (2019). Powerhouse of the mind: mitochondrial plasticity at the synapse. *Curr. Opin. Neurobiol.* 57, 149–155. doi: 10.1016/j.conb.2019.02.001

Rostène, W., Kitabgi, P., and Parsadaniantz, S. M. (2007). Chemokines: a new class of neuromodulator? *Nat. Rev. Neurosci.* 8, 895–903. doi: 10.1038/nrn2255

Rousseau, J., Tene Tadoum, S. B., Lavertu Jolin, M., Nguyen, T. T. M., Ajeawung, N. F., Flenniken, A. M., et al. (2023). The ATP6V1B2 DDOD/DOORS-Associated p.Arg506* Variant Causes Hyperactivity and Seizures in Mice. *Genes* 14, 1538. doi: 10.3390/genes14081538

Rowland, A. M., Richmond, J. E., Olsen, J. G., Hall, D. H., and Bamber, B. A. (2006). Presynaptic terminals independently regulate synaptic clustering and autophagy of GABAA receptors

in Caenorhabditis elegans. *J. Neurosci. Off. J. Soc. Neurosci.* 26, 1711–1720. doi: 10.1523/JNEUROSCI.2279-05.2006

Roy, S. (2014). Seeing the unseen: the hidden world of slow axonal transport. *Neurosci. Rev. J. Bringing Neurobiol. Neurol. Psychiatry* 20, 71–81. doi: 10.1177/1073858413498306

Safiulina, V. F., Fattorini, G., Conti, F., and Cherubini, E. (2006). GABAergic Signaling at Mossy Fiber Synapses in Neonatal Rat Hippocampus. *J. Neurosci.* 26, 597–608. doi: 10.1523/JNEUROSCI.4493-05.2006

Saini, P., Eyler, D. E., Green, R., and Dever, T. E. (2009). Hypusine-containing protein eIF5A promotes translation elongation. *Nature* 459, 118–121. doi: 10.1038/nature08034

Salogiannis, J., and Reck-Peterson, S. L. (2017). Hitchhiking: A Non-Canonical Mode of Microtubule-Based Transport. *Trends Cell Biol.* 27, 141–150. doi: 10.1016/j.tcb.2016.09.005

Sathyanesan, A., Zhou, J., Scafidi, J., Heck, D. H., Sillitoe, R. V., and Gallo, V. (2019). Emerging connections between cerebellar development, behaviour and complex brain disorders. *Nat. Rev. Neurosci.* 20, 298–313. doi: 10.1038/s41583-019-0152-2

Saxton, W. M., and Hollenbeck, P. J. (2012). The axonal transport of mitochondria. *J. Cell Sci.* 125, 2095–2104. doi: 10.1242/jcs.053850

Schafer, D. P., and Stevens, B. (2010). Synapse elimination during development and disease: immune molecules take centre stage. *Biochem. Soc. Trans.* 38, 476–481. doi: 10.1042/BST0380476

Schanzenbächer, C. T., Sambandan, S., Langer, J. D., and Schuman, E. M. (2016). Nascent Proteome Remodeling following Homeostatic Scaling at Hippocampal Synapses. *Neuron* 92, 358–371. doi: 10.1016/j.neuron.2016.09.058

Scharfman, H. E. (2007). The neurobiology of epilepsy. *Curr. Neurol. Neurosci. Rep.* 7, 348–354. doi: 10.1007/s11910-007-0053-z

Schönfeld, P., and Reiser, G. (2013). Why does brain metabolism not favor burning of fatty acids to provide energy? Reflections on disadvantages of the use of free fatty acids as fuel for brain. *J. Cereb. Blood Flow Metab. Off. J. Int. Soc. Cereb. Blood Flow Metab.* 33, 1493–1499. doi: 10.1038/jcbfm.2013.128

Schrimpf, S. P., Meskenaite, V., Brunner, E., Rutishauser, D., Walther, P., Eng, J., et al. (2005). Proteomic analysis of synaptosomes using isotope-coded affinity tags and mass spectrometry. *Proteomics* 5, 2531–2541. doi: 10.1002/pmic.200401198

Scott, D. A., Das, U., Tang, Y., and Roy, S. (2011). Mechanistic Logic Underlying the Axonal Transport of Cytosolic Proteins. *Neuron* 70, 441–454. doi: 10.1016/j.neuron.2011.03.022

Sha, Z., Zhao, J., and Goldberg, A. L. (2018). Measuring the Overall Rate of Protein Breakdown in Cells and the Contributions of the Ubiquitin-Proteasome and Autophagy-Lysosomal Pathways. *Methods Mol. Biol. Clifton NJ* 1844, 261–276. doi: 10.1007/978-1-4939-8706-1_17

Shannon, P., Pennacchio, L. A., Houseweart, M. K., Minassian, B. A., and Myers, R. M. (2002). Neuropathological changes in a mouse model of progressive myoclonus epilepsy: cystatin B deficiency and Unverricht-Lundborg disease. *J. Neuropathol. Exp. Neurol.* 61, 1085–1091.

Shigeoka, T., Jung, H., Jung, J., Turner-Bridger, B., Ohk, J., Lin, J. Q., et al. (2016). Dynamic Axonal Translation in Developing and Mature Visual Circuits. *Cell* 166, 181–192. doi: 10.1016/j.cell.2016.05.029

Sierra-Torre, V., Plaza-Zabala, A., Bonifazi, P., Abiega, O., Díaz-Aparicio, I., Tegelberg, S., et al. (2020). Microglial phagocytosis dysfunction in the dentate gyrus is related to local neuronal activity in a genetic model of epilepsy. *Epilepsia* 61, 2593–2608. doi: 10.1111/epi.16692

Siletti, K., Hodge, R., Mossi Albiach, A., Lee, K. W., Ding, S.-L., Hu, L., et al. (2023). Transcriptomic diversity of cell types across the adult human brain. *Science* 382, eadd7046. doi: 10.1126/science.add7046

Silvennoinen, K., Säisänen, L., Hyppönen, J., Rissanen, S. M., Karjalainen, P. A., D'Ambrosio, S., et al. (2023). Short- and long-interval intracortical inhibition in EPM1 is related to genotype. *Epilepsia* 64, 208–217. doi: 10.1111/epi.17466

Silverthorn, D. U. (2009). *Human physiology: an integrated approach*., 4th ed. Harlow: Pearson Education.

Simats, A., García-Berrocoso, T., Penalba, A., Giralt, D., Llovera, G., Jiang, Y., et al. (2018). CCL23: a new CC chemokine involved in human brain damage. *J. Intern. Med.* 283, 461–475. doi: 10.1111/joim.12738

Simons, M., and Nave, K.-A. (2015). Oligodendrocytes: Myelination and Axonal Support. *Cold Spring Harb. Perspect. Biol.* 8, a020479. doi: 10.1101/cshperspect.a020479

Singh, O. V., Yaster, M., Xu, J.-T., Guan, Y., Guan, X., Dharmarajan, A. M., et al. (2009). Proteome of synaptosome-associated proteins in spinal cord dorsal horn after peripheral nerve injury. *Proteomics* 9, 1241–1253. doi: 10.1002/pmic.200800636

Singh, S., Plotnikova, L., Karvonen, K., Ryytty, S., Hyppönen, J., Kälviäinen, R., et al. (2023). Generation of a human induced pluripotent stem cell line (UEFi004-A) from a patient with progressive myoclonic epilepsy type 1 (EPM1). *Stem Cell Res.* 73, 103248. doi: 10.1016/j.scr.2023.103248

Sipilä, J. O. T., Hyppönen, J., Kytö, V., and Kälviäinen, R. (2020). Unverricht-Lundborg disease (EPM1) in Finland: A nationwide population-based study. *Neurology* 95, e3117–e3123. doi: 10.1212/WNL.0000000000010911

Sipilä, S., Huttu, K., Voipio, J., and Kaila, K. (2004). GABA Uptake via GABA Transporter-1 Modulates GABAergic Transmission in the Immature Hippocampus. *J. Neurosci.* 24, 5877–5880. doi: 10.1523/JNEUROSCI.1287-04.2004

Skoff, R. P. (1980). Neuroglia: A Reevaluation of their Origin and Development. *Pathol. - Res. Pract.* 168, 279–300. doi: 10.1016/S0344-0338(80)80270-6

Smith, P. L. P., Hagberg, H., Naylor, A. S., and Mallard, C. (2014). Neonatal peripheral immune challenge activates microglia and inhibits neurogenesis in the developing murine hippocampus. *Dev. Neurosci.* 36, 119–131. doi: 10.1159/000359950

Somera-Molina, K. C., Nair, S., Van Eldik, L. J., Watterson, D. M., and Wainwright, M. S. (2009). Enhanced microglial activation and proinflammatory cytokine upregulation are linked to increased susceptibility to seizures and neurologic injury in a "two-hit" seizure model. *Brain Res.* 1282, 162–172. doi: 10.1016/j.brainres.2009.05.073

Song, J., Herrmann, J. M., and Becker, T. (2021). Quality control of the mitochondrial proteome. *Nat. Rev. Mol. Cell Biol.* 22, 54–70. doi: 10.1038/s41580-020-00300-2

Sorce, S., Myburgh, R., and Krause, K.-H. (2011). The chemokine receptor CCR5 in the central nervous system. *Prog. Neurobiol.* 93, 297–311. doi: 10.1016/j.pneurobio.2010.12.003

Sörensen, L., Ekstrand, M., Silva, J. P., Lindqvist, E., Xu, B., Rustin, P., et al. (2001). Late-onset corticohippocampal neurodepletion attributable to catastrophic failure of oxidative phosphorylation in MILON mice. *J. Neurosci. Off. J. Soc. Neurosci.* 21, 8082–8090. doi: 10.1523/JNEUROSCI.21-20-08082.2001

Sossin, W. S., and DesGroseillers, L. (2006). Intracellular trafficking of RNA in neurons. *Traffic Cph. Den.* 7, 1581–1589. doi: 10.1111/j.1600-0854.2006.00500.x

Sowa, J. E., and Tokarski, K. (2021). Cellular, synaptic, and network effects of chemokines in the central nervous system and their implications to behavior. *Pharmacol. Rep. PR* 73, 1595–1625. doi: 10.1007/s43440-021-00323-2

Soykan, T., Haucke, V., and Kuijpers, M. (2021). Mechanism of synaptic protein turnover and its regulation by neuronal activity. *Curr. Opin. Neurobiol.* 69, 76–83. doi: 10.1016/j.conb.2021.02.006

Spillane, M., Ketschek, A., Merianda, T. T., Twiss, J. L., and Gallo, G. (2013). Mitochondria coordinate sites of axon branching through localized intra-axonal protein synthesis. *Cell Rep.* 5, 1564–1575. doi: 10.1016/j.celrep.2013.11.022

Stahl-Meyer, J., Stahl-Meyer, K., and Jäättelä, M. (2021). Control of mitosis, inflammation, and cell motility by limited leakage of lysosomes. *Curr. Opin. Cell Biol.* 71, 29–37. doi: 10.1016/j.ceb.2021.02.003

Stellwagen, D., and Malenka, R. C. (2006). Synaptic scaling mediated by glial TNF-alpha. *Nature* 440, 1054–1059. doi: 10.1038/nature04671

Stevens, B., Allen, N. J., Vazquez, L. E., Howell, G. R., Christopherson, K. S., Nouri, N., et al. (2007). The classical complement cascade mediates CNS synapse elimination. *Cell* 131, 1164–1178. doi: 10.1016/j.cell.2007.10.036

Stoka, V., Turk, V., and Turk, B. (2016). Lysosomal cathepsins and their regulation in aging and neurodegeneration. *Ageing Res. Rev.* 32, 22–37. doi: 10.1016/j.arr.2016.04.010

Su, L.-J., Zhang, J.-H., Gomez, H., Murugan, R., Hong, X., Xu, D., et al. (2019). Reactive Oxygen Species-Induced Lipid Peroxidation in Apoptosis, Autophagy, and Ferroptosis. *Oxid. Med. Cell. Longev.* 2019, 5080843. doi: 10.1155/2019/5080843

Subbarayan, M. S., Joly-Amado, A., Bickford, P. C., and Nash, K. R. (2022). CX3CL1/CX3CR1 signaling targets for the treatment of neurodegenerative diseases. *Pharmacol. Ther.* 231, 107989. doi: 10.1016/j.pharmthera.2021.107989

Sudhof, T. C. (2004). The synaptic vesicle cycle. *Annu. Rev. Neurosci.* 27, 509–547. doi: 10.1146/annurev.neuro.26.041002.131412

Sun, C., and Schuman, E. M. (2022). Logistics of neuronal protein turnover: Numbers and mechanisms. *Mol. Cell. Neurosci.* 123, 103793. doi: 10.1016/j.mcn.2022.103793

Suzdak, P. D., Frederiksen, K., Andersen, K. E., Sørensen, P. O., Knutsen, L. J., and Nielsen, E. B. (1992). NNC-711, a novel potent and selective gamma-aminobutyric acid uptake inhibitor: pharmacological characterization. *Eur. J. Pharmacol.* 224, 189–198. doi: 10.1016/0014-2999(92)90804-d

Takaya, A., Peng, W.-X., Ishino, K., Kudo, M., Yamamoto, T., Wada, R., et al. (2015). Cystatin B as a potential diagnostic biomarker in ovarian clear cell carcinoma. *Int. J. Oncol.* 46, 1573–1581. doi: 10.3892/ijo.2015.2858

Takayama, F., Zhang, X., Hayashi, Y., Wu, Z., and Nakanishi, H. (2017). Dysfunction in diurnal synaptic responses and social behavior abnormalities in cathepsin S-deficient mice. *Biochem. Biophys. Res. Commun.* 490, 447–452. doi: 10.1016/j.bbrc.2017.06.061

Tang, J., Oliveros, A., and Jang, M.-H. (2019). Dysfunctional Mitochondrial Bioenergetics and Synaptic Degeneration in Alzheimer Disease. *Int. Neurourol. J.* 23, 5. doi: 10.5213/inj.1938036.018

Tang, Y., Das, U., Scott, D. A., and Roy, S. (2012). The slow axonal transport of alpha-synuclein--mechanistic commonalities amongst diverse cytosolic cargoes. *Cytoskelet. Hoboken NJ* 69, 506–513. doi: 10.1002/cm.21019

Tegelberg, S., Kopra, O., Joensuu, T., Cooper, J. D., and Lehesjoki, A. E. (2012). Early microglial activation precedes neuronal loss in the brain of the Cstb-/- mouse model of progressive myoclonus epilepsy, EPM1. *J. Neuropathol. Exp. Neurol.* 71, 40–53. doi: 10.1097/NEN.0b013e31823e68e1%20%5Bdoi%5D

Tenreiro, P., Rebelo, S., Martins, F., Santos, M., Coelho, E. D., Almeida, M., et al. (2017). Comparison of simple sucrose and percoll based methodologies for synaptosome enrichment. *Anal. Biochem.* 517, 1–8. doi: 10.1016/j.ab.2016.10.015

Török, I., Herrmann-Horle, D., Kiss, I., Tick, G., Speer, G., Schmitt, R., et al. (1999). Down-regulation of RpS21, a putative translation initiation factor interacting with P40, produces viable minute imagos and larval lethality with overgrown hematopoietic organs and imaginal discs. *Mol. Cell. Biol.* 19, 2308–2321. doi: 10.1128/MCB.19.3.2308

Town, T., Nikolic, V., and Tan, J. (2005). The microglial “activation” continuum: from innate to adaptive responses. *J. Neuroinflammation* 2, 24. doi: 10.1186/1742-2094-2-24

Treiman, D. M. (2001). GABAergic mechanisms in epilepsy. *Epilepsia* 42 Suppl 3, 8–12. doi: 10.1046/j.1528-1157.2001.042suppl.3008.x

Trstenjak Prebanda, M., Završnik, J., Turk, B., and Kopitar Jerala, N. (2019). Upregulation of Mitochondrial Redox Sensitive Proteins in LPS-Treated Stefin B-Deficient Macrophages. *Cells* 8, 1476. doi: 10.3390/cells8121476

Trstenjak-Prebanda, M., Biasizzo, M., Dolinar, K., Pirkmajer, S., Turk, B., Brault, V., et al. (2023). Stefin B Inhibits NLRP3 Inflammasome Activation via AMPK/mTOR Signalling. *Cells* 12, 2731. doi: 10.3390/cells12232731

Turk, B., Stoka, V., Rozman-Pungercar, J., Cirman, T., Droga-Mazovec, G., Oresić, K., et al. (2002). Apoptotic pathways: involvement of lysosomal proteases. *Biol. Chem.* 383, 1035–1044. doi: 10.1515/BC.2002.112

Turk, V., and Bode, W. (1991). The cystatins: protein inhibitors of cysteine proteinases. *FEBS Lett.* 285, 213–219.

Turrigiano, G. G. (2008). The self-tuning neuron: synaptic scaling of excitatory synapses. *Cell* 135, 422–435. doi: 10.1016/j.cell.2008.10.008

Tweedie-Cullen, R. Y., Reck, J. M., and Mansuy, I. M. (2009). Comprehensive mapping of post-translational modifications on synaptic, nuclear, and histone proteins in the adult mouse brain. *J. Proteome Res.* 8, 4966–4982. doi: 10.1021/pr9003739

Ulbrich, L., Cozzolino, M., Marini, E. S., Amori, I., De Jaco, A., Carrì, M. T., et al. (2014). Cystatin B and SOD1: Protein–Protein Interaction and Possible Relation to Neurodegeneration. *Cell. Mol. Neurobiol.* 34, 205–213. doi: 10.1007/s10571-013-0004-y

Vallejo, D., Codocedo, J. F., and Inestrosa, N. C. (2017). Posttranslational Modifications Regulate the Postsynaptic Localization of PSD-95. *Mol. Neurobiol.* 54, 1759–1776. doi: 10.1007/s12035-016-9745-1

van der Heijden, M. E., Gill, J. S., and Sillitoe, R. V. (2021). Abnormal Cerebellar Development in Autism Spectrum Disorders. *Dev. Neurosci.* 43, 181–190. doi: 10.1159/000515189

van Niel, G., D'Angelo, G., and Raposo, G. (2018). Shedding light on the cell biology of extracellular vesicles. *Nat. Rev. Mol. Cell Biol.* 19, 213–228. doi: 10.1038/nrm.2017.125

Van Oostrum, M., Blok, T. M., Giandomenico, S. L., Tom Dieck, S., Tushev, G., Fürst, N., et al. (2023). The proteomic landscape of synaptic diversity across brain regions and cell types. *Cell* 186, 5411-5427.e23. doi: 10.1016/j.cell.2023.09.028

Van Steenwinckel, J., Reaux-Le Goazigo, A., Pommier, B., Mauborgne, A., Dansereau, M.-A., Kitabgi, P., et al. (2011). CCL2 Released from Neuronal Synaptic Vesicles in the Spinal Cord Is a Major Mediator of Local Inflammation and Pain after Peripheral Nerve Injury. *J. Neurosci.* 31, 5865–5875. doi: 10.1523/JNEUROSCI.5986-10.2011

Vardar, G., Chang, S., Arancillo, M., Wu, Y.-J., Trimbuch, T., and Rosenmund, C. (2016). Distinct Functions of Syntaxin-1 in Neuronal Maintenance, Synaptic Vesicle Docking, and Fusion in Mouse Neurons. *J. Neurosci. Off. J. Soc. Neurosci.* 36, 7911–7924. doi: 10.1523/JNEUROSCI.1314-16.2016

Verbovšek, U., Motaln, H., Rotter, A., Atai, N. A., Gruden, K., Van Noorden, C. J. F., et al. (2014). Expression analysis of all protease genes reveals cathepsin K to be overexpressed in glioblastoma. *PloS One* 9, e111819. doi: 10.1371/journal.pone.0111819

Verstreken, P., Ly, C. V., Venken, K. J. T., Koh, T.-W., Zhou, Y., and Bellen, H. J. (2005). Synaptic mitochondria are critical for mobilization of reserve pool vesicles at Drosophila neuromuscular junctions. *Neuron* 47, 365–378. doi: 10.1016/j.neuron.2005.06.018

Vilhardt, F. (2005). Microglia: phagocyte and glia cell. *Int. J. Biochem. Cell Biol.* 37, 17–21. doi: 10.1016/j.biocel.2004.06.010

Völgyi, K., Háden, K., Kis, V., Gulyássy, P., Badics, K., Györffy, B. A., et al. (2017). Mitochondrial Proteome Changes Correlating with β-Amyloid Accumulation. *Mol. Neurobiol.* 54, 2060–2078. doi: 10.1007/s12035-015-9682-4

Voogd, J., and Glickstein, M. (1998). The anatomy of the cerebellum. *Trends Neurosci.* 21, 370–375. doi: 10.1016/s0166-2236(98)01318-6

Wakamatsu, N., Kominami, E., Takio, K., and Katunuma, N. (1984). Three forms of thiol proteinase inhibitor from rat liver formed depending on the oxidation-reduction state of a sulfhydryl group. *J. Biol. Chem.* 259, 13832–13838.

Wall, M. J., and Usowicz, M. M. (1997). Development of action potential-dependent and independent spontaneous GABAA receptor-mediated currents in granule cells of postnatal rat cerebellum. *Eur. J. Neurosci.* 9, 533–548. doi: 10.1111/j.1460-9568.1997.tb01630.x

Wang, J., He, J., Fan, Y., Xu, F., Liu, Q., He, R., et al. (2022). Extensive mitochondrial proteome disturbance occurs during the early stages of acute myocardial ischemia. *Exp. Ther. Med.* 23, 85. doi: 10.3892/etm.2021.11008

Wang, Q., Zhang, S., Liu, T., Wang, H., Liu, K., Wang, Q., et al. (2018). Sarm1/Myd88-5 Regulates Neuronal Intrinsic Immune Response to Traumatic Axonal Injuries. *Cell Rep.* 23, 716–724. doi: 10.1016/j.celrep.2018.03.071

Wang, S., Long, H., Hou, L., Feng, B., Ma, Z., Wu, Y., et al. (2023). The mitophagy pathway and its implications in human diseases. *Signal Transduct. Target. Ther.* 8, 304. doi: 10.1038/s41392-023-01503-7

Wang, X., Ellison, J. A., Siren, A. L., Lysko, P. G., Yue, T. L., Barone, F. C., et al. (1998). Prolonged expression of interferon-inducible protein-10 in ischemic cortex after permanent occlusion of the middle cerebral artery in rat. *J. Neurochem.* 71, 1194–1204. doi: 10.1046/j.1471-4159.1998.71031194.x

Washbourne, P. (2015). Synapse assembly and neurodevelopmental disorders. *Neuropsychopharmacol. Off. Publ. Am. Coll. Neuropsychopharmacol.* 40, 4–15. doi: 10.1038/npp.2014.163

Watson, A. E. S., Goodkey, K., Footz, T., and Voronova, A. (2020). Regulation of CNS precursor function by neuronal chemokines. *Neurosci. Lett.* 715, 134533. doi: 10.1016/j.neulet.2019.134533

Wendt, W., Lübbert, H., and Stichel, C. C. (2008). Upregulation of cathepsin S in the aging and pathological nervous system of mice. *Brain Res.* 1232, 7–20. doi: 10.1016/j.brainres.2008.07.067

Wilson, C., and González-Billault, C. (2015). Regulation of cytoskeletal dynamics by redox signaling and oxidative stress: implications for neuronal development and trafficking. *Front. Cell. Neurosci.* 9, 381. doi: 10.3389/fncel.2015.00381

Wishart, T. M., Parson, S. H., and Gillingwater, T. H. (2006). Synaptic Vulnerability in Neurodegenerative Disease. *J. Neuropathol. Exp. Neurol.* 65, 733–739. doi: 10.1097/01.jnen.0000228202.35163.c4

Wolf, M. E., and Kapatos, G. (1989). Flow cytometric analysis of rat striatal nerve terminals. *J. Neurosci. Off. J. Soc. Neurosci.* 9, 94–105. doi: 10.1523/JNEUROSCI.09-01-00094.1989

Wu, W. W., Wang, G., Baek, S. J., and Shen, R.-F. (2006). Comparative study of three proteomic quantitative methods, DIGE, cICAT, and iTRAQ, using 2D gel- or LC-MALDI TOF/TOF. *J. Proteome Res.* 5, 651–658. doi: 10.1021/pr050405o

Xie, Z., Zhao, M., Yan, C., Kong, W., Lan, F., Narengaowa, null, et al. (2023). Cathepsin B in programmed cell death machinery: mechanisms of execution and regulatory pathways. *Cell Death Dis.* 14, 255. doi: 10.1038/s41419-023-05786-0

Yang, A. J., Chandswangbhuvana, D., Margol, L., and Glabe, C. G. (1998). Loss of endosomal/lysosomal membrane impermeability is an early event in amyloid Abeta1-42 pathogenesis. *J. Neurosci. Res.* 52, 691–698. doi: 10.1002/(SICI)1097-4547(19980615)52:6%3C691::AID-JNR8%3E3.0.CO;2-3

Yang, J., Liu, X., Bhalla, K., Kim, C. N., Ibrado, A. M., Cai, J., et al. (1997). Prevention of apoptosis by Bcl-2: release of cytochrome c from mitochondria blocked. *Science* 275, 1129–1132. doi: 10.1126/science.275.5303.1129

Yarana, C., Sanit, J., Chattipakorn, N., and Chattipakorn, S. (2012). Synaptic and nonsynaptic mitochondria demonstrate a different degree of calcium-induced mitochondrial dysfunction. *Life Sci.* 90, 808–814. doi: 10.1016/j.lfs.2012.04.004

Yi, M., Weaver, D., and Hajnóczky, G. (2004). Control of mitochondrial motility and distribution by the calcium signal: a homeostatic circuit. *J. Cell Biol.* 167, 661–672. doi: 10.1083/jcb.200406038

Yoshimura, T., Matsushima, K., Tanaka, S., Robinson, E. A., Appella, E., Oppenheim, J. J., et al. (1987). Purification of a human monocyte-derived neutrophil chemotactic factor that has peptide sequence similarity to other host defense cytokines. *Proc. Natl. Acad. Sci. U. S. A.* 84, 9233–9237. doi: 10.1073/pnas.84.24.9233

Zabielski, P., Lanza, I. R., Gopala, S., Heppelmann, C. J. H., Bergen, H. R., Dasari, S., et al. (2016). Altered Skeletal Muscle Mitochondrial Proteome As the Basis of Disruption of Mitochondrial Function in Diabetic Mice. *Diabetes* 65, 561–573. doi: 10.2337/db15-0823

Zerovnik, E., Pompe-Novak, M., Skarabot, M., Ravnikar, M., Musevic, I., and Turk, V. (2002). Human stefin B readily forms amyloid fibrils in vitro. *Biochim. Biophys. Acta* 1594, 1–5. doi: 10.1016/s0167-4838(01)00295-3

Zhao, L., Zhao, J., Zhong, K., Tong, A., and Jia, D. (2022). Targeted protein degradation: mechanisms, strategies and application. *Signal Transduct. Target. Ther.* 7, 113. doi: 10.1038/s41392-022-00966-4

Zheng, J. Q., Kelly, T. K., Chang, B., Ryazantsev, S., Rajasekaran, A. K., Martin, K. C., et al. (2001). A functional role for intra-axonal protein synthesis during axonal regeneration from adult sensory neurons. *J. Neurosci. Off. J. Soc. Neurosci.* 21, 9291–9303. doi: 10.1523/JNEUROSCI.21-23-09291.2001

Zhong, Z., Umemura, A., Sanchez-Lopez, E., Liang, S., Shalapour, S., Wong, J., et al. (2016). NF-κB Restricts Inflammasome Activation via Elimination of Damaged Mitochondria. *Cell* 164, 896–910. doi: 10.1016/j.cell.2015.12.057

Zhou, L., Kong, G., Palmisano, I., Cencioni, M. T., Danzi, M., De Virgiliis, F., et al. (2022). Reversible CD8 T cell-neuron cross-talk causes aging-dependent neuronal regenerative decline. *Science* 376, eabd5926. doi: 10.1126/science.abd5926

Zipp, F., Bittner, S., and Schafer, D. P. (2023). Cytokines as emerging regulators of central nervous system synapses. *Immunity* 56, 914–925. doi: 10.1016/j.immuni.2023.04.011

Zlotnik, A., and Yoshie, O. (2012). The chemokine superfamily revisited. *Immunity* 36, 705–716. doi: 10.1016/j.immuni.2012.05.008

Appendices

Appendix 1. Differentially expressed mitochondrial proteins in cerebellar synaptosomes from *Cstb*$^{-/-}$ mice.

Biological function	Protein name	Gene ID	Fold change (*Cstb*$^{-/-}$/wt)	
			P14	P30
Respiratory chain	Cytochrome c, somatic	*Cycs*	-6.46	0.38
	NADH dehydrogenase [ubiquinone] iron-sulfur protein 8	*Ndufs8*	1.90	
	NADH dehydrogenase [ubiquinone] 1 alpha subcomplex subunit 6	*Ndufa6*	1.64	1.75
	NADH dehydrogenase [ubiquinone] 1 alpha subcomplex subunit 5	*Ndufa5*	2.05	
	NADH dehydrogenase [ubiquinone] iron-sulfur protein 5	*Ndufs5*	2.66	
	NADH dehydrogenase [ubiquinone] 1 alpha subcomplex subunit 10	*Ndufa10*	1.86	
	Cytochrome c oxidase assembly factor 6	*Coa6*	1.79	
	Cytochrome c oxidase, subunit 6B1	*Cox6b1*	26.87	5.99
	ATP synthase, H+ transporting, mitochondrial F0 complex, subunit G	*Atp5l*	2.93	
	NADH dehydrogenase [ubiquinone] 1 beta subcomplex subunit 11, mitochondrial	*Ndufb11*		0.64
	Cytochrome c oxidase subunit 2	*mt-Co2*		0.65
	ATP synthase protein 8	*mt-Atp8*		0.60
	ATP synthase subunit f, mitochondrial	*Atp5j2*		2.51
	Cytochrome b-c1 complex subunit 6, mitochondrial	*Uqcrh*		0.62
	NADH dehydrogenase [ubiquinone] flavoprotein 1, mitochondrial	*Ndufv1*		1.51
	NADH dehydrogenase [ubiquinone] 1 subunit C2	*Ndufc2*		0.70
	Succinate dehydrogenase [ubiquinone] iron-sulfur subunit, mitochondrial	*Sdhb*		1.82
	NADH dehydrogenase [ubiquinone] 1 beta subcomplex subunit 4	*Ndufb4*		0.68
	NADH dehydrogenase [ubiquinone] 1 beta subcomplex subunit 7	*Ndufb7*		0.47

	Cytochrome b-c1 complex subunit Rieske, mitochondrial	*Uqcrfs1*		0.87
	Cytochrome b-c1 complex subunit 1, mitochondrial	*Uqcrc1*		1.56
	ATP synthase subunit delta, mitochondrial	*Atp5d*		0.67
	NADH dehydrogenase [ubiquinone] flavoprotein 2, mitochondrial	*Ndufv2*		1.35
	Cytochrome b-c1 complex subunit 2, mitochondrial	*Uqcrc2*		1.29
	NADH dehydrogenase [ubiquinone] 1 alpha subcomplex subunit 9, mitochondrial	*Ndufa9*		0.71
Carbohydrate and lipid metabolism	Succinate-CoA ligase, GDP-forming, alpha subunit	*Suclg1*	2.73	
	D-2-hydroxyglutarate dehydrogenase	*D2hgdh*	3.07	
	Isopentenyl-diphosphate delta isomerase	*Idi1*	2.05	
	Malate dehydrogenase, mitochondrial	*Mdh2*		1.43
	Acyl-CoA-binding protein	*Dbi*		0.39
	Non-specific lipid-transfer protein	*Scp2*		2.61
	Very long-chain specific acyl-CoA dehydrogenase, mitochondrial	*Acadvl*		1.35
	Peroxisomal multifunctional enzyme type 2	*Hsd17b4*		1.29
	Isocitrate dehydrogenase [NADP], mitochondrial	*Idh2*		2.17
	Hydroxyacyl-coenzyme A dehydrogenase, mitochondrial	*Hadh*		1.93
	Glycerol-3-phosphate dehydrogenase, mitochondrial	*Gpd2*		0.77
	D-beta-hydroxybutyrate dehydrogenase, mitochondrial	*Bdh1*		1.68
	Calcium-binding mitochondrial carrier protein Aralar1	*Slc25a12*		0.57
	3-ketoacyl-CoA thiolase, mitochondrial	*Acaa2*		1.45
	Cytosolic acyl coenzyme A thioester hydrolase	*Acot7*		2.96
	Sideroflexin-5	*Sfxn5*		0.66
	Electron transfer flavoprotein subunit beta	*Etfb*		1.21
ROS metabolism	Superoxide dismutase 1, soluble	*Sod1*	-1.64	
	4-trimethylaminobutyraldehyde dehydrogenase	*Aldh9a1*	1.69	
	Catalase	*Cat*		1.44
	Peroxiredoxin-2	*Prdx2*		1.33
	Thioredoxin-dependent peroxide reductase, mitochondrial	*Prdx3*		1.43
	Peroxiredoxin-4	*Prdx4*		1.73
Maintenance	MICOS complex subunit Mic25	*Chchd6*	2.32	
	Single-stranded DNA binding protein 1	*Ssbp1*	-3.50	
	Mitochondrial fission regulator 1-like	*Mtfr1l*		0.85
	Endonuclease G, mitochondrial	*Endog*		0.84
	MICOS complex subunit Mic60	*Immt*		0.75
Other	Mitochondrial Rho GTPase 2	*Rhot2*	1.91	

	Coiled-coil domain-containing protein 58	*Ccdc58*	2.21	
	Dehydrogenase/reductase SDR family member 7B	*Dhrs7b*	-2.27	
	Quinone oxidoreductase	*Cryz*	1.46	
	Methylmalonate-semialdehyde dehydrogenase [acylating], mitochondrial	*Aldh6a1*	1.51	
	Isobutyryl-CoA dehydrogenase, mitochondrial	*Acad8*	1.65	
	Alanine aminotransferase 2	*Gpt2*	3.35	
	Ornithine aminotransferase, mitochondrial	*Oat*	1.71	1.79
	Hydroxymethylglutaryl-CoA lyase, mitochondrial	*Hmgcl*	2.35	
	Valacyclovir hydrolase	*Bphl*	2.03	
	Ubiquinone biosynthesis monooxygenase COQ6, mitochondrial	*Coq6*	1.99	
	Dihydropteridine reductase	*Qdpr*	1.92	7.00
	ADP/ATP translocase 1	*Slc25a4*	1.63	
	ADP/ATP translocase 2	*Slc25a5*	2.30	
	28S ribosomal protein S9, mitochondrial	*Mrps9*	1.68	
	39S ribosomal protein L47, mitochondrial	*Mrpl47*	1.71	
	SRA stem-loop-interacting RNA-binding protein, mitochondrial	*Slirp*	2.15	
	39S ribosomal protein L11, mitochondrial	*Mrpl11*	1.90	
	Mitochondrial import inner membrane translocase subunit Tim13	*Timm13*	2.89	3.54
	Nardilysin	*Nrd1*	-1.50	
	ATPase family AAA domain-containing protein 1	*Atad1*	2.86	0.66
	Reactive oxygen species modulator 1	*Romo1*	3.15	
	Mitochondrial import receptor subunit TOM40 homolog	*Tomm40*	-1.83	
	Mitochondrial glutamate carrier 2	*Slc25a18*	1.78	
	Mitochondrial import receptor subunit TOM20 homolog	*Tomm20*		0.12
	Persulfide dioxygenase ETHE1, mitochondrial	*Ethe1*		5.22
	Mitochondrial import inner membrane translocase subunit Tim9	*Timm9*		2.13
	Aflatoxin B1 aldehyde reductase member 2	*Akr7a5*		1.35
	3-hydroxyisobutyryl-CoA hydrolase, mitochondrial	*Hibch*		0.70
	Cytosolic 10-formyltetrahydrofolate dehydrogenase	*Aldh1l1*		1.45
	Phosphate carrier protein, mitochondrial	*Slc25a3*		0.72
	Sideroflexin-3	*Sfxn3*		0.65
	Glyoxalase domain-containing protein 4	*Glod4*		1.74
	Ferredoxin-2, mitochondrial	*Fdx2*		0.45
	Calcium uptake protein 3, mitochondrial	*Micu3*		0.64
	Haloacid dehalogenase-like hydrolase domain-containing protein 3	*Hdhd3*		1.31

	ATP-dependent (S)-NAD(P)H-hydrate dehydratase	*Naxd*		1.29
	Glutamine amidotransferase-like class 1 domain-containing protein 3A, mitochondrial	*Gatd3a*		1.55
	Aldehyde dehydrogenase, mitochondrial	*Aldh2*		1.47
	Prohibitin-2	*Phb2*		0.65
	Histidine triad nucleotide-binding protein 1	*Hint1*		1.31
	Voltage-dependent anion-selective channel protein 2	*Vdac2*		0.68
	Voltage-dependent anion-selective channel protein 1	*Vdac1*		0.67
	Guanylate kinase	*Guk1*		1.56
	2-oxoisovalerate dehydrogenase subunit beta, mitochondrial	*Bckdhb*		3.66
	Dephospho-CoA kinase domain-containing protein	*Dcakd*		1.94

Appendix 2. Differentially expressed mRNA transcripts in cerebellar synaptosomes from *Cstb*$^{-/-}$ mice.

Biological function	Cellular location	Gene ID	Fold change (*Cstb*$^{-/-}$/wt)	
			P30	P45
Inflammation and defense response	Extracellular space	*C1qa*	2.09	
		C4b	4.52	5.04
		Ccl4	12.24	6.44
		Ccl6	5.40	2.65
		Cd14	2.64	2.75
		Cstb	0.09	0.12
		Cxcl13	133.05	152.05
		Lgals3bp		3.19
		Lpl	13.46	9.18
		Serpinf1		0.46
	Lysosome	*Cd68*	2.12	
		Cst7	37.83	19.75
		Tmem9b		0.73
	Other	*Alox5ap*	0.49	0.36
		C3ar1	4.99	3.51
		Ctse	3.72	7.63
		Cybb	14.62	14.79
		Dcstamp		33.30
		Erbin		1.79
		Hsd11b1	0.56	0.50
		Lat2	4.67	
		Lst1		0.21
		Ptgs1	0.56	
		Selplg		0.48
		Usp18		9.52
Apoptosis	Extracellular space	*C3*		19.81
		Ccl12	5.02	
		Ccl3	16.77	32.40
		Ccl5	8.03	8.17
		Cxcl10	10.49	16.13
		Igf1	5.51	4.59
		Lgals3	2.90	
		Lox		4.53
		Nell1		1.77

		Ntf3		0.40
		Spp1	4.37	4.52
		Sulf1		1.66
	Lysosome	*Ctsd*	1.80	1.99
		Ctsh	1.94	
		Ctsz		1.72
		Grn		1.94
		Srgn	1.85	1.65
	Mitochondria	*Bcl2a1d*	4.71	
	Other	*Bcl2a1a*	14.05	
		Birc5		5.48
		Clec7a	69.56	35.03
		Dab2	2.34	
		Egln2		1.49
		Gjb6	0.55	
		Ifi27l2a	11.34	5.78
		Ifit3	3.44	3.97
		Ifit3b		4.43
		Top2a		6.77
		Tyrobp	1.95	
Stress response	Extracellular space	*Capg*		6.11
		Cxcl16	3.55	4.18
		Lyz2	3.19	2.27
		P2ry12		0.39
		Wfdc17	7.61	9.42
	Lysosome	*Gfap*	2.43	4.12
		H2-K1		2.12
		Ifitm3	3.19	2.70
		Irgm1		2.62
	Other	*Ch25h*		30.70
		Ifit1	6.22	7.23
		Mpeg1	3.00	3.38
		Nrep		0.73
		Oasl2	15.66	8.26
		Omg		0.71
		Pclaf		5.25
		Plek	2.74	
		Rtp4	4.16	3.39
		Slamf9	5.71	

Other function	Extracellular space	*Dmp1*	0.46	
	Lysosome	*Hexa*	1.64	1.49
		Snapin		0.71
	Mitochondria	*Echdc2*		0.55
		Rab24		0.72
		Slc25a3	0.77	
	Other	*Anln*		0.57
		Apbb1ip	2.67	
		Atoh7		0.57
		AU020206	2.78	2.27
		Cacna1g		1.87
		Cd52	5.04	3.19
		Cd72		3.99
		Cdk6		19.33
		Cenpa		3.15
		Crybb1	0.11	
		Cyp51		0.73
		Dpys	20.69	6.91
		Ggact		0.70
		Gmfg		0.30
		Gpr34		0.44
		Hs3st1		0.62
		Limd2		0.61
		Marchf4		2.29
		Msmo1		0.59
		Rab2a		0.78
		Sez6l2		1.55
		Snhg20		0.56
		Tef		1.49
		Tk1	45.20	
		Tmem52	0.40	
		Trmt9b		0.72
		Txndc9		0.70
		Zfp511		0.63